Prepared for submission to JHEP IPPP/14/23, DCPT/14/46

Constrained Dirac gluino mediation

Daniel Busbridge

Institute for Particle Physics Phenomenology,
Durham University, South Road
Durham, DH1 3LE, UK

E-mail: d.w.busbridge@durham.ac.uk

Abstract: We perform a comparison study of the Constrained Minimal Supersymmetric Standard Model and Constrained General Gauge Mediation with and without a heavy Dirac gluino. These extremely simple models have very few free parameters and exhibit the characteristic features of *supersoftness* and *supersafeness*. We determine the characteristic low energy spectra, the production cross sections of key processes at the Large Hadron Collider and the degree of fine tuning for a representative range of parameters for each model.

Keywords: Dirac gauginos, SUSY breaking, Supersymmetry

ArXiv ePrint: 1408.4605

arXiv:1408.4605v2 [hep-ph] 27 Aug 2014

Contents

1 Introduction **2**

2 Constrained Dirac gluino mediation **5**

2.1 Overview 5

2.2 Boundary conditions at the Messenger scale 6

2.2.1 D-term breaking effective operators 6

2.2.2 Combined D and F term 7

2.3 One loop threshold corrections at the Dirac gluino mass 9

2.3.1 Significance 9

2.3.2 Threshold corrections 9

3 Numerical setup **11**

4 Spectra **11**

4.1 Constrained General Gauge Mediation 19

4.2 Overview 21

5 Cross sections **21**

6 Electroweak symmetry breaking and fine tuning **24**

7 Conclusions **28**

8 Acknowledgements **29**

A Additional plots **30**

A.1 Constrained Minimal Supersymmetric Standard Model 30

A.2 Constrained General Gauge Mediation 34

B Renormalisation Group equations with Dirac gluino decoupling **46**

B.1 SUSY parameters 46

B.2 SUSY breaking parameters 48

1 Introduction

In light of the data taken by the ATLAS and CMS collaborations during Run I of the Large Hadron Collider (LHC), many popular Ultraviolet (UV) completions of the Minimal Supersymmetric Standard Model (MSSM) are now severely challenged as 'natural' realisations of microscopic physics:

- The discovery of a particle closely resembling the Standard Model (SM) Higgs Boson [1, 2] with a mass $m_{\rm h} = 125.9 \pm 0.4$ GeV [3] typically requires one loop corrections to its mass to be the same order as its tree level contribution[1]

$$m_{\rm h}^2 \simeq m_{\rm Z}^2\, c_{2\beta}^2 + \frac{3}{2\,\pi^2}\frac{m_{\rm t}^4}{v^2}\left[\log\left(\frac{m_{\tilde{\rm t}_1}\, m_{\tilde{\rm t}_2}}{m_{\rm t}^2}\right) + \frac{X_t^2}{m_{\tilde{\rm t}_1}\, m_{\tilde{\rm t}_2}}\left(1 - \frac{X_t^2}{12\, m_{\tilde{\rm t}_1}\, m_{\tilde{\rm t}_2}}\right)\right] \tag{1.1}$$

  if it is identified with the lightest Charge Parity (CP) even neutral MSSM scalar. Here $X_t = A_t - \mu\, \cot(\beta)$ is the stop mixing parameterk β is the ArcTan of the Two Higgs-Doublet Model (2HDM) vacuum parameters

$$\langle {\rm H}_u \rangle = \frac{1}{\sqrt{2}}\,(0 \quad v_u)^T, \quad \langle {\rm H}_d \rangle = \frac{1}{\sqrt{2}}\,(v_d \quad 0)^T, \quad t_\beta \equiv \frac{v_u}{v_d} \tag{1.2}$$

  and μ is the Higgsino mass parameter. Without increasing the field content beyond the MSSM, raising the Higgs mass this leaves residual tuning in electroweak minimisation conditions.

- The non-observation of strongly interacting sparticles by ATLAS (CMS) has put stringent bounds on gluino and squark masses: $m_{\tilde{\rm g}} \gtrsim 1350$ $(1000 - 1200)$ GeV, $m_{\tilde{q}} \gtrsim 780$ (780) GeV in simplified models with degenerate squark masses and a neutralino Lightest Ordinary Supersymmetric Particle (LOSP) with mass $m_{\tilde{\chi}_1^0} = 0$ ($m_{\tilde{\chi}_1^0} < 80$) GeV [4, 5]. If the stops and gluinos are heavy for the entire Renormalisation Group (RG) flow they lead to a large logarithmic dependence of Electroweak Symmetry Breaking (EWSB) upon the UV parameters.

There are many ways of reducing tuning. A well studied example is the Next to Minimal Supersymmetric Standard Model (NMSSM) which adds to the MSSM a SM gauge singlet chiral superfield which acquires a Vaccum Expectation Value (VEV) to dynamically solve the *μ-problem*. New quartic Higgs interactions are present which raise the tree level Higgs mass so that a smaller fraction is required from radiative corrections. Unfortunately, these interactions are suppressed at large t_β, where the D-term contributions to the tree level Higgs mass are maximised. Typically $m_{\tilde{\rm t}} \sim 1$ TeV is required if perturbativity holds all the way to the Grand Unified Theory (GUT) scale [6, 7], leaving the NMSSM with a *little hierarchy problem*. If one also adds a hypercharge neutral $\mathrm{SU(2)_L}$ triplet as is done in the Triplet Extended NMSSM, further quartic Higgs interactions can be induced that allow the correct Higgs mass to be achieved at tree level, removing heavy stops as

[1] We use $c_\theta \equiv \cos(\theta)$, $s_\theta \equiv \sin(\theta)$ and $t_\theta \equiv \tan(\theta)$ throughout.

a requirement [8, 9]. The direct constraints on the gluino and squarks stops still remain however, so this is not a complete solution.

Solutions accounting for the non-observation of Supersymmetry (SUSY) are also available: compressed spectra [10–12] softens jet activity, R Parity Violation ($\not{R}$) reduces the about of Missing Transverse Energy ($\not{E}_T$) [13] and Flavoured Gauge Mediation (FGM) [14, 15] can break the squark mass degeneracy, weakening the reduced limits at current experiments. Combining these mechanisms with models that generate natural spectra can give a plausible explanation of SUSY non-observation *and* the Higgs mass.

Instead of using a combination of the above, one can use a Dirac gluino to achieve both. A Dirac gluino doesn't enter the scalar Renormalisation Group Equations (RGEs) at one loop. This is known as *supersoftness*. The Dirac gluino does however give the squarks a one loop threshold correction at the Dirac gluino mass, acting as a low scale messenger for the strong sector of the SM. In this situation, larger $m_{\widetilde{\mathrm{t}}}$ can be more acceptable as the RG running will be shorter and so will induce smaller corrections to the parameters involved in EWSB [16]. The electroweak sector will then less UV sensitive. Models with Dirac gauginos have been studied in a wide range of scenarios [16–64]. The simplest known way of generating a Dirac gluino mass m_{D3} is to generate it at the messenger scale M by integrating out the messenger sector coupled to a source of D term breaking

$$\delta m_{D3} = \quad = \frac{y\, g_3}{16\,\pi^2}\frac{D'}{M}, \tag{1.3}$$

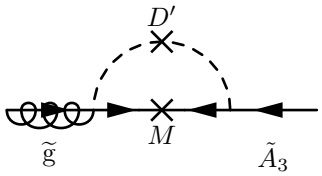

where D' is the SUSY breaking D-term VEV of a U(1)′ gauge group in the hidden sector: $\langle \mathcal{W}'_\alpha \rangle = \theta_\alpha\, D'$ and M is the messenger scale and y is couples vector-like messengers $(\Phi, \bar{\Phi})$ to the chiral field A_3 containing the right handed component of the Dirac gluino $\widetilde{\mathrm{g}}_R = (\tilde{A}_3)^\dagger$

$$W_{\mathrm{Mess}} = \sqrt{2}\, y\, \bar{\Phi}\, A_3\, \Phi + M\, \bar{\Phi}\, \Phi. \tag{1.4}$$

This theory is RG evolved to the physical Dirac gluino mass where we must switch to an effective theory with the gluino and the sgluons integrated out. This generates one loop threshold corrections

for the squarks

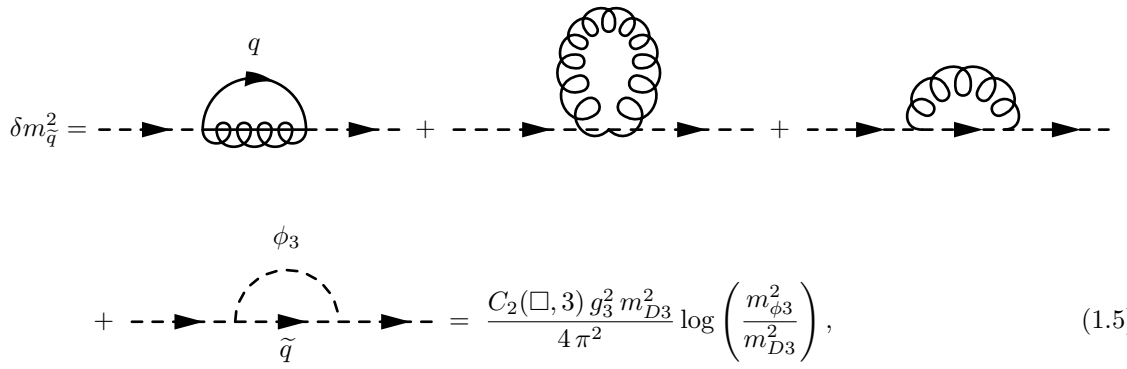

$$= \frac{C_2(\square, 3)\, g_3^2\, m_{D3}^2}{4\,\pi^2} \log\left(\frac{m_{\phi 3}^2}{m_{D3}^2}\right), \tag{1.5}$$

where $C_2(\square, 3)$[2] is the quadratic Casimir for the fundamental representation under the gauge group $\mathrm{SU}(3)_\mathrm{C}$, and

$$m_{\phi 3}^2 = m_3^2 + 4\, m_{3D}^2 + B_3, \qquad\qquad m_{\sigma 3}^2 = m_3^2 - B_3, \tag{1.8}$$

are the soft masses squared for the CP-even ϕ_3 and CP-odd σ_3[3] that we will refer to as the sgluon and pseudosgluon (collectively as sgluons for simplicity). Here, m_3^2 is the sgluon soft mass squared and B_3 is the sgluon bilinear term (see sec. 2.2.2). The theory is then RG evolved to the SUSY scale m_SUSY which we take to be the geometric stop mass $m_\mathrm{SUSY} = \sqrt{m_{\widetilde{t}_1}\, m_{\widetilde{t}_2}}$ where the renormalisation scale dependence for the calculation of the spectrum is minimised [65–67].

If the majority of the squark mass is generated through integrating out the gluino and its corresponding scalar degrees of freedom, the sensitivity of electroweak parameters to the parameters defined at M is reduced as the most sensitive period of running is now effectively from m_{D3} rather than M to m_SUSY. It is straightforward to give Dirac masses to all of the gauginos in the MSSM in this way, each accompanied by analogous threshold corrections to the scalar spectrum, though this can introduces further complications such as tachyons and electroweak precision measurements.

The dominant diagram for squark production at the LHC in the MSSM is t-channel gluino exchange which requires the presence of the chirality flipping Majorana gluino propagator (see fig. 1). With a purely Dirac gluino this is essentially negligible. For a characteristic Majorana

[2] We use $C_2(\mathbf{r}, i)$ to denote the quadratic Casimir of the representation $\mathbf{r}$ under the i^th gauge group. In this paper we use

$$C_2(\square, N) = C_2(\bar{\square}, N) = \frac{N^2 - 1}{2 \times N}, \qquad\qquad C_2(\mathbf{Ad}, N) = N \tag{1.6}$$

for $\mathrm{SU}(N)$ gauge groups and

$$C_2(q, 1) = q^2 \tag{1.7}$$

for $\mathrm{U}(1)$ gauge groups, where q is the charge under that gauge group.

[3] We decompose A_3 as

$$A_3 = \frac{1}{\sqrt{2}}(\phi_3 + i\,\sigma_3). \tag{1.9}$$

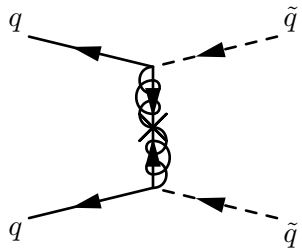

Figure 1. The dominant tree-level contribution to squark-squark production at the LHC requires a chirality flipping Marjoana gluino propagator. This is absent in models with Dirac gluinos, greatly the suppressing squark-squark production cross-section.

gluino spectrum, where squarks should be at least as heavy as gluinos from a UV perspective [68], the relevant bounds from ATLAS and CMS are $m_{\tilde{q}} = m_{\tilde{g}} \gtrsim 1700 - 1800$ GeV for $m_{\rm LSP} \lesssim 700$ GeV. In a supersoft model, gluinos are naturally absent from the spectrum, the ATLAS (CMS) bounds on first two generation squarks are moderately reduced to $m_{\tilde{q}_{1,2}} \gtrsim 850$ (780) GeV with $m_{\rm LSP} = 0$ and no bound with $m_{\rm LSP} \gtrsim 300$ GeV, rendering them *supersafe* [44, 55, 56]. The number of events involving electroweak sparticles at the LHC will also be reduced as the dominant processes with these sparticles as final states are those of the decay chains of the gluinos and squarks whose production is suppressed.

We will first construct two simple models that that have the following properties:

- Natural from the point of view of EWSB — electroweak sparticles all at electroweak scale.
- A minimal set of free parameters in the UV.
- *Supersoftess* to reduce fine tuning.
- *Supersafeness* to aleviate collider bounds.

We will then implement these models and the supersoft mechanism into a spectrum generator and perform a study, discussing the consequences for hadron collider phenomenology and fine tuning.

2 Constrained Dirac gluino mediation

2.1 Overview

As the LHC is a proton-proton collider, the non-observation of SUSY, and particularly of gluinos, indicates that the strongly interacting SUSY particles should be moderately heavy to evade exclusion. To achieve this, we supplement the Constrained Minimal Supersymmetric Standard Model (CMSSM) and Constrained General Gauge Mediation (CGGM) with a Dirac gluino. We will refer to these scenarios as *Constrained Dirac gluino mediation*. Due to the one loop supersoft nature of the Dirac gauginos, the higher scale of the strong sector is not transferred to the electroweak sector through RG running, and so electroweak sparticles can remain light (depending on the region of parameter space). Specifically, we couple $\mathrm{SU}(3)_{\rm C} \times \mathrm{SU}(2)_{\rm L} \times \mathrm{U}(1)_Y$ to either the CMSSM or the CGGM, and couple only $\mathrm{SU}(3)_{\rm C}$ to a sector of D term breaking to the mechanism of [16] (see fig. 2

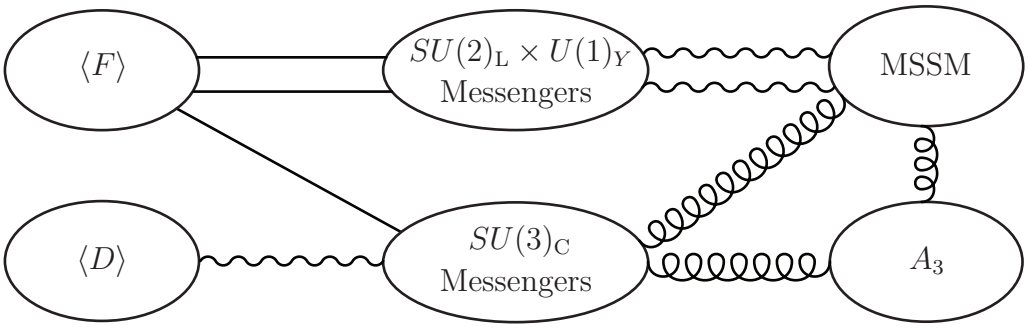

Figure 2. The different sectors used in our setup.

for the CGGM setup). The field content is the same as the MSSM plus the chiral superfield A_3 detailed in table 1. The A_3 is often referred to as an Extended Superpartner (ESP) due to its potential origin as the chiral superfield component of $\mathcal{N} = 2$ vector multiplets.

We will now recap the effects of integrating out a messenger sector in terms of the presence of D term SUSY breaking before moving on to discuss the full UV boundary conditions of the model.

2.2 Boundary conditions at the Messenger scale

2.2.1 D-term breaking effective operators

Fox, Nelson and Weiner (FNW) [16] identified two operators generated by D-term breaking in the presence of ESPs

$$\begin{aligned}\mathcal{L}^{(1)}_{\rm Supersoft} = \sqrt{2}\int d^2\theta\, \frac{\mathcal{W}'\cdot\mathcal{W}_3^a\, A_3^a}{M} &= \frac{D'}{M}\left(i\,\widetilde{\mathrm{g}}^a\cdot\tilde{A}_3^a + \sqrt{2}\,A_3^a\, D_3^a\right) + \cdots \\ &= m_{D3}\left(i\,\widetilde{\mathrm{g}}^a\cdot\tilde{A}_3^a + \sqrt{2}\,A_3^a\, D_3^a\right) + \cdots, \qquad (2.1)\\ \mathcal{L}^{(2)}_{\rm Supersoft} = \int d^2\theta\, \frac{\mathcal{W}'\cdot\mathcal{W}'\, A_3^a\, A_3^a}{M^2} &= \left(\frac{D'}{M}\right)^2 A_3^a\, A_3^a \\ &= B_3\, A_3^a\, A_3^a, \qquad (2.2)\end{aligned}$$

where M is the scale of physics integrated out to generate the operators in eqs. 2.1, and 2.1, and D' is the VEV of a hidden sector $U(1)'$: $\langle \mathcal{W}'_\alpha \rangle = \theta_\alpha\, D'$. The "$\cdots$" in eq. 2.1 correspond to operators that vanish upon including their hermitian conjugates. In a messenger setup, both of these operators are generated at one loop, leading to a tachyon in the spectrum. Indeed, this is the original reason for abandoning these models [17]. There is one further operator generated at two loops by D-term breaking identified by Csáki et al. [58]

$$\begin{aligned}\mathcal{L}^{(1)}_{\text{Not supersoft}} = \int d^4\theta\, \frac{S^\dagger e^V S + \tilde{S}^\dagger e^{-V}\tilde{S}}{M^2}\, A_3^\dagger A_3 = \left(\frac{D'}{M}\right)^2 A_3^\dagger A_3 \\ = m_{A_3}^2\, A_3^\dagger A_3 \qquad (2.3)\end{aligned}$$

	$\mathrm{SU(3)_C}$	$\mathrm{SU(2)_L}$	$\mathrm{U(1)_Y}$
A_3	**Ad**	**1**	0

Table 1. Additional field content required to give a Dirac mass to the gluino.

where S and $\tilde{S}$ are singlets under the SM but charged under the $U(1)'$. These give rise to the non-vanishing $D' \propto |S|^2 - |\tilde{S}|^2$ and break the $U(1)'$ gauge symmetry. Note that the operator in eq. 2.3 is still picks out a coefficient $\sim (D'/M)^2$. Upon introducing messenger mixing, 2.3 is generated at one loop instead of two, and then the mixing freedom can be used to tune[4] 2.2 to be two loop size [29, 34, 58]. We then find the phenomenologically acceptable boundary conditions

$$m_{D3} \sim \frac{1}{16\pi^2}\frac{D'}{M}, \qquad m^2_{A_3} \sim \frac{1}{16\pi^2}\left(\frac{D'}{M}\right)^2, \qquad B_3 \sim \frac{\varepsilon}{16\pi^2}\left(\frac{D'}{M}\right)^2, \tag{2.4}$$

where $\varepsilon \sim 1/(16\pi^2)$ is a parameter that arises due to a cancellation between different contributions to B_3[5] . Note that the operator 2.3 is not supersoft at two loops, however, and will generate

$$K_{\mathrm{Sfermion}} = \int d^4\theta \, \frac{S^\dagger e^V S + \tilde{S}^\dagger e^{-V}\tilde{S}}{M^2}\, q^\dagger q \tag{2.5}$$

as can be observed from the squark two loop beta function

$$(16\pi^2)^2 \beta^{(2)}_{m_q^2} = 32\, g_3^2\, m^2_{A_3} + \cdots . \tag{2.6}$$

Supersoftness is then broken at two loops, rendering a UV sensitivity to the scale at which the Dirac gluino mass is generated [69].

2.2.2 Combined D and F term

Upon integrating out the messenger sector, we still have the MSSM superpotential

$$W_{\mathrm{MSSM}} = y_{\mathrm{u}}\, \overline{\mathrm{u}}\, q \cdot \mathrm{H}_u - y_{\mathrm{d}}\, \bar{\mathrm{d}}\, q \cdot \mathrm{H}_d - y_{\mathrm{e}}\, \bar{\mathrm{e}}\, \ell \cdot \mathrm{H}_d + \mu\, \mathrm{H}_u \cdot \mathrm{H}_d \tag{2.7}$$

and a soft lagrangian conveniently decomposed into

$$\mathcal{L}_{\mathrm{Soft}} = \mathcal{L}^F_{\mathrm{Soft}} + \mathcal{L}^D_{\mathrm{Soft}}. \tag{2.8}$$

[4] The tuning is typically $\mathcal{O}\left(\frac{1}{16\pi^2}\right)$.

[5] Strictly this is a cancellation between terms linear and quadratic in D', though this is not so important for our discussion.

$\mathcal{L}^F_{\rm Soft}$ is the standard soft lagrangian of the MSSM supplemented with A_3

$$\begin{aligned}
-\mathcal{L}^F_{\rm Soft} = \frac{1}{2}\Big(&M_3\,\widetilde{\rm g}\cdot\widetilde{\rm g} + M_2\,\widetilde{\rm W}\cdot\widetilde{\rm W} + M_1\,\widetilde{\rm B}\cdot\widetilde{\rm B} + {\rm h.c.}\Big)\\
&+ \big(a_{\rm u}\,\overline{\rm u}\,q\cdot{\rm H}_u - a_{\rm d}\,\overline{\rm d}\,q\cdot{\rm H}_d - a_{\rm e}\,\bar{\rm e}\,\ell\cdot{\rm H}_d + {\rm h.c.}\big)\\
&+ m_q^2|q|^2 + m_{\rm u}^2|\overline{\rm u}|^2 + m_{\rm d}^2|\overline{\rm d}|^2 + m_\ell^2|\ell|^2 + m_{\rm e}^2|\bar{\rm e}|^2 + m^2_{A_3^F}|A_3|^2\\
&+ (B_3\,A_3\,A_3 + {\rm h.c.})\\
&+ m^2_{{\rm H}_u}|{\rm H}_u|^2 + m^2_{{\rm H}_d}|{\rm H}_d|^2 + (B_\mu\,{\rm H}_u\cdot{\rm H}_d + {\rm h.c.}),
\end{aligned} \tag{2.9}$$

where the M_i are the Majorana gaugino massses, a_i are the scalar trilinears, the m_i^2 are the soft masses squared and the B_i are the scalar bilinears. The boundary conditions for these terms at $m_{\rm GUT}$ in the CMSSM are [70]

$$m^2_{\tilde f} = m_0^2, \qquad \tilde f = q, \overline{\rm u}, \overline{\rm d}, \ell, {\rm e}, {\rm H}_u, {\rm H}_d, A_3^F, \tag{2.10}$$

$$M_i = M_{1/2}, \qquad i = 1,2,3, \tag{2.11}$$

$$a_i\,y_i^{-1} = A_0, \qquad i = {\rm u}, {\rm d}, {\rm e}, \tag{2.12}$$

with B_μ and μ determined from EWSB at the low scale

$$m_{\rm Z}^2 = \frac{m^2_{{\rm H}_d} - m^2_{{\rm H}_u}}{\sqrt{1-s^2_{2\beta}}} - m^2_{{\rm H}_u} - m^2_{{\rm H}_d} - 2\,|\mu|^2, \tag{2.13}$$

$$s_{2\beta} = \frac{2\,B_\mu}{m^2_{{\rm H}_u} + m^2_{{\rm H}_d} + 2\,|\mu|^2} \tag{2.14}$$

and $B_3 = 0$ for simplicity. The boundary conditions at $m_{\rm Mess}$ for General Gauge Mediation (GGM) are [71]

$$M_i = \frac{g_i^2}{16\,\pi^2}\,\Lambda_{G_i}, \qquad i = 1,2,3, \tag{2.15}$$

$$a_i = 0, \qquad i = {\rm u}, {\rm d}, {\rm e}, \tag{2.16}$$

$$m^2_{\tilde f} = 2\sum_{i=1}^{3} C_2(\mathbf{r}^i_{\tilde f}, i)\,k_i\,\frac{g_i^4}{(16\,\pi^2)^2}\,\Lambda^2_{S_i}, \qquad \tilde f = q, \overline{\rm u}, \overline{\rm d}, \ell, {\rm e}, {\rm H}_u, {\rm H}_d, A_3^F, \tag{2.17}$$

with B_μ and μ again determined from EWSB at the low scale as in eqs. 2.13 and 2.14. $C_2(\mathbf{r}^i_{\tilde f}, i)$ is the quadratic Casimir of the representation $\mathbf{r}^i_{\tilde f}$ under the $i^{\rm th}$ gauge group (see eqs. 1.6 and 1.7) and $k_i = (3/5, 1, 1)$ is the standard GUT normalisation. To compare like with like, we will take the CGGM parameter space

$$\Lambda_{G_i} = \Lambda_G, \qquad \Lambda_{S_i} = \Lambda_S, \qquad i = 1,2,3, \tag{2.18}$$

and looking along the line $\Lambda_S = \Lambda_G$ gives the boundary conditions of the Minimal Gauge Mediated Supersymmetry Breaking (mGMSB) [72–74] subspace of models originally developed in [75–80]. We concede that we have not solved the B_μ problem of Gauge Mediated Supersymmetry Breaking (GMSB). With a future study one could take supplement GMSB with a Dirac gluino. Then as was studied in [81–84] t_β would be taken as an output rather than input, and a small value of B_μ would be specified at the high scale. $\mathcal{L}^D_{\rm Soft}$ contains the operators, including the non-standard soft terms [85] generated by the D-term SUSY breaking discussed in 2.2.1

$$\begin{aligned} -\mathcal{L}^D_{\rm Soft} = & \left(i\, m_{D3}\, \widetilde{\mathrm{g}}^a \cdot \tilde{A}^a_3 + \mathrm{h.c.} \right) + \frac{m^2_{\phi 3}}{2}\, \phi_3^2 + \frac{m^2_{\sigma 3}}{2}\, \sigma_3^2 \\ & + 2\, g_3\, m_{D3}\, \phi_3^a \left(q^\dagger\, T^a\, q + \overline{\mathrm{u}}^\dagger\, T^a\, \overline{\mathrm{u}} + \overline{\mathrm{d}}^\dagger\, T^a\, \overline{\mathrm{d}} \right), \end{aligned} \tag{2.19}$$

where ϕ_3, σ_3, $m^2_{\phi_3}$ and $m^2_{\sigma_3}$ are as defined in eqs. 1.9 and 1.8 and the T^a are the generators of $\mathrm{SU}(3)_\mathrm{C}$ in the fundamental representation. The second line in 2.19 is the origin of the supersoftness of these models, and provides the additional interaction required for the diagram on the second line of 1.5, cutting off the sensitivity to the UV scale where m_{D3} is generated. Finally, for both the CMSSM and CGGM we take

$$m_{D3} = \frac{1}{16\pi^2}\Lambda_D, \qquad m^2_{A^D_3} = \frac{c_1^2}{16\pi^2}\,\Lambda_D^2, \qquad B_3 = 0, \tag{2.20}$$

where c_1 represents $\mathcal{O}(1)$ mixings in the messenger sector that have been tuned to make B_3 phenomenologically negligible as already discussed.

2.3 One loop threshold corrections at the Dirac gluino mass

2.3.1 Significance

The Dirac gluinos and the sgluons play the role of messengers D-term SUSY for the strongly interacting sparticles. As our calculation will be performed in $\overline{\rm DR}$, a mass-independent scheme, in order to treat the large hierarchy between the gluino mass and the rest of the SUSY spectrum correctly, we integrate out the gluino and the sgluons, resulting in shifts of the parameters at the gluino mass. This leads to a different behaviour of the RG compared to the MSSM. The most important contributions to take into account are the corrections to squark masses and to the strong gauge coupling g_3. We will see that this alters where EWSB occurs and can increase the naturalness of these models.

2.3.2 Threshold corrections

Squark masses: The gluino in these models is not pure Dirac, although in some regions of parameter space this may be approximately true. Consequently, instead of using the analytic formulae in eq. 1.5, we will numerically compute the full 1-loop threshold correction to squark

masses[6]

$$m_{\widetilde{q}}^2 \to m_{\widetilde{q}}^2 - \Pi_{\widetilde{q}}^{\widetilde{g}}(m_{\widetilde{q}}) - \Pi_{\widetilde{q}}^{\phi_3}(m_{\widetilde{q}}) \tag{2.21}$$

where

$$\Pi_{\widetilde{q}}^{\widetilde{g}}(p) = \frac{g_3^2}{6\,\pi^2}\,|(Z_g)_{i,1}|^2\,G_0(p, m_{\widetilde{g}_i}, 0), \qquad \Pi_{\widetilde{q}}^{\phi_3}(p) = \frac{g_3^2}{3\,\pi^2}\,m_{D3}^2\,B_0(p, m_{\widetilde{q}}, m_{\phi_3}) \tag{2.22}$$

and Z_g is the matrix that diagonalises the gluino mass matrix $m_{\widetilde{g}}$

$$m_{\widetilde{g}} = \begin{pmatrix} M_3 & m_{D3} \\ m_{D3} & 0 \end{pmatrix}, \qquad Z_g\,m_{\widetilde{g}}\,Z_g^\dagger = \mathrm{diag}(m_{\widetilde{g}_1}, m_{\widetilde{g}_2}) \tag{2.23}$$

where $m_{\widetilde{g}}$ is in the $(\widetilde{g}, \tilde{A}_3)$ basis. B_0 and G_0 are scalar integrals [86, 87].

Strong gauge coupling: The 1-loop threshold corrections to g_3 at m_{D3} are [88]

$$g_3 \to g_3 \left\{1 \pm \frac{g_3^2}{16\,\pi^2}\left[\sum_i \log\left(\frac{m_{\widetilde{g}_i}^2}{m_{D3}^2}\right) + \frac{1}{4}\log\left(\frac{m_{\phi_3}^2}{m_{D3}^2}\right)\right]\right\} \tag{2.24}$$

where the positive (negative) contribution occurs when running from the UV (Infrared (IR)) to the IR (UV) and all parameters are evaluated at the renomalisation scale $\mu(m_{D3}) = m_{D3}$.

Quark masses: We do not implement the quark mass threshold corrections from the gluinos and sgluons. To correctly do this would be quite technical and we anticipate that the overall impact on the areas we are interested in (such as the SUSY spectrum, EWSB and tuning) should be minimal; correction of this kind must be proportional to chiral symmetry breaking and since the quarks are essentially massless at m_{D3} the remaining correction is proportional to the Majorana gluino mass. For the top quark [86]

$$\delta m_{\mathrm{t}} = -\frac{g_3^2}{12\,\pi^2}\sin(\theta_{\widetilde{\mathrm{t}}})\,M_3\left[B_0(0, M_3, m_{\widetilde{\mathrm{t}}_1}) - B_0(0, M_3, m_{\widetilde{\mathrm{t}}_2})\right], \tag{2.25}$$

where $\theta_{\widetilde{\mathrm{t}}}$ is the stop mixing angle. This will alter the yukawa couplings in the UV and hence only affect the running of UV parameters that depend on the yukawa couplings. We expect the low energy physics to be largely unaffected however, and instead we include the loop contributions to the quark masses from gluinos and sgluons at m_{Z} and m_{SUSY}. By doing this we making a systematic error proportional to $(16\pi^2)^{-2} \times \log(m_{D3}/m_{\mathrm{SUSY}}) \times \log(m_{GUT}/m_{\mathrm{SUSY}}) \lesssim 0.1\%$.

[6] There is no contribution from $\Pi_{\widetilde{q}}^{\sigma_3}(m_{\widetilde{q}})$ as the σ_3 coupling to squarks is zero.

Sparticle	Lower Mass Limit at 95 % CL (GeV)	Reference
Neutralino (stable)	45.5	[3]
Neutralino (unstable)	96.8	[97, 98]
Sneutrino	41	[3]
Chargino	103.5	[99, 100]
Sleptons	100.2	[101]

Table 2. The strongest most model independent non-hadron collider limits on LOSP and NLSP masses. The lightest neutralino $\widetilde{\chi}_1^0$ is assumed to be bino-like, and allowed to decay to the gravitino $\tilde{G}$ in GMSB, emitting a photon.

3 Numerical setup

We use the standard top-down approach where we fix a set of UV boundary conditions at either $m_{\rm GUT}$ in the CMSSM or $m_{\rm Mess}$ in CGGM. The low energy spectrum is found through RG evolution, and then the corresponding flavour observables and fine tuning are calculated.

To achieve this, we have used the Mathematica package `SARAH` 4.3.0 [89–94] to generate source code for the spectrum generator `SPheno` 3.3.2 [95, 96]. `SPheno` solves the RG equations taking into account the presence of the Dirac gluino at one and two loops. This program then calculates the one loop masses for all particles in the model, the branching ratios for all kinematically allowed two body decays and the branching ratios for three body decays involving intermediate W and Z bosons.

The UV boundary conditions discussed in section 2.2.2 are implemented we can solve the EWSB minimisation conditions for μ and B_μ. We only study the $\mu > 0$ case in order to maximise the effect from stop mixing upon the Higgs sector. The `SPheno` code has been modified to include an intermediate step in RG running where the gluino and its corresponding scalar degrees of freedom are integrated out at the gluino mass. This implements the EWSB mechanism of supersoft models outlined in [16]. The masses for the gluino and the real sgluon are calculated at the this intermediate scale instead of $m_{\rm SUSY}$. A schematic of this algorithm is shown in fig. 3.

4 Spectra

On each of the parameter space plots we include the relevant limits on SUSY particle masses. As production cross section is suppressed for all SUSY particles in models with Dirac gluinos (shown in section 5), we take only the strongest most model independent limits available set by lepton colliders, outlined in table 2. For the CMSSM, the stable neutralino limit is applied, whereas for CGGM the unstable limit is used instead. The red, purple and green solid lines indicate the limit on the slepton, neutralino and sneutrino masses, and the blue dashed line indicates the limit on the chargino masses.

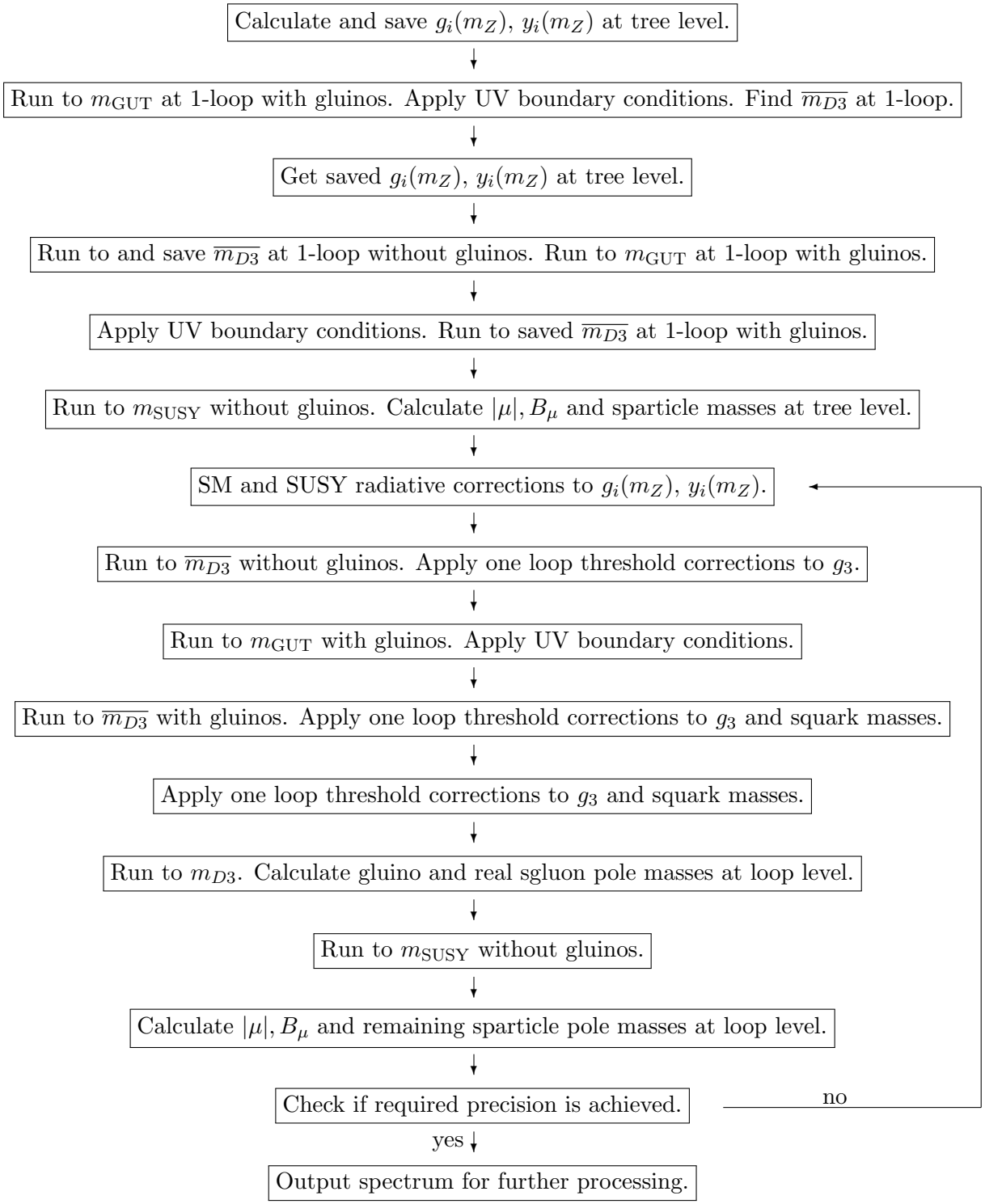
Calculate and save $g_i(m_Z)$, $y_i(m_Z)$ at tree level.
Run to $m_{\rm GUT}$ at 1-loop with gluinos. Apply UV boundary conditions. Find $\overline{m_{D3}}$ at 1-loop.
Get saved $g_i(m_Z)$, $y_i(m_Z)$ at tree level.
Run to and save $\overline{m_{D3}}$ at 1-loop without gluinos. Run to $m_{\rm GUT}$ at 1-loop with gluinos.
Apply UV boundary conditions. Run to saved $\overline{m_{D3}}$ at 1-loop with gluinos.
Run to $m_{\rm SUSY}$ without gluinos. Calculate $|\mu|, B_\mu$ and sparticle masses at tree level.
SM and SUSY radiative corrections to $g_i(m_Z)$, $y_i(m_Z)$.
Run to $\overline{m_{D3}}$ without gluinos. Apply one loop threshold corrections to g_3.
Run to $m_{\rm GUT}$ with gluinos. Apply UV boundary conditions.
Run to $\overline{m_{D3}}$ with gluinos. Apply one loop threshold corrections to g_3 and squark masses.
Apply one loop threshold corrections to g_3 and squark masses.
Run to m_{D3}. Calculate gluino and real sgluon pole masses at loop level.
Run to $m_{\rm SUSY}$ without gluinos.
Calculate $|\mu|, B_\mu$ and remaining sparticle pole masses at loop level.
Check if required precision is achieved.
no
yes
Output spectrum for further processing.

Figure 3. Algorithm used to calculate the spectrum. Adapted from fig. 1 in [95]. Note that apart from where it explicitly states running to a saved value of $\overline{m_{D3}}$, the scale is found by requiring a solution to $\mu(m_{D3}) = m_{D3}$. This typically updates with each iteration since it depends on the behaviour of g_3 whose running is determined by the location of $\overline{m_{D3}}$.

Points below and to the left of these lines are excluded at the 95% Confidence Level (CL). We will present three types of graphs in the $(m_0, M_{1/2})$ and (Λ_G, Λ_S) planes to illustrate the similarities and differences between spectra:

- Gradients of Higgs boson masses with contours of the parameters entering into the one loop Higgs mass approximation in eq. 1.1.
- LOSP species with mass contours of the typical candidates.
- Next to Lightest Ordinary Supersymmetric Particle (NLOSP) species.

In the MSSM the two loop contribution from gluinos gives quite a significant contribution. Because the two loop Higgs mass has not yet been computed in the presence of a Dirac gluino, we will not impose achieving the correct value as a strict requirement, as we would be incorrectly ruling out viable regions of parameter space. Although the full calculation will be completed in the future [102], the effective field theory framework used here requires a different approach. At the gluino scale, one would need to match the theory onto a theory with broken SUSY with RGEs. This requires removing the approximation that e.g. the stop-Higgs quartic coupling and the Higgs-top yukawa terms remain equal along the RG flow

$$y_t \, \bar{t} \, q \cdot H_u \longleftrightarrow |y_t|^2 |\widetilde{t}|^2 |H_u|^2.$$

Instead, the coefficients of the operators $\bar{t} \, q \cdot H_u$ and $|\widetilde{t}|^2 |H_u|^2$ should have different RGEs below the Dirac gluino mass. After applying threshold corrections to each coupling, flowing down from the gluino mass to the SUSY scale would then correctly include the two loop contributions to the Higgs mass with gluino integrated out. With the new non-SUSY RGE calculators becoming available [93, 103], the possibility to correctly incorporate these kinds of particle threshold effects into spectrum generators in the future is a very interesting possibility

Only a subset of the scans are presented in the body of the text. The remaining parameter configurations can be found in appendix A. The generic dependence of the spectrum and low energy parameters on the UV boundary conditions can be inferred by analysing the cases we present.

We first present the comparison of the CMSSM with and without a Dirac gluino. We scan

$$0 \text{ TeV} \leq m_0 \leq 6 \text{ TeV} \qquad\qquad 0 \text{ TeV} \leq M_{1/2} \leq 4 \text{ TeV} \tag{4.1}$$

and take a moderate and large $t_\beta = 10, 25$. In the presence of a Dirac gluino, we set $m_{D3}(m_{\rm GUT}) = 5, 7.5, 10$ TeV which, due to RG running, lead to a significant spread of physical Dirac gluino masses that can be estimated using

$$\overline{m_{D3}}|_{\rm approx} = \left[m_{D3}(\Lambda) \, \Lambda^{\frac{3 \, g_3^2(\Lambda)}{8 \, \pi^2}} \right]^{\frac{1}{1 + \frac{3 \, g_3^2(\Lambda)}{8 \, \pi^2}}} \tag{4.2}$$

where Λ can be any scale, but is most conveniently taken as the UV scale.

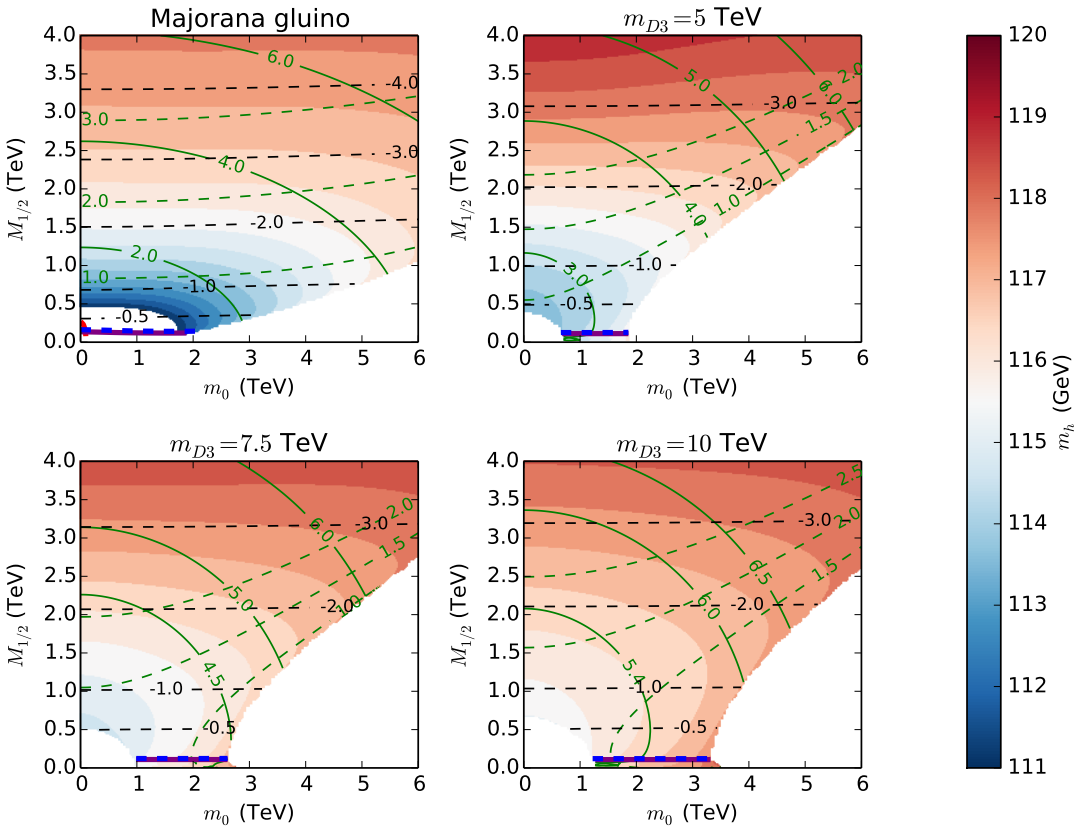

Figure 4. Higgs sector parameters in the CMSSM with $t_\beta = 10$ and m_{D3} fixed as indicated. The gradient indicates the Higgs mass. The black dashed, green dashed and green solid lines are contours of $a_{\rm t}(m_{\rm SUSY})$, $\mu(m_{\rm SUSY})$, and $m_{\rm SUSY}$ respectively. All contours unless otherwise specified are in TeV.

The first thing to note is that there is a new region of parameter space in the $(m_0, M_{1/2})$ plane opening up for very low $M_{1/2}$ but non-zero m_0 in the presence of a Dirac gluino. This region isn't populated in the MSSM due to an absence of EWSB when $m^2_{\rm H_u}$ isn't pushed negative enough for a positive $|\mu|^2$ solution; at this point in parameter space in the CMSSM one needs extra logs from M_3 to push the squark mass up along the RG trajectory. In the case of a Dirac gluino, one can essentially ignore the need for a Majorana gluino mass, as the threshold correction on its own is enough to lift the squark mass in the IR, triggering EWSB for even zero $M_{1/2}$. Here however, the Large Electron Positron Collider (LEP) bound on the chargino mass becomes important, putting an experimental lower limit on $M_{1/2}$ of $\mathcal{O}(100)$ GeV.

Higgs: In figures 4 and 16 we show the Higgs mass and the parameters entering the one loop Higgs mass formula in eq. 1.1. Even though we are taking $A_0(m_{\rm GUT}) = 0$, a non-zero value is

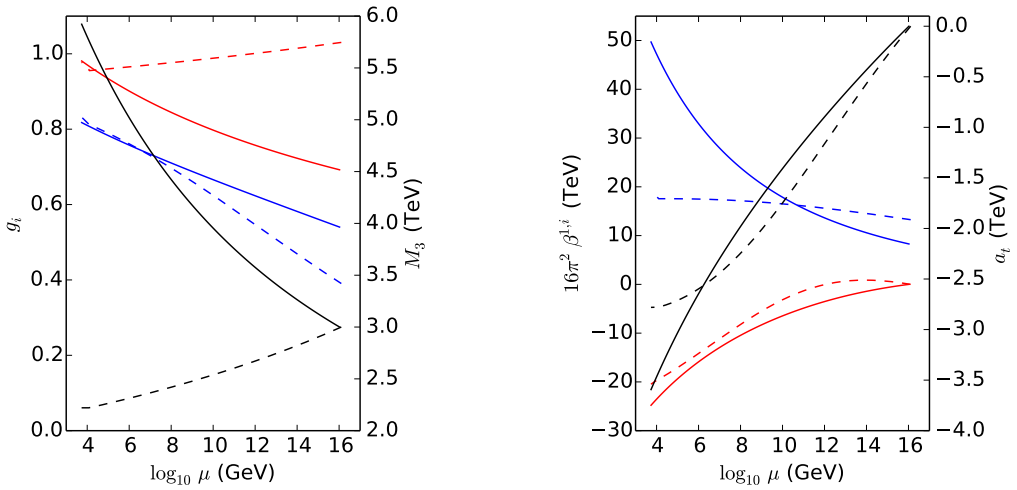

Figure 5. RG evolution of dominant parameters contributing to the running of $a_{\rm t}$ in the CMSSM with $m_0 = 4.5$ TeV, $M_{1/2} = 4$ TeV, $m_{D3} = 5$ TeV and $t_\beta = 25$. Solid lines correspond to the CMSSM and dashed lines correspond to the CMSSM supplemented with a Dirac gluino. **Left**: The blue, red and black lines show the evolution of $y_{\rm t}$, g_3 and M_3 respectively. **Right**: The blue, red and black lines show the evolution of $\frac{32}{3}\,y_{\rm t}\,g_3^2\,M_3$, $a_{\rm t}\left(18\,|y_{\rm t}|^2 - \frac{16}{3}\,g_3^2\right)$ and $a_{\rm t}$ respectively.

generated by running. In the large y_t limit (see eq. B.28 for the complete expression)

$$16\pi^2\beta^{(1)}_{a_{\rm t}} \supset a_{\rm t}\left[18\,|y_{\rm t}|^2 + \frac{16}{3}\,\left(\theta_{\widetilde{\rm g}} - 2\right)\,g_3^2\right] + \frac{32}{3}\,y_{\rm t}\,g_3^2\,M_3\,\theta_{\widetilde{\rm g}}, \tag{4.3}$$

where

$$\theta_{\widetilde{\rm g}} = 1 \quad \text{if} \quad \mu \geq \overline{m_{D3}}, \qquad\qquad \theta_{\widetilde{\rm g}} = 0 \quad \text{if} \quad \mu < \overline{m_{D3}}. \tag{4.4}$$

with the precise definitions given in appendix B. In the CMSSM without a gluino, $\theta_{\widetilde{\rm g}} = 1$ always in eq. 4.3. Note that we do not observe the more negative values of $a_{\rm t}$ in the presence of the gluino that were found in [104]. This can be understood by considering the running of the Majorana gluino mass in the presence of a Dirac gluino

$$16\pi^2\beta^{(1)}_{M_3} = -6\,g_3^2\,M_3 \qquad \text{MSSM} \tag{4.5}$$

$$16\pi^2\beta^{(1)}_{M_3} = 0 \qquad \text{MSSM with Dirac Gluino.} \tag{4.6}$$

Because we are taking $a_{\rm t}(m_{\rm GUT}) = 0$ then the gluino term dominates for most of the flow, and in the CMSSM, this term becomes larger that in the CMSSM with a Dirac gluino as demonstrated in fig. 5. The contours of $m_{\rm SUSY}$ in the presence of a Dirac gluino are increased to the minimum squark mass possible in the model (i.e. determined by eq. 1.5). For large values of m_0 and $M_{1/2}$ contours of $m_{\rm SUSY}$ across the different models approach each other.

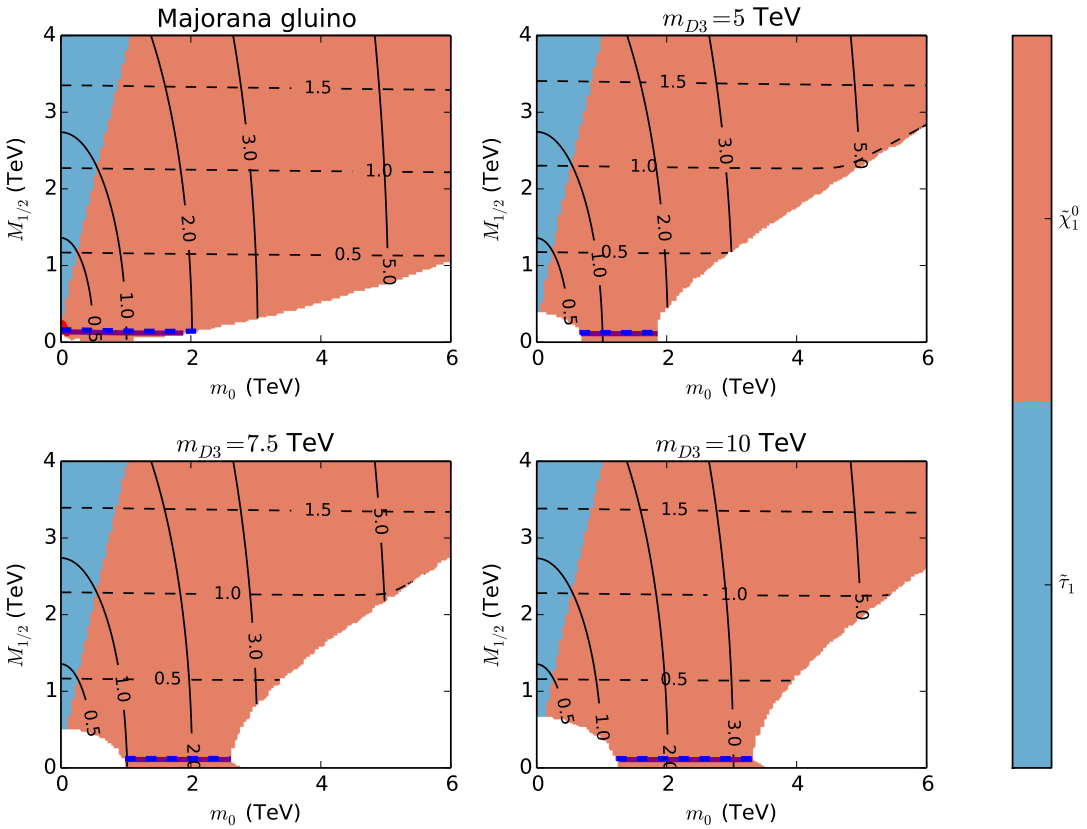

Figure 6. LOSP species in the CMSSM with $t_\beta = 10$ and m_{D3} fixed as indicated. The black dashed and black solid lines are contours of lightest neutralino mass $m_{\tilde{\chi}_1^0}$ and stau mass $m_{\tilde{\tau}}$ in TeV.

The μ parameter is seen to increase with increasing Dirac gluino mass. This can be understood by considering the EWSB conditions in the large t_β limit

$$|\mu|^2 = -m_{\mathrm{H}_u}^2 - \frac{m_{\mathrm{Z}}^2}{2} + \mathcal{O}(t_\beta^{-2}). \tag{4.7}$$

$m_{\mathrm{H}_u}^2$ is driven negative by the squark soft scalar masses

$$16\pi^2 \beta^{(1)}_{m_{\mathrm{H}_u}^2} \supset 6\,|y_{\mathrm{t}}|^2 \left(m_q^2 + m_{\mathrm{t}}^2\right) \tag{4.8}$$

which are in turn determined by the Dirac gluino mass through eq. 1.5. The values of μ in the MSSM for moderate $(m_0, M_{1/2})$ are actually lower with a Dirac gluino than without. Considering the RG equation for y_{t}

$$16\pi^2 \beta^{(1)}_{y_{\mathrm{t}}} \supset \frac{8}{3}(\theta_{\tilde{\mathrm{g}}} - 3)\, g_3^2. \tag{4.9}$$

This term causes y_{t} to decrease in the flow from the IR to the UV. In the MSSM, the strong

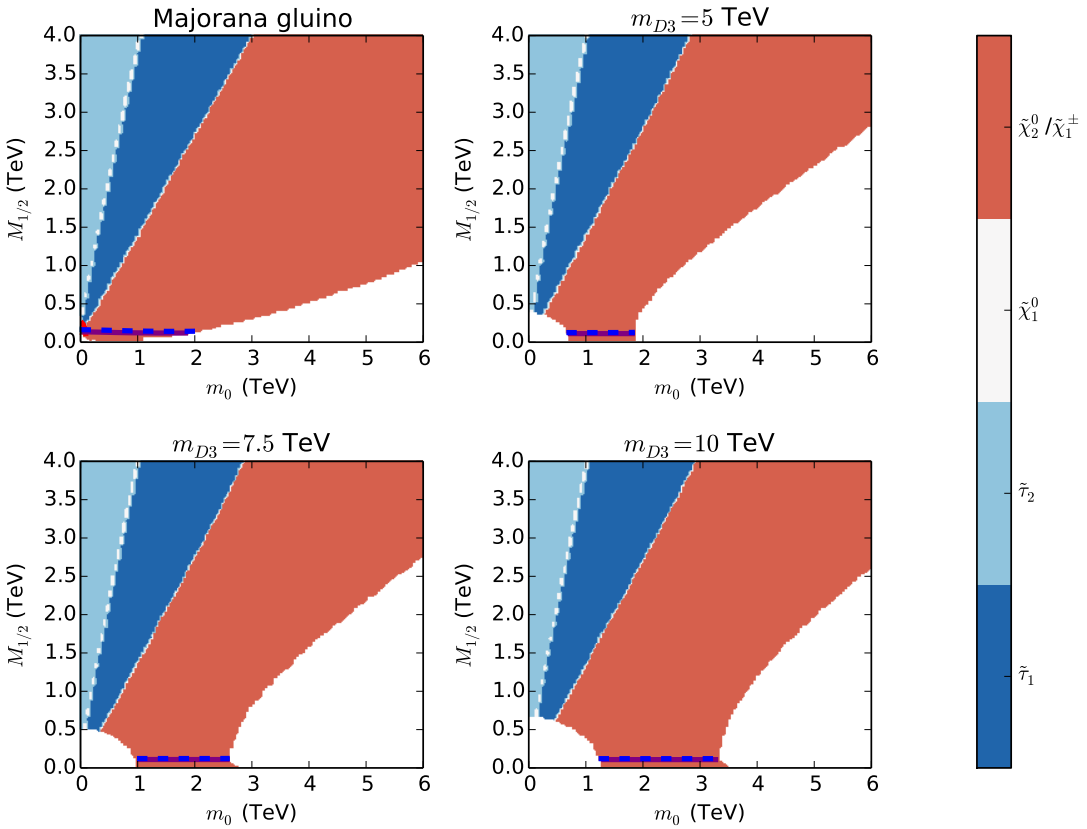

Figure 7. NLOSP species in the CMSSM with $t_\beta = 10$ and m_{D3} fixed as indicated.

interactions retain asymptotic freedom, whereas with a Dirac gluino present, g_3 remains roughly constant along the entire flow. In the Dirac gluino case, this causes y_t to decrease much more rapidly, and so the the integrated term of eq. 4.8 with a Dirac gluino than without.

The lower limit on squark masses translates into a lower limit on the Higgs mass. Apart from at low $(m_0, M_{1/2})$ where we get a separation between the strong and electroweak sectors it is difficult to distinguish the CMSSM with and without a gluino. The presence of a Dirac gluino allows us, for a given Higgs mass, to realise a lighter electroweak scalar spectrum for low $(m_0, M_{1/2})$.

LOSP: The LOSP candidate in the presence of a Dirac gluino is essentially unchanged in the CMSSM. The blue regions in figs. 6 and 17 have a charged stau $\widetilde{\tau}_1$ as the LOSP and so are excluded. The remainder of the parameter space is entirely bino-like neutralino $\widetilde{\chi}_1^0$ LOSP, a good dark matter candidate.

NLOSP: The NLOSP candidate in the presence of a Dirac gluino is similarly relatively unchanged essentially when compared to the Majorana case. The light blue regions in figs. 7 and 18 have the second lightest stau $\widetilde{\tau}_2$ as the NLOSP but are excluded as the corresponding region has a

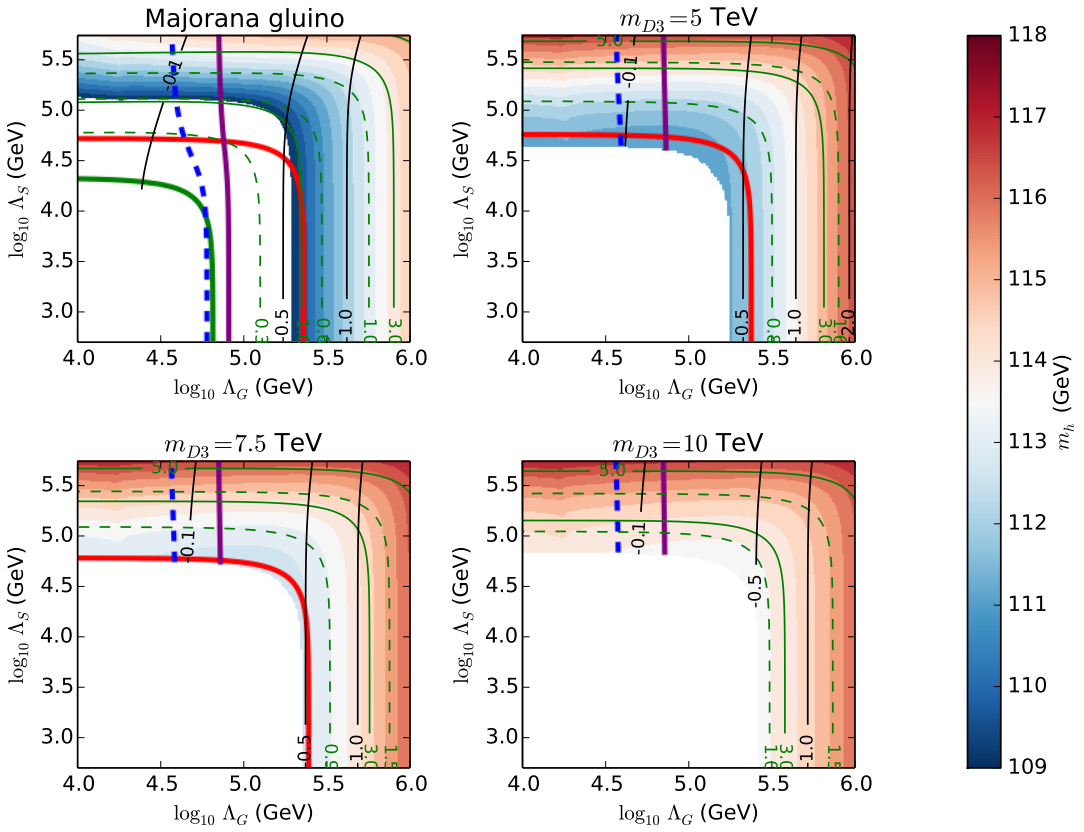

Figure 8. Higgs sector parameters in CGGM with $t_\beta = 10$, $m_{\rm Mess} = 10^7$ GeV and m_{D3} fixed as indicated. The gradient indicates the Higgs mass. The black dashed, green dashed and green solid lines are contours of $a_{\rm t}(m_{\rm SUSY})$, $\mu(m_{\rm SUSY})$, and $m_{\rm SUSY}$ respectively. All contours unless otherwise specified are in TeV.

lightest stau $\widetilde{\tau}_1$ LOSP. The dark blue region has lightest stau $\widetilde{\tau}_1$ LOSP and leads to one lepton and $\not{E}_T$ or jets and $\not{E}_T$ in the final state, as does the red region with wino-like chargino $\widetilde{\chi}^\pm$ NLOSP. This chargino $\widetilde{\chi}^\pm$ is also coincident with the wino-like neutralino $\widetilde{\chi}^0_2$ which instead leads to either entirely $\not{E}_T$ in the final state or $\not{E}_T$ with either two leptons of opposite sign or a jet.

It is clear that nature of the light spectrum is largely unaffected by the presence of a Dirac gluino, except that it is now possible to raise the strongly interacting sector almost[7] independently of the electroweak sector, giving some freedom to aleviate the tension with results at hadron collider experiments to date.

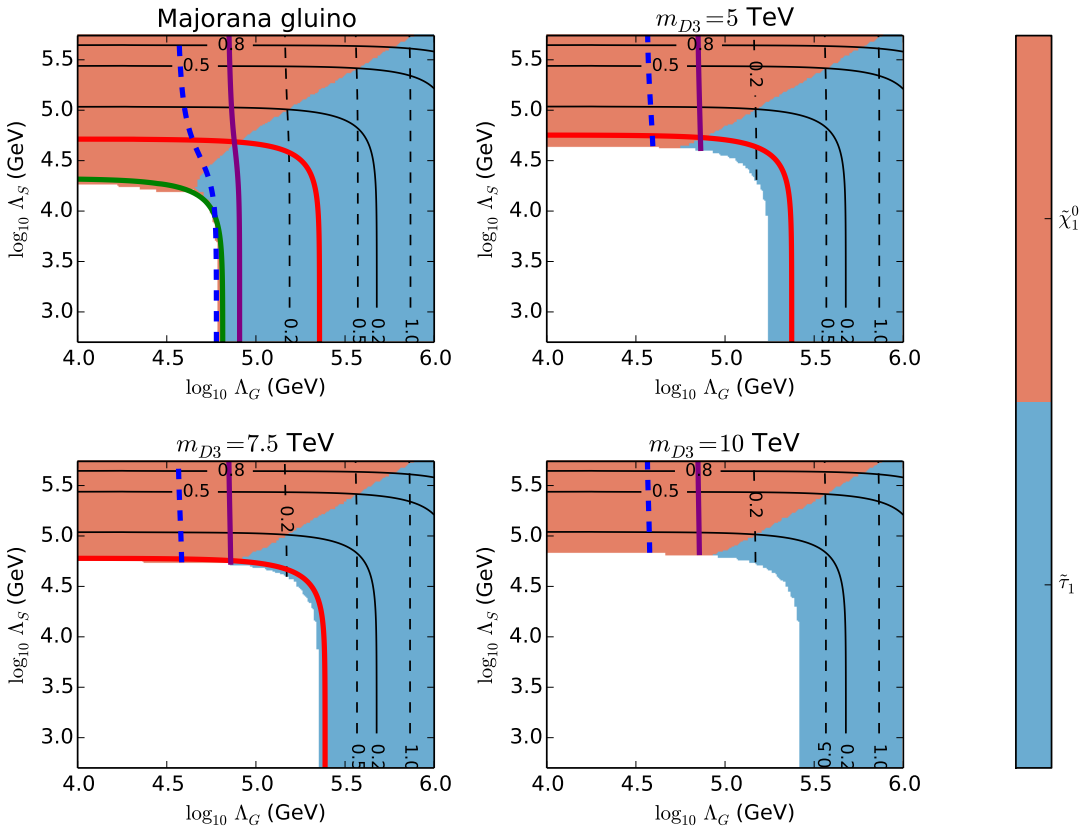

Figure 9. LOSP species in CGGM with $t_\beta = 10$, $m_{\rm Mess} = 10^7$ GeV and m_{D3} fixed as indicated. The black dashed and black solid lines are contours of lightest neutralino mass $m_{\widetilde{\chi}_1^0}$ and stau mass $m_{\widetilde{\tau}}$ in TeV.

4.1 Constrained General Gauge Mediation

We now present the comparison of CGGM with and without Dirac gluino. A recent comprehensive study of the parameter space of CGGM was done in [105]. We scan

$$10^3 \text{ GeV} \leq \Lambda_G \leq 10^7 \text{ GeV} \qquad 10^3 \text{ GeV} \leq \Lambda_S \leq 10^7 \text{ GeV} \tag{4.10}$$

whilst taking $t_\beta = 10, 25$ and again we again take $m_{D3}(m_{\rm GUT}) = 5, 7.5, 10$ TeV in the presence of a Dirac gluino. We take two messenger scales $m_{\rm Mess} = 10^7$ GeV and 10^{12} GeV to represent short and long periods of running.

The theoretically allowed parameter space is reduced by the presence of a Dirac gluino as is seen in fig. 9. Although viable EWSB is occurring, the the lightest stau $\widetilde{\tau}_1$ is being driven tachyonic for a larger portion of the parameter space. This is induced by the Dirac gluino much for much

[7] There will always arise terms proportional to $(16\,\pi^2)^{-1}\log(m_{D3}/m_{\rm SUSY})$, and there two loop sensitivity to the sgluon soft mass in eq. 2.6 present.

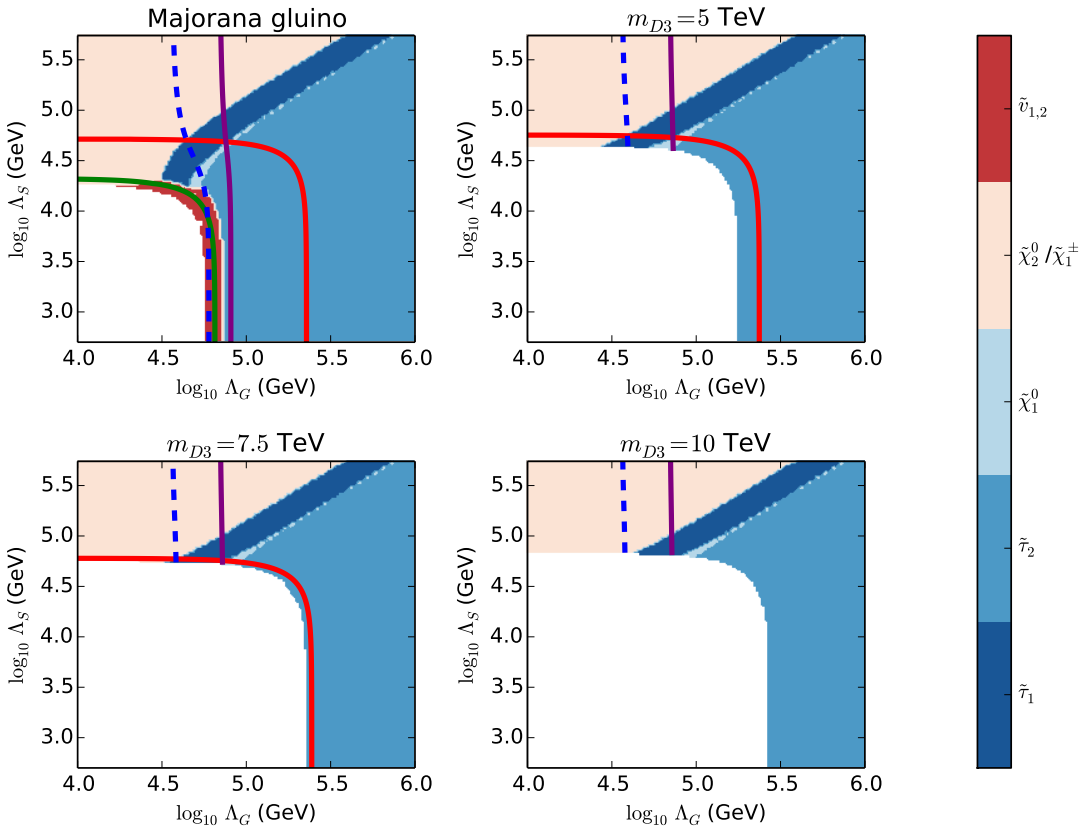

Figure 10. NLOSP species in CGGM with $t_\beta = 10$, $m_{\rm Mess} = 10^7$ GeV and m_{D3} fixed as indicated. The black dashed and black solid lines are contours of lightest neutralino mass $m_{\tilde{\chi}_1^0}$ and stau mass $m_{\tilde{\tau}}$ in TeV.

higher UV stau mass set by eq. 2.17. This is caused by larger values of $|\mu|^2$ for a given (Λ_G, Λ_S) by the threshold corrections at the Dirac gluino scale, driving the smallest eigenvalue of the stau mass matrix

$$m^2_{\tau,\rm mat} = \begin{pmatrix} m^2_{\ell_{3,3}} + D\,\text{terms} & v\,(a^*_\tau\, c_\beta - \mu\, y_\tau\, s_\beta) \\ v\,(a_\tau c_\beta - \mu^*\, y_\tau\, s_\beta) & m^2_{\rm e_{3,3}} + D\,\text{terms} \end{pmatrix} \tag{4.11}$$

negative.

Higgs: In figures 8, 20, 21 and 22 we show the Higgs mass and the parameters entering the one loop Higgs mass formula in eq. 1.1. The characteristic properties here are essentially unchanged from the CMSSM counterpart as we have only considered the CMSSM case $A_0 = 0$.

LOSP: The LOSP candidates in CGGM with and without a Dirac gluino are similar to those of the CMSSM as can be seen in figs. 9, 23, 24 and 25. The difference here is that the blue regions that correspond to stau $\tilde{\tau}_1$ LOSP are now viable as the Lightest Supersymmetric Particle (LSP) in these models is the gravitino $\tilde{G}$. The stau can either be long lives produce a missing energy

signature or it can undergo the decay $\widetilde{\tau} \to \tilde{G}\,\tau$ inside the detector depending on its mass. If it does decay it will lead to one lepton and $\not{E}_T$ or jets and $\not{E}_T$. The remainder of the parameter space is has entirely bino-like neutralino $\widetilde{\chi}_1^0$ LOSP. This could appear a dark matter candidate on collider time-scales, but it may also undergo the decay $\widetilde{\chi}_1^0 \to \tilde{G}\,\gamma$. This decay is responsible for the stronger lower bounds on the neutralino mass $m_{\widetilde{\chi}_1^0}$ in CGGM.

NLOSP: In CGGM we have a sneutrino NLOSP candiate in addition to those found in the CMSSM. These are shown in figs. 10, 26, 27 and 28. This only happens without a Dirac gluino however, as in the region where a sneutrino $\widetilde{\nu}$ NLOSP would be achieved, the lightest stau $\widetilde{\tau}_1$ has already been pushed tachyonic. The region with sneutrino $\widetilde{\nu}$ NLOSP is ruled out by collider searches. The remaining NLOSP candidates have the same decays as seen in the CMSSM except that they may be accompanied by an additional photon in the final state.

4.2 Overview

Overall, one sees that when each the CMSSM and CGGM are supplemented with a Dirac gluino, very little changes in the electroweak spectrum. This is of course by construction since the effective theory is essentially the MSSM without a gluino. The Higgs mass however, is raised across the whole parameter space and can be made largely independent of $(m_0, M_{1/2})$ or (Λ_G, Λ_S) at sufficiently low values of these parameters. Note that this is different to having non-universal scalar masses and gaugino masses, since giving a large mass to squarks and or gluinos in the UV will lead to a very large value for μ, giving very heavy Higgsinos and non-SM-like Higgses as well as being accompanied by considerable fine tuning. The Wino mass will also be lifted along the RG flow since

$$(16\,\pi^2)^2 \beta_{M_2} \supset 48\,(g_2\,g_3)^3\,M_3 \tag{4.12}$$

causes M_2 to increase by ~ 500 GeV for a 10 TeV Majorana gluino. A characteristic plot of the spectra in the CMSSM with and without a Dirac gluino is shown in fig. 11. Since the overall result is a light set of electroweak particles with the neutralino as the LOSP, the detailed phenomenology is expected to be very similar to that of the *well-tempered neutralino* [106, 107]. One could also take all of the orderings of our electroweak states and map them on to the analysis in [108].

5 Cross sections

Here we present the Leading Order (LO) cross sections at 8 and 13 TeV LHC with and without a Dirac gluino in the CMSSM. We fixed $t_\beta = 10$, $m_0 = 200\,\text{GeV}$ and scanned over

$$M_{1/2} \in [200, 1600]\,\text{GeV} \qquad \text{CMSSM}$$
$$M_{1/2} = 400,\ m_{D3} \in [500, 5000]\,\text{GeV} \qquad \text{CMSSM with Dirac gluino}$$

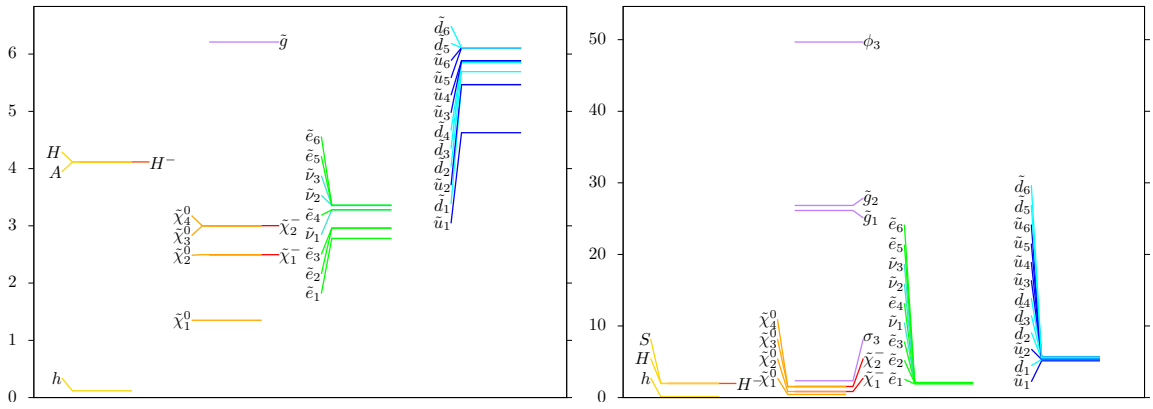

Figure 11. Sparticle spectra the CMSSM (left) and the CMSSM with a Dirac gluino (right) for the benchmark points in table 5

leading to the spread of squark masses shown in fig. 12. For disquark production, we can see that there is suppression in the Dirac gluino case of approximately two orders of magnitude. Note that this is only true for disquark production, but is not true for squark-antisquark production as the dominant diagrams required for these processes do not involve the Majorana nature of gluinos as was discussed in [44, 55].

Digluino production is only displayed for the CMSSM without a Dirac gluino, since for the parameter space displayed, di-gluino production is kinematically forbidden in the Dirac gluino case. Similarly, disgluon production is kinematically forbidden. The dipseudosgluon production rate, however, is relatively high due to its light mass and its large $\mathrm{SU}(3)_\mathrm{C}$ charge. Since this particle is the lightest strongly interacting sparticle and is CP-odd, it has no particles to decay into [8] in the CMSSM this will be stable particle. The pseudosgluon could possibly form colour singlet bound states in an analogous way to the gluon-gluino bound states R_0 in [109, 110]. It was also shown in [111] that until the non-perturbative aspects of $\widetilde{\mathrm{g}}\,\widetilde{\mathrm{g}}$ in the early universe production are understood, is is not possible to constrain gluino LOSP as a dark matter candidate. We leave this curious investigation for future study. In any case, the LOSP will be the dominant dark matter component as many more of them are expected to be produced in the early universe. Direct searches for dark matter should not be an issue as σ_3 only interacts strongy, and the $\mathrm{SU}(3)_\mathrm{C}$ charge of the nucleus is zero. It is also simple to allow both the sgluon and the pseudosgluon undergo the loop decay via squarks studied in [63] by taking m_{D3} complex.

Finally we display the product of branching ratios approximation for the cross section for two

[8] This is the $\phi_O = 0$ case of [63] since we have a pure pseudoscalar in our setup and therefore no $\sigma\,\tilde{q}\,\tilde{q}^\dagger$ couplings that allow the loop decay to gluons.

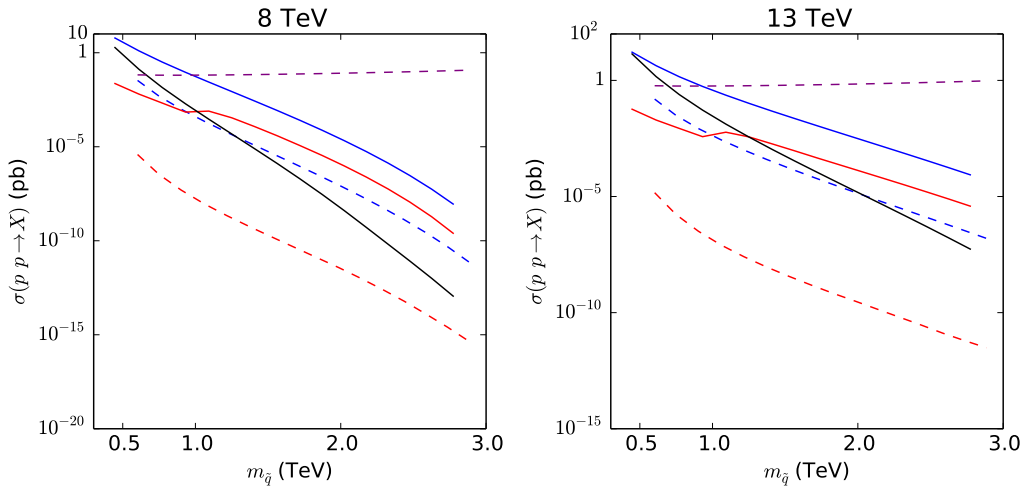

Figure 12. LO cross sections for various processes at 8 TeV (left) and 13 TeV (right) LHC. The solid and dashed lines indicate cross sections in the CMSSM with and without a Dirac gluino respectively. The blue, black and purple lines indicate total disquark ($\widetilde{q}_i\,\widetilde{q}_j$), digluino ($\widetilde{g}_i\,\widetilde{g}_j$) dipseudosgluon production ($\sigma_3\,\sigma_3$). The red lines indicate cross section $\times$ branching ratio for processes beginning with disquark production and ending up with two jets, two same sign leptons and $\not{E}_T$ in the final state. The cross sections were calculated using `Madgraph5_aMC@NLO` using the MSTW2008lo68cl PDF set. All two and three body branching ratios were calculated using `SPheno` 3.3.2.

jets, two same sign leptons and missing energy

$$2 \times \Big[\sum_{i \leq j} \sigma(\mathrm{p\,p} \to \widetilde{\mathrm{u}}_i\,\widetilde{\mathrm{u}}_j) \times \mathrm{Br}(\widetilde{\mathrm{u}}_i \to \mathrm{jet} + \ell^+ + \not{E}) \times \mathrm{Br}(\widetilde{\mathrm{u}}_j \to \mathrm{jet} + \ell^+ + \not{E}) + \sum_{i \leq j} \sigma(\mathrm{p\,p} \to \widetilde{\mathrm{d}}_i\,\widetilde{\mathrm{d}}_j) \times \mathrm{Br}(\widetilde{\mathrm{d}}_i \to \mathrm{jet} + \ell^- + \not{E}) \times \mathrm{Br}(\widetilde{\mathrm{d}}_j \to \mathrm{jet} + \ell^- + \not{E}) \Big],$$

where the squark branching ratios are given by all possible combinations of kinematically allowed decays leading to one jet, one lepton and missing energy

$$\mathrm{Br}(\widetilde{\mathrm{u}}_i \to \mathrm{jet} + \ell^+ + \not{E}) \sim \mathrm{Br}(\widetilde{\mathrm{u}}_i \to \mathrm{d}\,\widetilde{\chi}_1^+) \times \mathrm{Br}(\widetilde{\chi}_1^+ \to \ell^+\,\nu\,\widetilde{\chi}_1^0) + \cdots . \tag{5.1}$$

Although this approximation misses effects coming from off-shell intermediate sparticles in the decay chain that increase the cross section $\times$ branching ratio, it can still serve as an indicator of what to expect if one simulated the high multiplicity final states fully. All branching ratios are calculated as a function of the parameter space scanned by `SPheno`. All other branching ratios are SM branching ratios which can are given in table 3. All decay products in the chain considered are displayed in table 4. Whilst the Majorana case still allows a number of events visible at the LHC given an integrated luminosity of 23.26 fb^{-1} such that the same sign lepton analyses [112] are sensitive in the direct squark (via sleptons) models, the case with a Dirac gluino is far beyond producing any same

Decaying particle	Decay products	Branching fraction
Z	invisible	0.2000 ± 0.0006
W^+	$\mathrm{e}^+ \nu_\mathrm{e}$	0.1075 ± 0.0013
	$\mu^+ \nu_\mu$	0.1057 ± 0.0015
	$\tau^+ \nu_\tau$	0.1125 ± 0.0020
τ^+	$\overline{\nu}_\tau \mathrm{e}^+ \nu_\mathrm{e}$	0.1783 ± 0.0004
	$\overline{\nu}_\tau \mu^+ \nu_\mu$	0.1741 ± 0.0004
t^-	$\mathrm{W}^+ \mathrm{b}$	0.91 ± 0.04

Table 3. SM branching ratios used in calculation of branching ratios $\times$ cross sections. All are the world averages taken from [3].

Particle	Relevant Decay Products
$\widetilde{\mathrm{u}}_{1,\ldots,6}$	$\mathrm{d}_{1,2,3}\, \widetilde{\chi}^+_{1,2}$
$\widetilde{\mathrm{d}}_{1,\ldots,6}$	$\mathrm{u}_{1,2}\, \widetilde{\chi}^-_{1,2}$
$\widetilde{\chi}^+_2$	$\mathrm{e}^+_{1,\ldots,3}\, \widetilde{\nu}_{1,2,3}$; $\nu_{1,2,3}\, \widetilde{\mathrm{e}}^+_{1,\ldots,6}$; $\mathrm{W}^+\, \widetilde{\chi}^0_{1,2}$; $\mathrm{Z}\, \widetilde{\chi}^+_1$
$\widetilde{\chi}^+_1$	$\mathrm{e}^+_{1,\ldots,3}\, \widetilde{\nu}_{1,2,3}$; $\nu_{1,2,3}\, \widetilde{\mathrm{e}}^+_{1,\ldots,6}$; $\mathrm{W}^+\, \widetilde{\chi}^0_{1,2}$
$\widetilde{\chi}^0_2$	$\mathrm{Z}\, \widetilde{\chi}^0_1$
$\widetilde{\mathrm{e}}^-_{1,\ldots,6}$	$\mathrm{e}^-_{1,\ldots,3}\, \widetilde{\chi}^0_{1,2}$; $\nu_{1,\ldots,3}\, \widetilde{\chi}^+_1$
$\widetilde{\nu}_{1,2,3}$	$\widetilde{\chi}^+_{1,2}\, \mathrm{e}^-_{1,2,3}$; $\widetilde{\chi}^0_{1,2}\, \nu_{1,2,3}$

Table 4. Decays considered for the squark to one jet, one lepton and $\not{E}_T$.

sign dileptons plus two jet events at the LHC with the current integrated luminosity. In addition, the Majorana digluino production is the dominant process leading to two same-sign dipletons with $\widetilde{\mathrm{g}} \to 2\,\mathrm{jets} + l^\pm + \not{E}$. This decay is simply absent with a heavy Dirac gluino.

One feature to note is that in the MSSM, there is a rise in the branching ratio $\times$ cross section for 1 TeV squarks in both the 8 and 13 TeV cases. This doesn't occur in with a Dirac gluino in the parameter space studied. In the MSSM, we are raising $M_{1/2}$ in order to raise the squark masses. As this happens, a gap between the lightest chargino and the sneutrino masses opens up. The chains that involving $\widetilde{\chi}^+_1 \to \widetilde{\nu}\, \ell^+$ account for 10 % of the overall branching ratio of a squark into one lepton, one jet and $\not{E}_T$ and only turn on once $M_{1/2}$ becomes large enough. In the Dirac gluino case this channel never opens up as we raise m_{D3} to raise the squark masses instead of $M_{1/2}$.

6 Electroweak symmetry breaking and fine tuning

As has already been indicated, EWSB in a model with a Dirac gluino is triggered much closer to the electroweak scale. As is well understood in most SUSY models, it is the stop mass (and at two loops a Majorana gluino mass) that causes this to happen. The same is true with a Dirac gluino. The difference here is that the stop mass can be negligible along the whole RG flow until the Dirac gluino mass is reached. The supersoft contribution from integrating out the gluino is applied to the

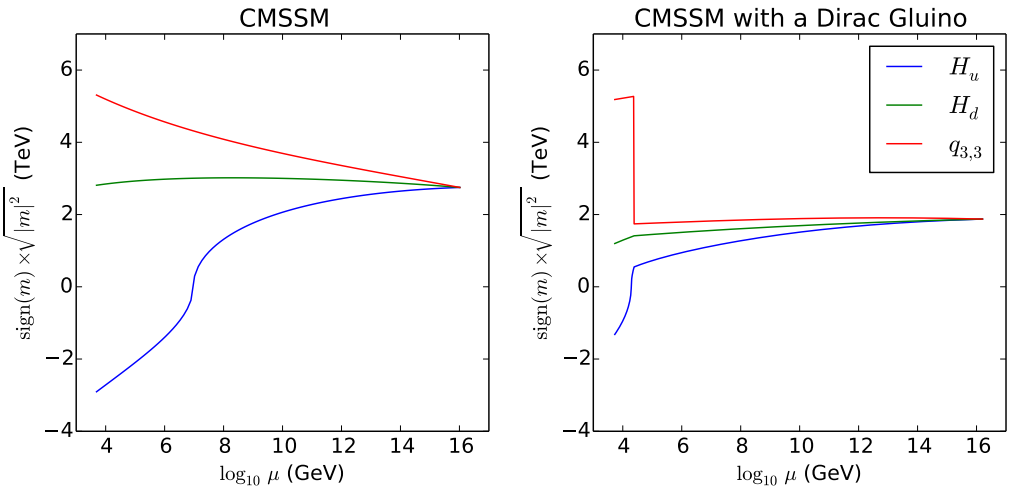

Figure 13. RGE of $m^2_{\mathrm{H}_u}$ (blue), $m^2_{\mathrm{H}_d}$ (green) and $m^2_{\tilde{q}_{3,3}}$ (red) from the GUT scale to the SUSY scale in the CMSSM (left) and the CMSSM with a Dirac gluino (right) for the benchmark points given in table 5

Model	m_0 (TeV)	$M_{1/2}$ (TeV)	m_{D3} (TeV)	$m_{\mathrm{h}}^{(1)}$ (GeV)	$m_{\mathrm{h}}^{(2)}$ (GeV)
CMSSM	2.750	3.000	N/A	118.1	127.4
CMSSM + DG	1.875	1.000	10.00	117.3	unknown

Table 5. Benchmark points for the RGE of parameters in the CMSSM with and without a Dirac gluino shown in figure 13.

squark masses, and they drive $m^2_{\mathrm{H}_u}$ negative for the remainder of the flow through its RG equation given in eq. 4.8. This effect is demonstrated in fig. 13. The upshot is that for a particularly large final squark mass, there is some control over how large $m^2_{\mathrm{H}_u}$ (and consequently $|\mu|^2$) is. In the Leading Log (LL) approximation at one loop we find

$$m^2_{\mathrm{H}_u}(m_{\mathrm{SUSY}}) = m^2_{\mathrm{H}_u}(m_{\mathrm{GUT}}) - \beta^{(1)}_{m^2_{\mathrm{H}_u}} \times \log\left(\frac{m_{\mathrm{GUT}}}{m_{\mathrm{SUSY}}}\right) \approx m_0^2\left[1 - \frac{3\,|y_{\mathrm{t}}|^2}{4\,\pi^2}\right] \times \log\left(\frac{m_{\mathrm{GUT}}}{m_0}\right) \quad (6.1)$$

in the CMSSM and

$$m^2_{\mathrm{H}_u}(m_{\mathrm{SUSY}}) \approx m_0^2 - (m_0^2 + m_q^2) \times \frac{3\,|y_{\mathrm{t}}|^2}{4\,\pi^2} \times \log\left(\frac{m_{D3}}{m_0 + m_q}\right) \quad (6.2)$$

in the CMSSM with a Dirac gluino where m_q^2 is given by eq. 1.5. Since $m^2_{\mathrm{H}_d}$ is so linked to the electroweak UV sensitivity, it is reasonable to expect that Dirac gluinos have the ability to reduce the amount of fine tuning in the presence of larger squark masses.

To quantify the impact this difference in triggering EWSB has on fine tuning, we take the

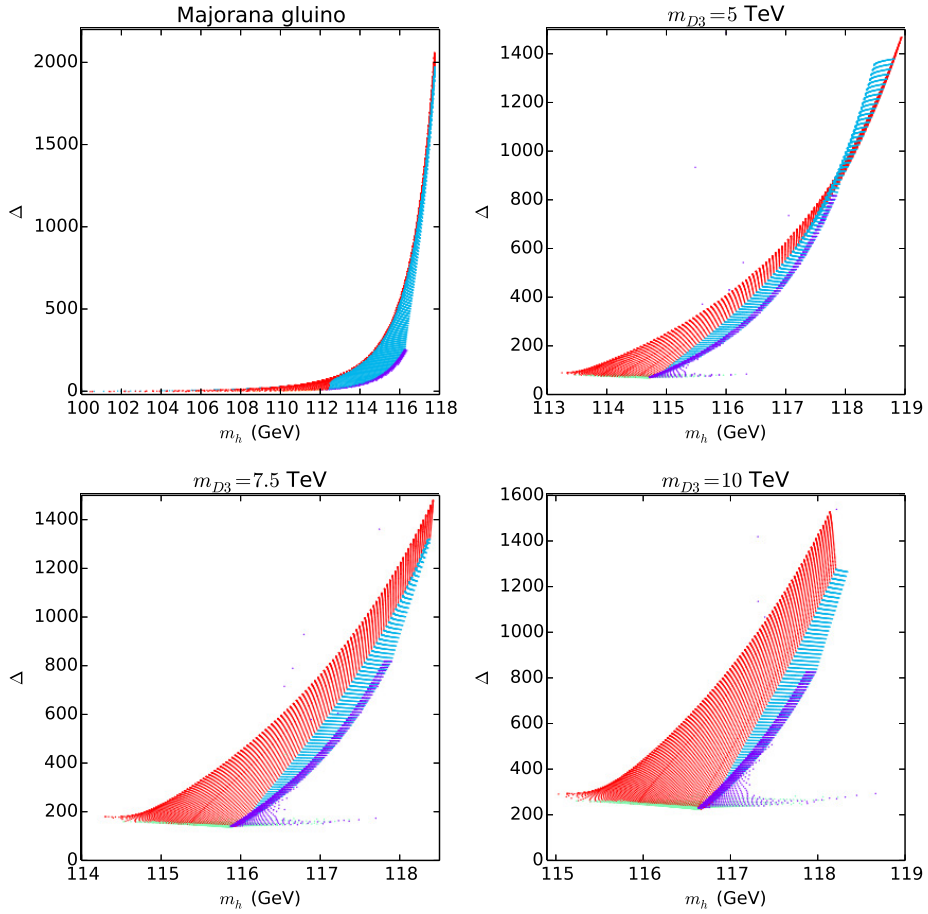

Figure 14. Fine tuning in the CMSSM with $t_\beta = 10$ and m_{D3} fixed as indicated. The red, purple, blue, and green regions correspond to μ, m_0, $M_{1/2}$ and m_{D3} as the dominant source of tuning.

measure Δ from [113]

$$\Delta \equiv \max\left[\mathrm{Abs}(\Delta_{\mathcal{O}})\right], \qquad \Delta_{\mathcal{O}} \equiv \frac{\partial \log v^2}{\partial \log \mathcal{O}} \tag{6.3}$$

such that Δ^{-1} gives a measure of how tuned the parameters $\mathcal{O}$ need to be tuned to achieve the observed EWSB scale v. This was calculated at the SUSY using the routines generated by `SARAH` modified to include the thresholds discussed in section 2.3.2 where appropriate. Since we are interested in UV sensitivity, we take the $\mathcal{O}$s as the set of parameters that would be fixed by the UV model at either the GUT scale in CMSSM or the messenger scale in CGGM. These are

$$\mathcal{O}|_{\mathrm{CMSSM}} \in \{m_0, M_{1/2}, \mu, B_\mu, m_{D3}\}, \quad \mathcal{O}|_{\mathrm{CGGM}} \in \{\Lambda_G, \Lambda_S, m_{\mathrm{Mess}}, \mu, B_\mu, m_{D3}\}. \tag{6.4}$$

The tuning in the CMSSM for the parameter space investigated in section 4 is shown in figs.

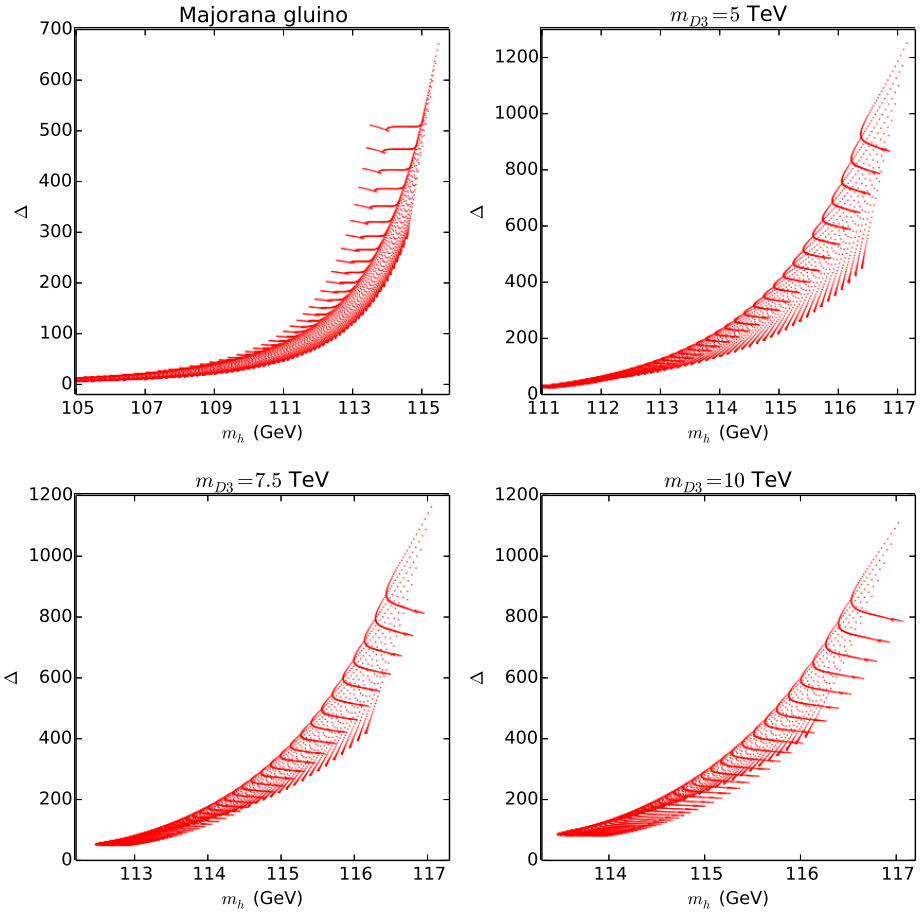

Figure 15. Fine tuning in the CMSSM with $t_\beta = 10$, $m_{\rm Mess} = 10^7$ GeV and m_{D3} fixed as indicated. The dominant source of tuning is entirely from the μ parameter.

14 and 19, and the tuning in CGGM is shown in figs. 15, 29, 30 and 31.

In the CMSSM and in CGGM it is observed that, for a given Higgs mass, new points exist with a reduction in fine tuning of typically up to a factor of two or three. In the CMSSM also a line of points opening up with moderately large Higgs mass mass but low ($\Delta \sim 200$) fine tuning. These points occur where the two terms in eq. 6.2 approximately cancel, giving low — $\mathcal{O}(0.5 - 1\,\text{TeV})$ — values of m_{H_u} and μ. The strip is very thin, since an increase in either m_0 or $M_{1/2}$ makes the right hand side become more positive in eq. 6.2, leaving no EWSB and decreasing m_0 or $M_{1/2}$ leads to a reduction in the Higgs mass. Unfortunately since these points are at very low values of $M_{1/2}$ that give rise to neutralino and chargino masses that are excluded by LEP.

The reduction in tuning in CGGM is less drastic than that seen in the CMSSM. This is because the mechanism reduces tuning through making logarithms smaller. Where in the CMSSM we have the log reduced $\log(m_{\rm GUT}/m_{\rm SUSY}) \to \log(m_{D3}/m_{\rm SUSY})$, whereas in CGGM this is only the factor $\log(m_{\rm Mess}/m_{\rm SUSY}) \to \log(m_{D3}/m_{\rm SUSY})$. Similarly, the reduction in fine tuning in CGGM is less

drastic in the case of the lower messenger scale than the higher messenger scale. In the CMSSM one can see the full range of UV parameters becoming the dominant source of tuning whereas in CGGM it is mainly the μ parameter across the entire space. However, in both the CMSSM and CGGM, all the underlying UV parameters considered do have associated tunings across the respective parameter spaces.

7 Conclusions

We have constructed a set of simple UV models with the supersoft mechanism introduced in [16] by extending the MSSM field content by only what was required to give the gluino a Dirac mass. We then performed the first implementation of the supersoft mechanism into a state of the art spectrum generator and carried out an analysis of the spectra, the production rates at LHC8 and LHC13, and fine tuning.

In the presence of a Dirac gluino, we find that it is possible to essentially decouple the strong sparticles without affecting the electroweak spectrum except that one finds that the pseudosgluon usually remains light and may even be a novel dark matter candidate by forming neutral bound states with other strongly interacting particles.

The decoupling of the strongly interacting sparticles from the electroweak sparticles has been shown to give a handle on the production cross sections at the LHC. Using a product of branching ratios approximation, we have shown that the Dirac gluino completely removes the same sign dilepton sign dilepton as a visible signature in current LHC data. A full simulation of the decay chain needs to be done to confirm this and it should also include the usually subdominant purely electroweak contributions to these events as these may now be important. It would also be interesting to investigate how many charginos and neutralinos are still produced in these cases with t-channel squarks.

Taking account the spectra and cross section suppression, we find that the final states of these models at the LHC are therefore altered in the following way:

- The number of events involving the Majorana gluino propagator are suppressed by roughly two orders of magnitude. This includes the same sign dilepton events.
- Events involving the pair production of gluinos are absent.
- The mass hierarchy between the strong and electroweak sectors causes hard jets in a SUSY cascade to be harder than usual.
- LOSP candidates are typical, yielding a number of leptons and missing energy in the final stages of a cascade. In the case of CGGM this may also include the emission of a photon.
- The number of events with jets and missing energy will increase in the case of a stable pseudosgluon.

Unfortunately there are no smoking gun signatures for these models. Their main distinguishing characteristic is that there are different numbers of each type of visible event compared to models without a Dirac gluino — generally fewer. Note that for models of this type, a new lepton collider such as the International Linear Collider (ILC) or Compact Linear Collider (CLIC) would be able to simply bypass the strong sparticle sector and directly probe the much lighter accessible electroweak states.

Finally, the allowed tuning in these models is found to reduced. In allowed regions of parameter space, the reduction for a given Higgs mass is generally by a factor of two or three, although one has to keep in consideration that a reduction in fine tuning is being achieved whilst the gluino mass is being taken up to ten times of greater that which is usually considered for precisely reasons of tuning.

There are two obvious extensions of this study:

- The accuracy of the Higgs mass calculation needs improving in order to say something more concrete and more tightly constrain the model. In order to achieve this, the full set of general broken SUSY two loop RGEs should be used below the Dirac gluino mass, allowing a two loop accurate Higgs mass prediction. This should be possible with the general two loop RGE calculators on the market [93, 103]. Since these calculations are in $\overline{\text{MS}}$ scheme, one would need to take care to convert to the $\overline{\text{DR}}$ scheme before implementing them into a SUSY spectrum generator [114].
- In our study of the CMSSM, we kept the A terms zero for simplicity. As was noted in [104], the presence of additional scalar octets allows g_3 to remain much larger over the RG flow, and can consequently generate large negative A terms in the IR providing one starts with a negative A term. This model has the potential to reduce tuning much further by allowing a reduction in the squark masses and at the same time the length of flowing between the Dirac gluino mass and the SUSY scale.

8 Acknowledgements

I would like to thank Alberto Mariotti for useful discussions, Florian Lyonnet for guidance with `PyR@TE` and Florian Staub for help with `SARAH`. I would also like to thank Valya Khoze for many fruitful discussions, helpful comments and support during this project. DB is supported by a U.K. Science and Technology Facilities Council (STFC) studentship.

A Additional plots

A.1 Constrained Minimal Supersymmetric Standard Model

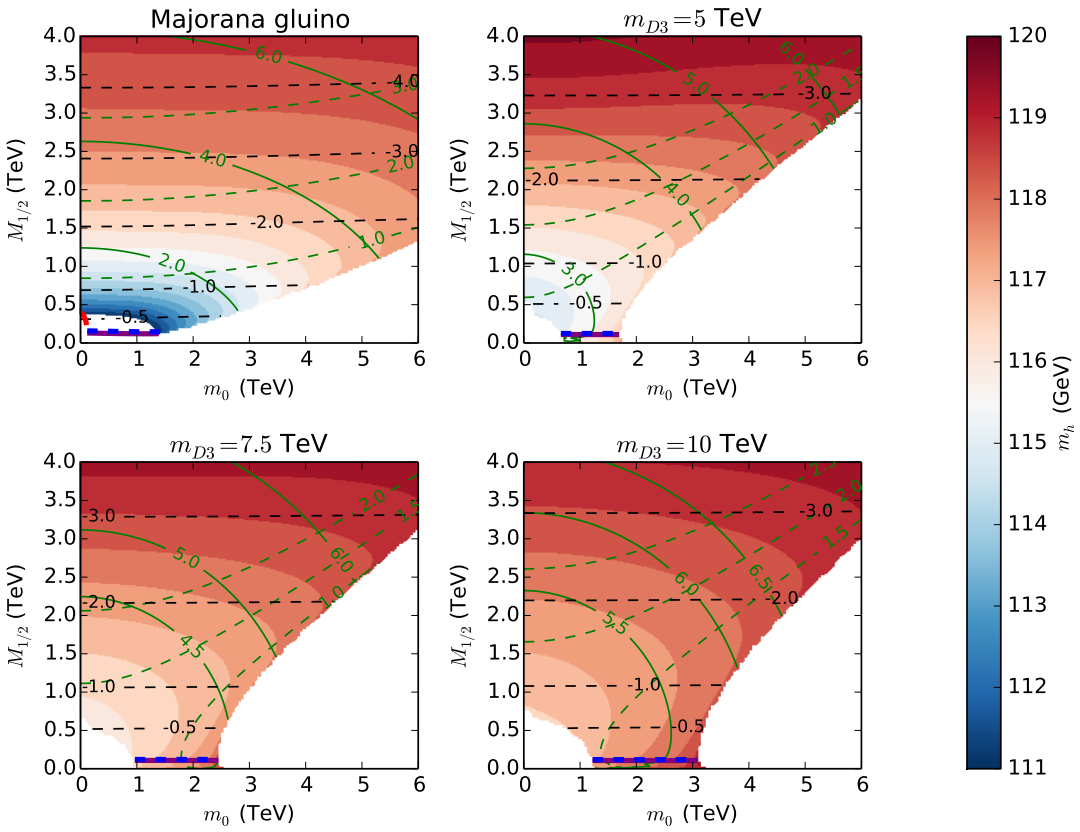

Figure 16. Higgs sector parameters in the CMSSM with $t_\beta = 25$ and m_{D3} fixed as indicated. The gradient indicates the Higgs mass. The black dashed, green dashed and green solid lines are contours of $a_t(m_{\rm SUSY})$, $\mu(m_{\rm SUSY})$, and $m_{\rm SUSY}$ respectively. All contours unless otherwise specified are in TeV.

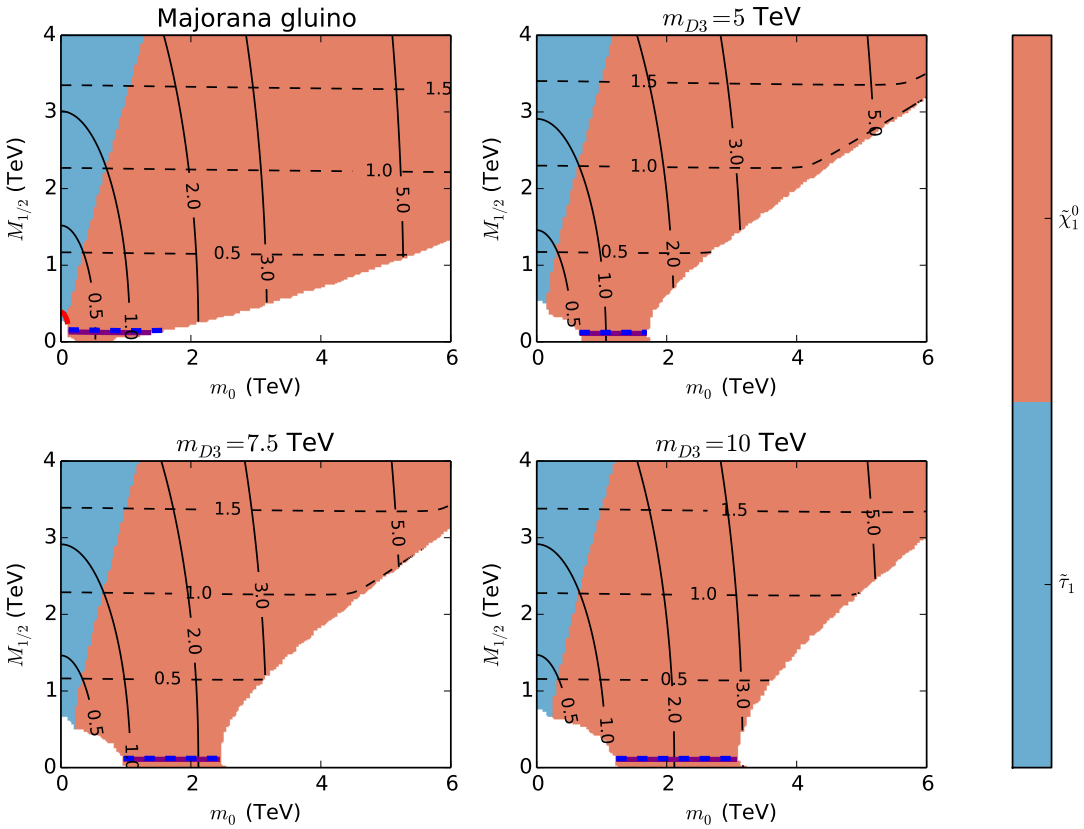

Figure 17. LOSP species in the CMSSM with $t_\beta = 25$ and m_{D3} fixed as indicated. The black dashed and black solid lines are contours of lightest neutralino mass $m_{\tilde{\chi}_1^0}$ and stau mass $m_{\tilde{\tau}}$ in TeV.

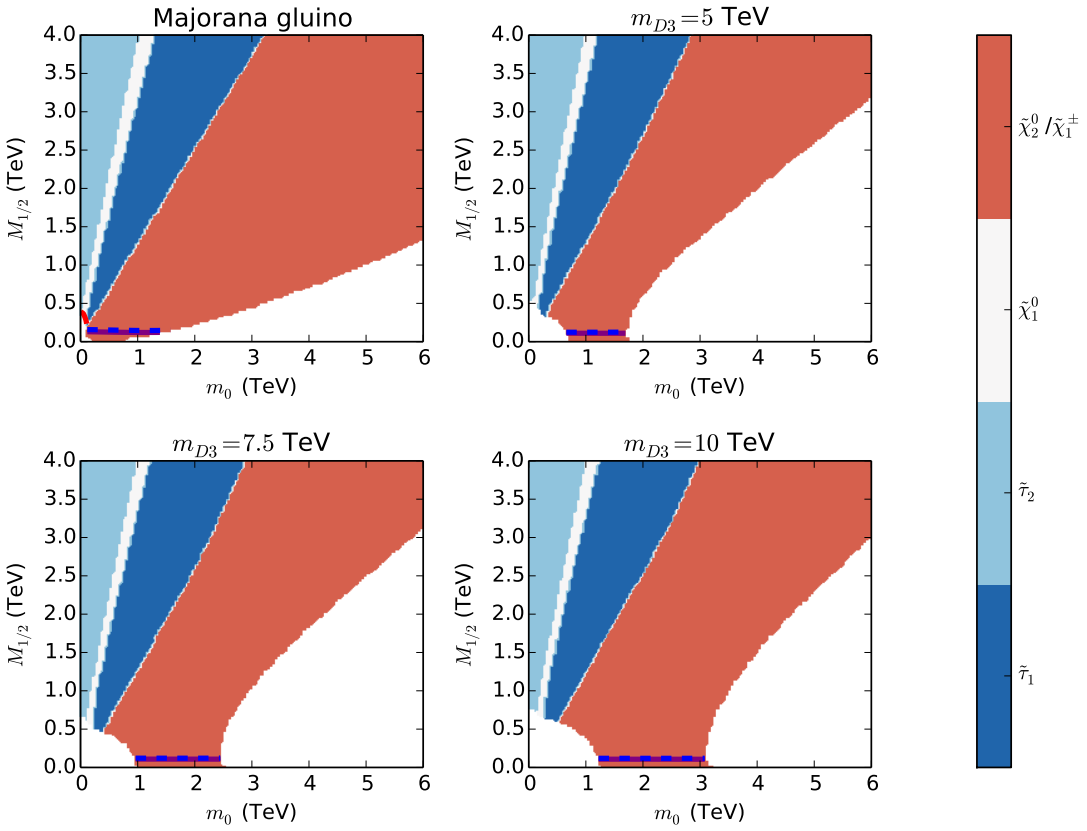

Figure 18. NLOSP species in the CMSSM with $t_\beta = 25$ and m_{D3} fixed as indicated

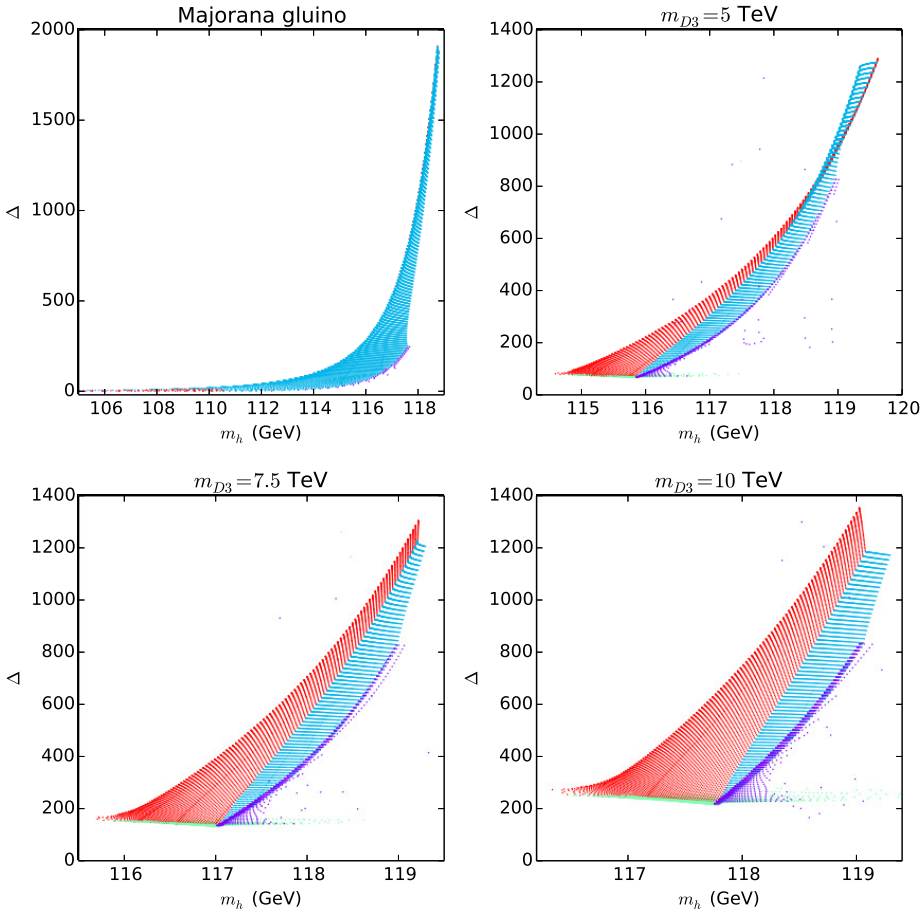

Figure 19. Fine tuning in the CMSSM with $t_\beta = 25$ and m_{D3} fixed as indicated. The red, purple, blue, and green regions correspond to μ, m_0, $M_{1/2}$ and m_{D3} as the dominant source of tuning.

A.2 Constrained General Gauge Mediation

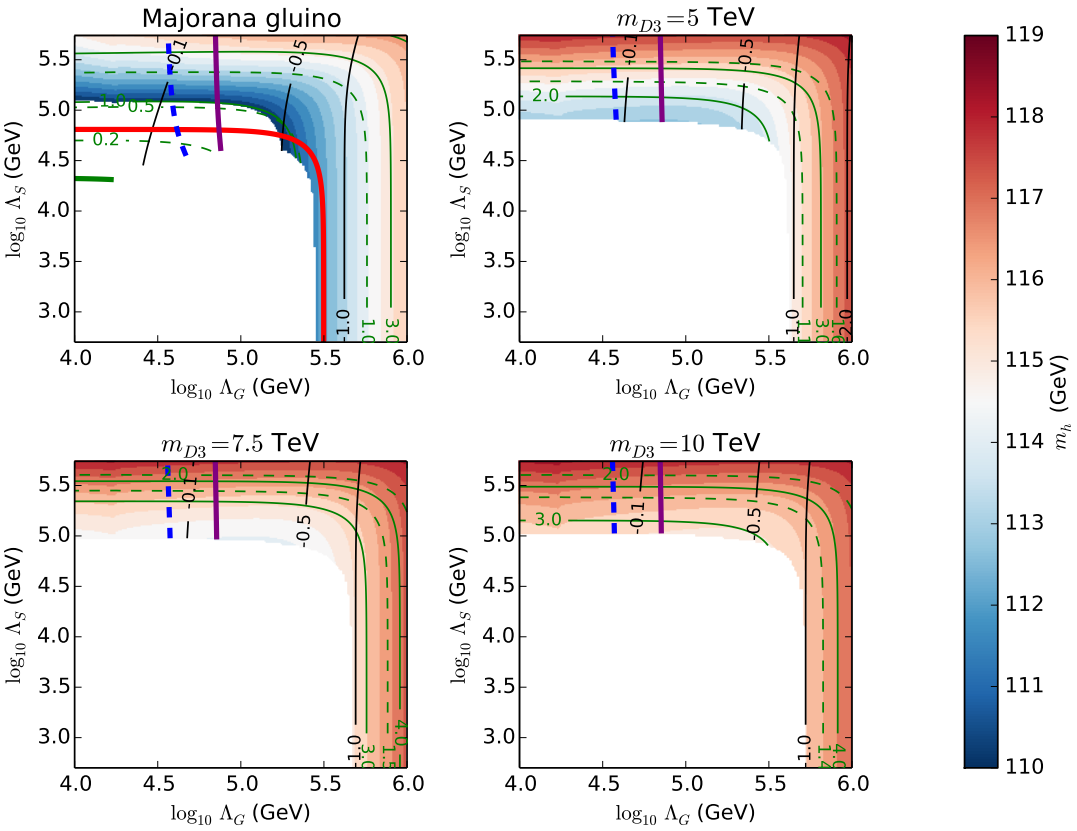

Figure 20. Higgs sector parameters in CGGM with $t_\beta = 25$, $m_{\rm Mess} = 10^7$ GeV and m_{D3} fixed as indicated. The gradient indicates the Higgs mass. The black dashed, green dashed and green solid lines are contours of $a_{\rm t}(m_{\rm SUSY})$, $\mu(m_{\rm SUSY})$, and $m_{\rm SUSY}$ respectively. All contours unless otherwise specified are in TeV.

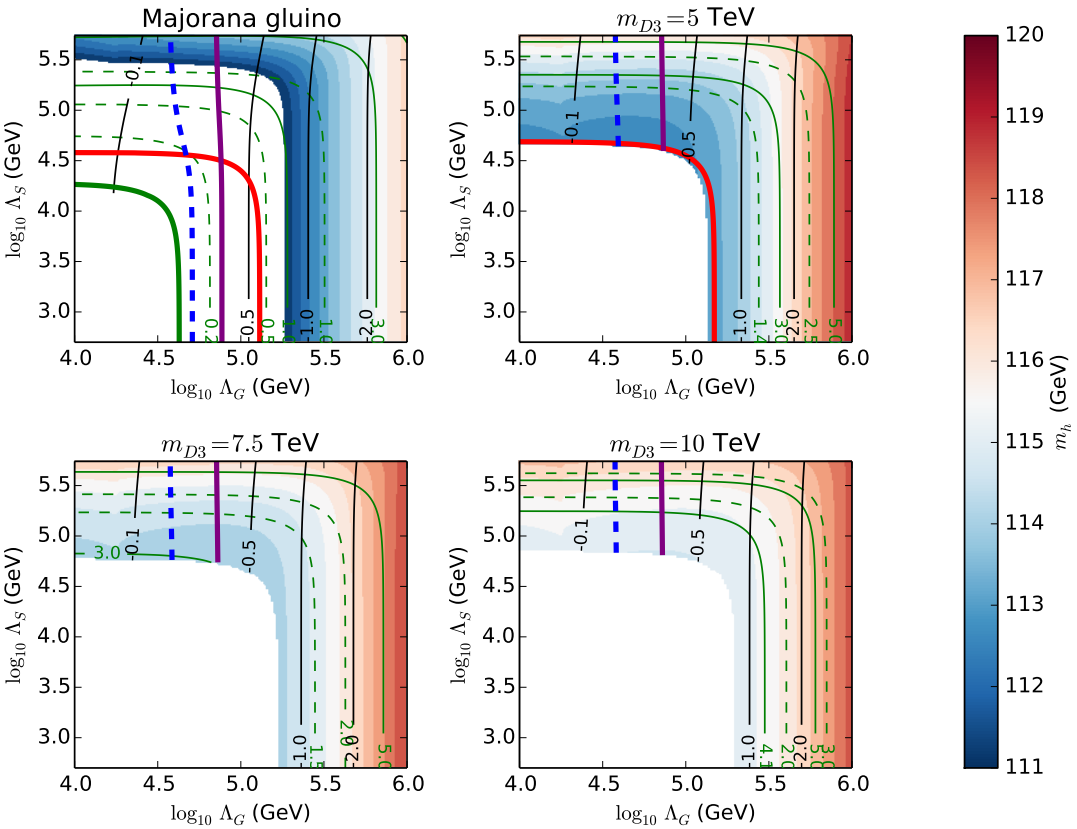

Figure 21. Higgs sector parameters in CGGM with $t_\beta = 10$, $m_{\rm Mess} = 10^{12}$ GeV and m_{D3} fixed as indicated. The gradient indicates the Higgs mass. The black dashed, green dashed and green solid lines are contours of $a_{\rm t}(m_{\rm SUSY})$, $\mu(m_{\rm SUSY})$, and $m_{\rm SUSY}$ respectively. All contours unless otherwise specified are in TeV.

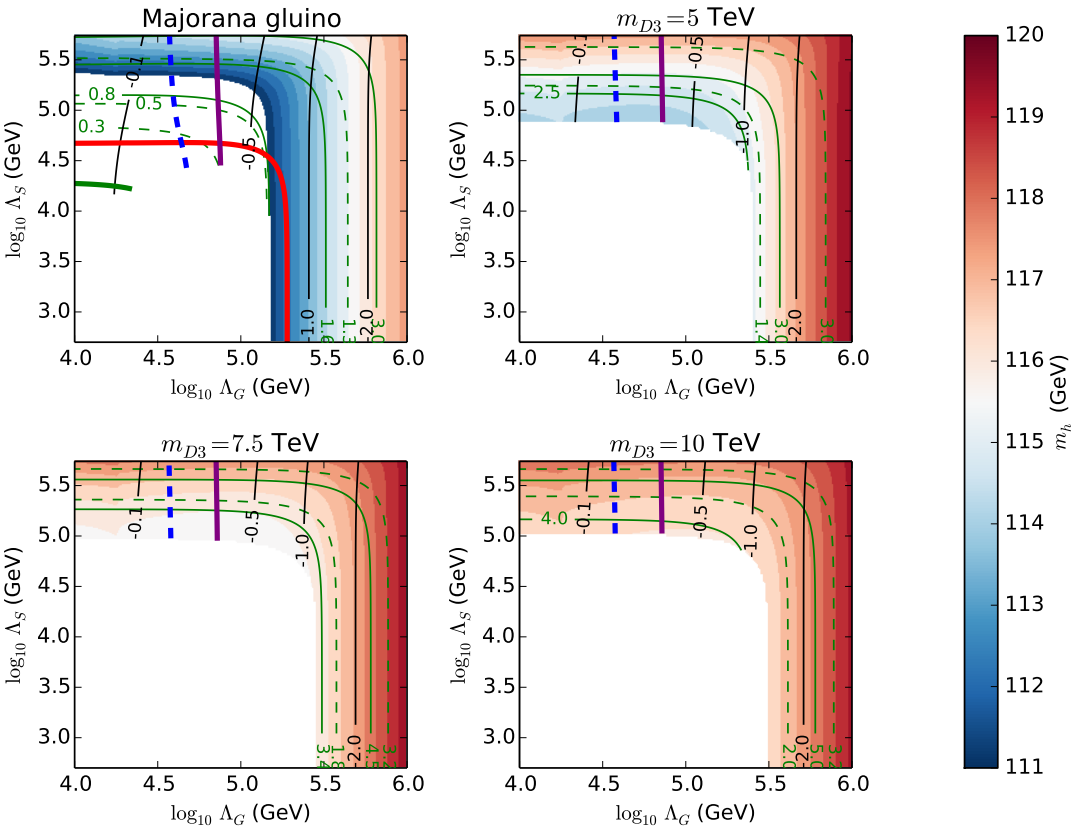

Figure 22. Higgs sector parameters in CGGM with $t_\beta = 25$, $m_{\rm Mess} = 10^{12}$ GeV and m_{D3} fixed as indicated. The gradient indicates the Higgs mass. The black dashed, green dashed and green solid lines are contours of $a_{\rm t}(m_{\rm SUSY})$, $\mu(m_{\rm SUSY})$, and $m_{\rm SUSY}$ respectively. All contours unless otherwise specified are in TeV.

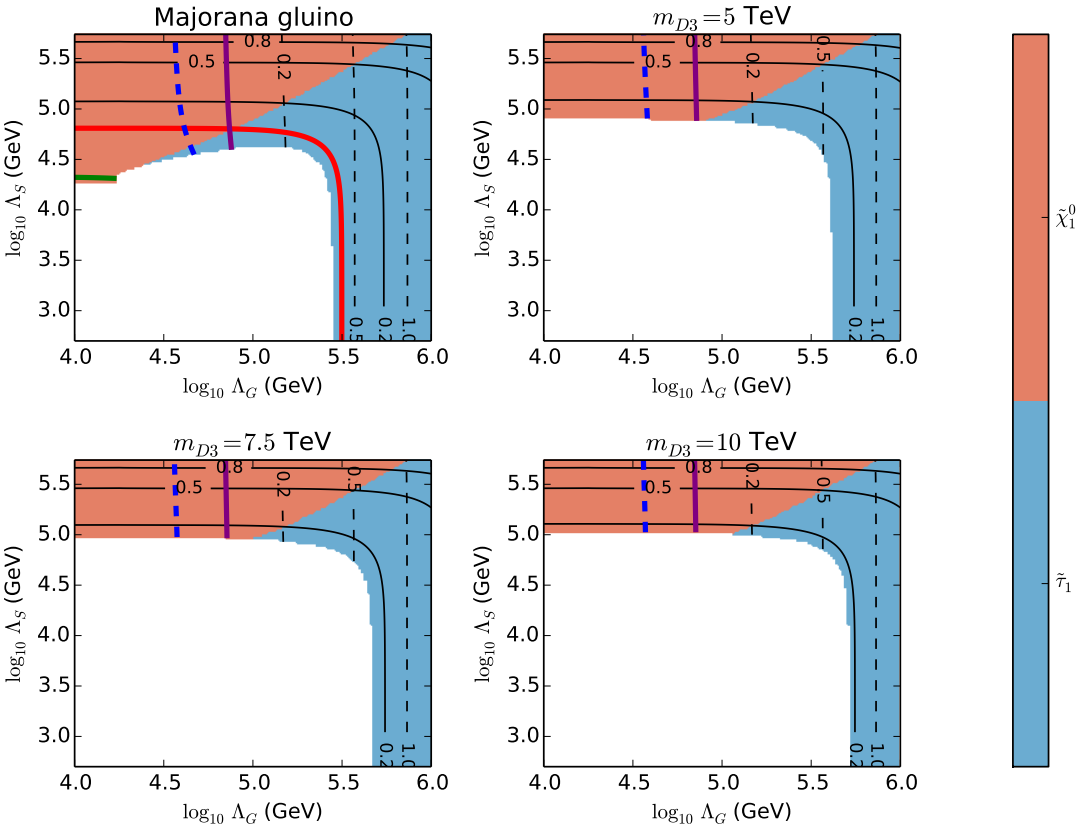

Figure 23. LOSP species in CGGM with $t_\beta = 25$, $m_{\rm Mess} = 10^7$ GeV and m_{D3} fixed as indicated. The black dashed and black solid lines are contours of lightest neutralino mass $m_{\tilde{\chi}_1^0}$ and stau mass $m_{\tilde{\tau}}$ in TeV.

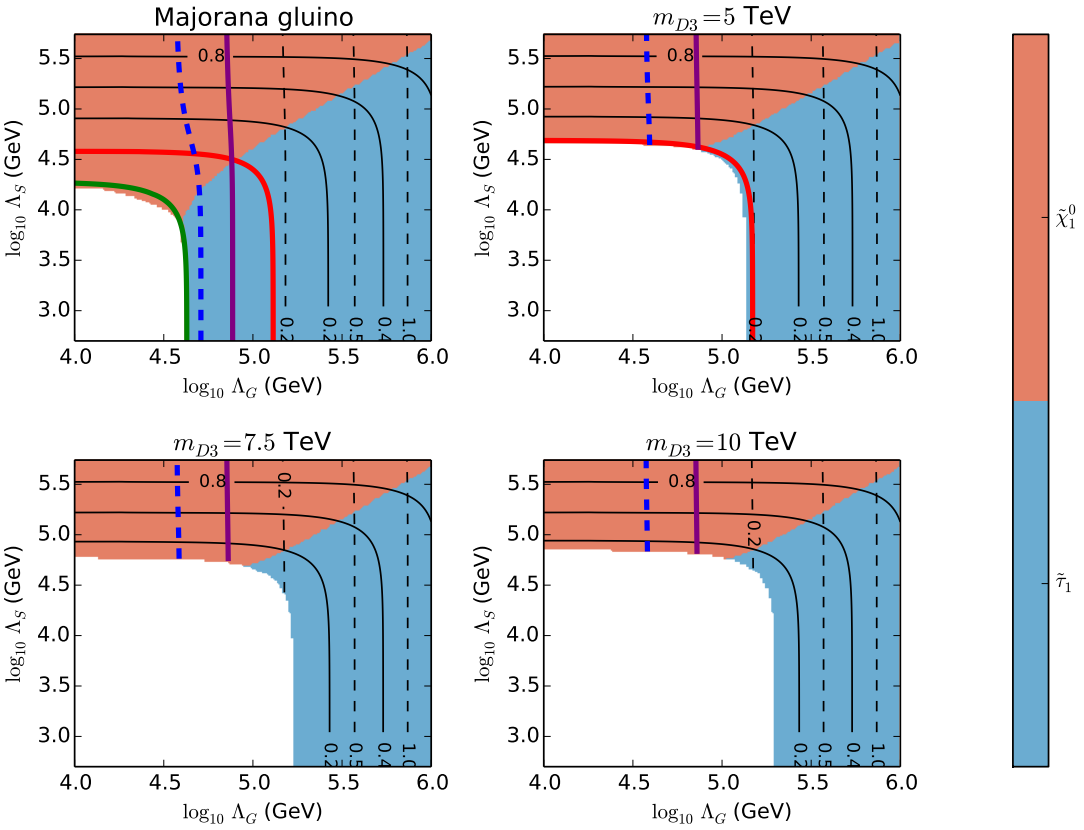

Figure 24. LOSP species in CGGM with $t_\beta = 10$, $m_{\rm Mess} = 10^{12}$ GeV and m_{D3} fixed as indicated. The black dashed and black solid lines are contours of lightest neutralino mass $m_{\tilde{\chi}_1^0}$ and stau mass $m_{\tilde{\tau}}$ in TeV.

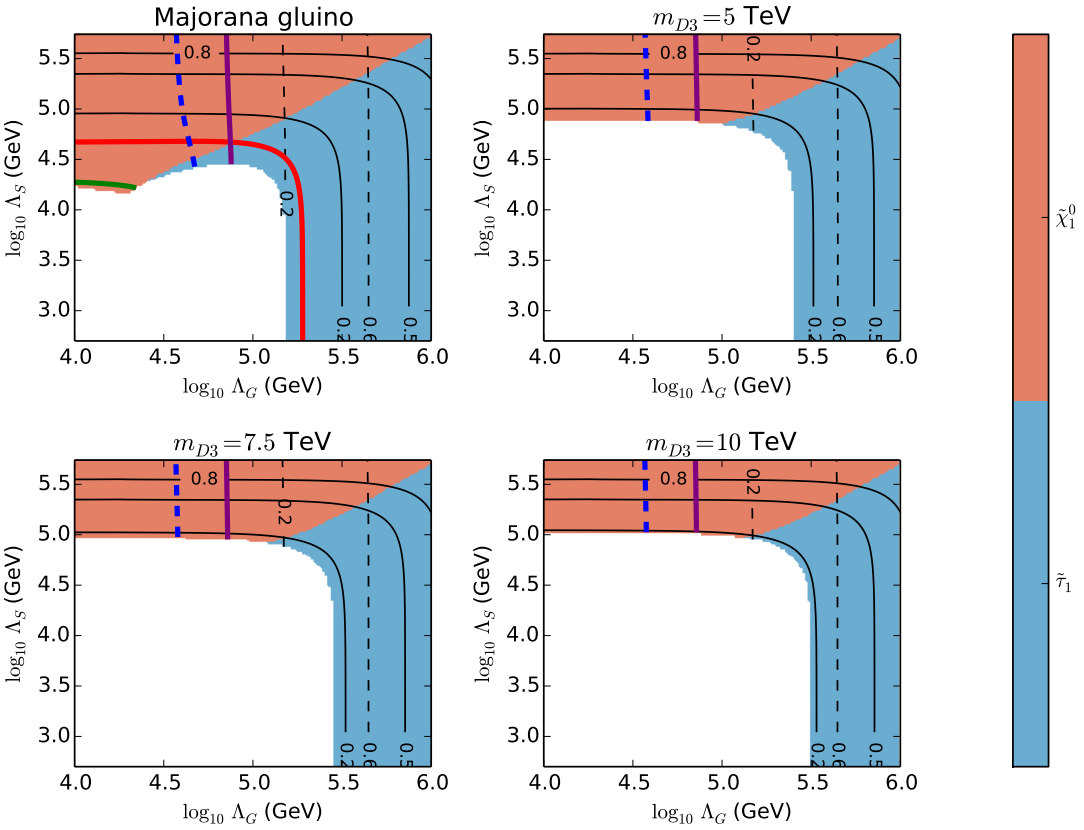

Figure 25. LOSP species in CGGM with $t_\beta = 25$, $m_{\rm Mess} = 10^{12}$ GeV and m_{D3} fixed as indicated. The black dashed and black solid lines are contours of lightest neutralino mass $m_{\tilde{\chi}_1^0}$ and stau mass $m_{\tilde{\tau}}$ in TeV.

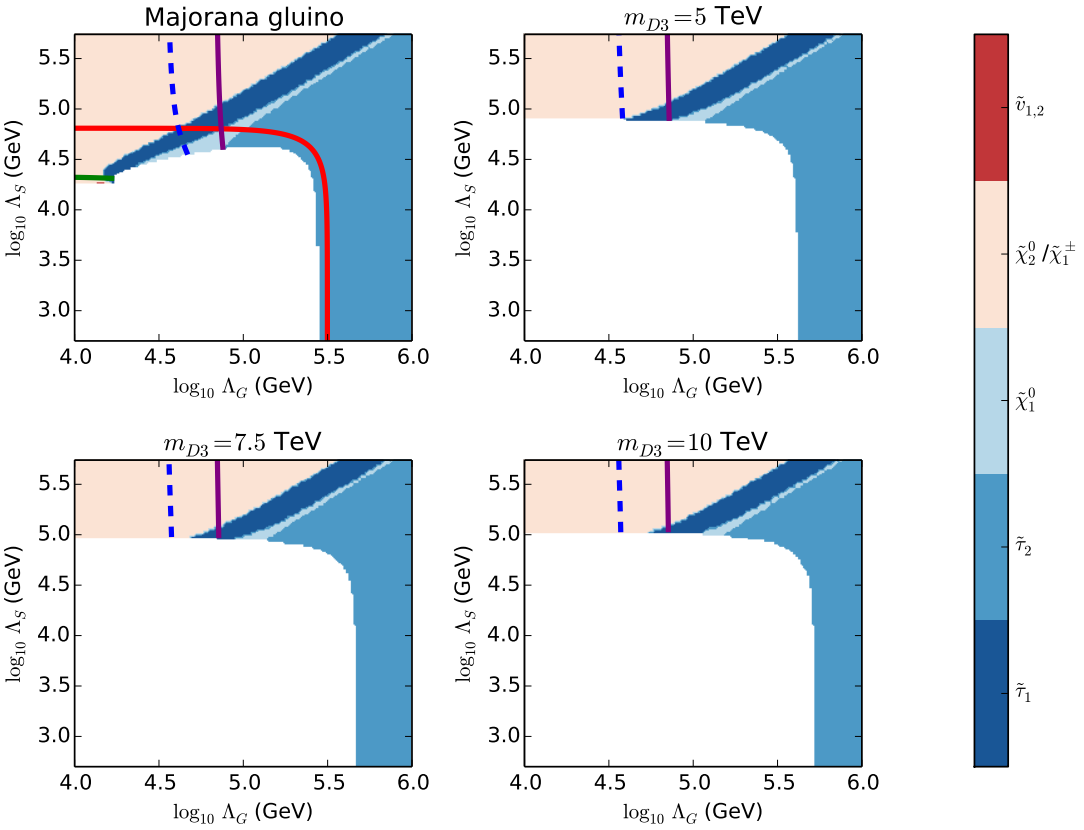

Figure 26. NLOSP species in CGGM with $t_\beta = 25$, $m_{\rm Mess} = 10^7$ GeV and m_{D3} fixed as indicated. The black dashed and black solid lines are contours of lightest neutralino mass $m_{\tilde{\chi}_1^0}$ and stau mass $m_{\tilde{\tau}}$ in TeV.

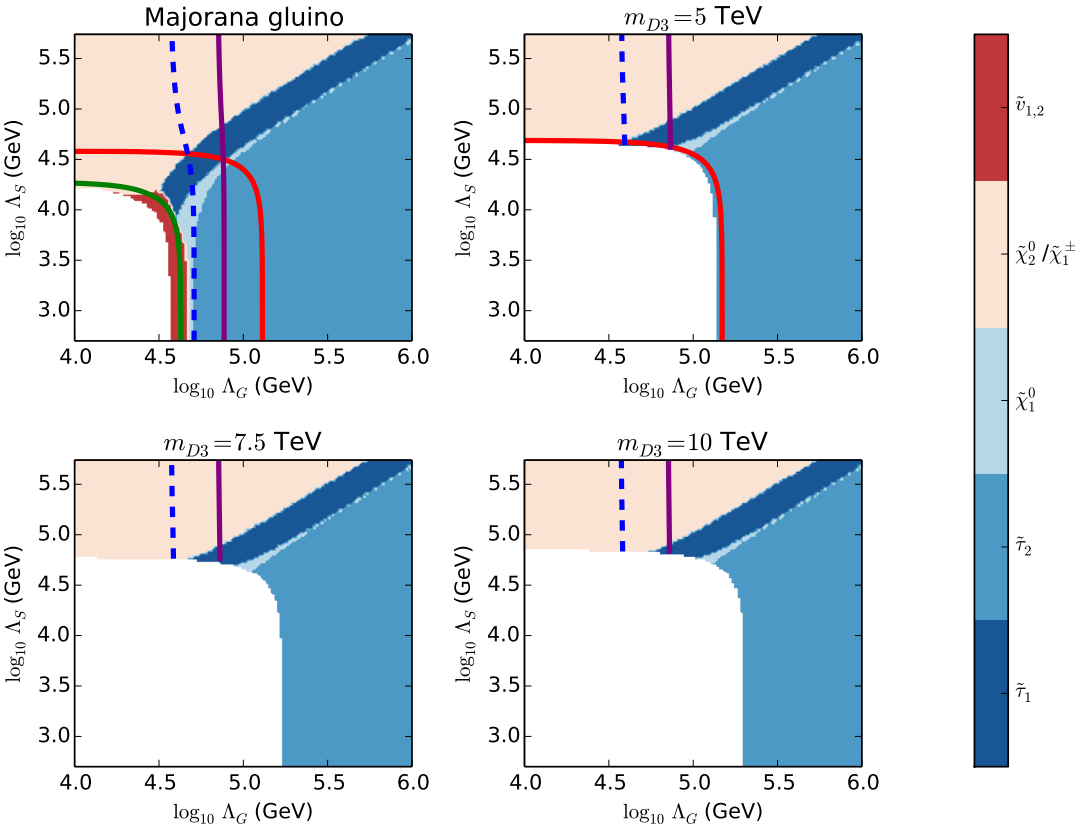

Figure 27. NLOSP species in CGGM with $t_\beta = 10$, $m_{\rm Mess} = 10^{12}$ GeV and m_{D3} fixed as indicated. The black dashed and black solid lines are contours of lightest neutralino mass $m_{\tilde{\chi}_1^0}$ and stau mass $m_{\tilde{\tau}}$ in TeV.

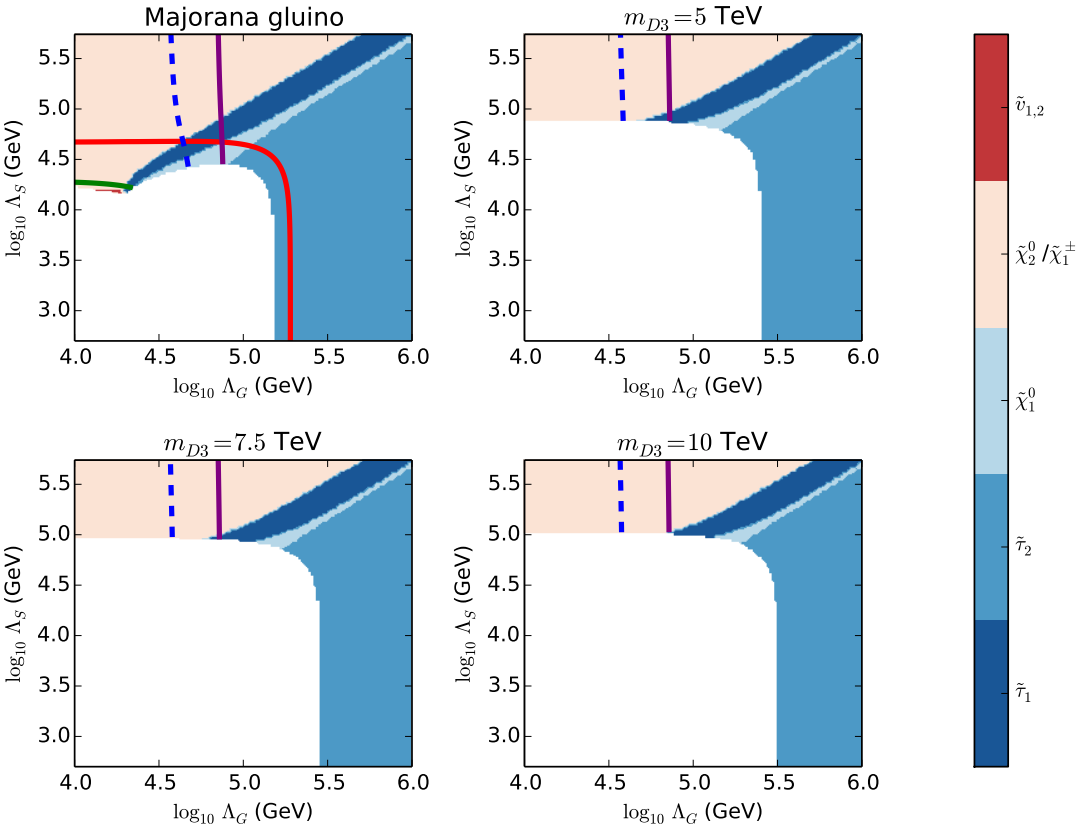

Figure 28. NLOSP species in CGGM with $t_\beta = 25$, $m_{\rm Mess} = 10^{12}$ GeV and m_{D3} fixed as indicated. The black dashed and black solid lines are contours of lightest neutralino mass $m_{\tilde{\chi}_1^0}$ and stau mass $m_{\tilde{\tau}}$ in TeV.

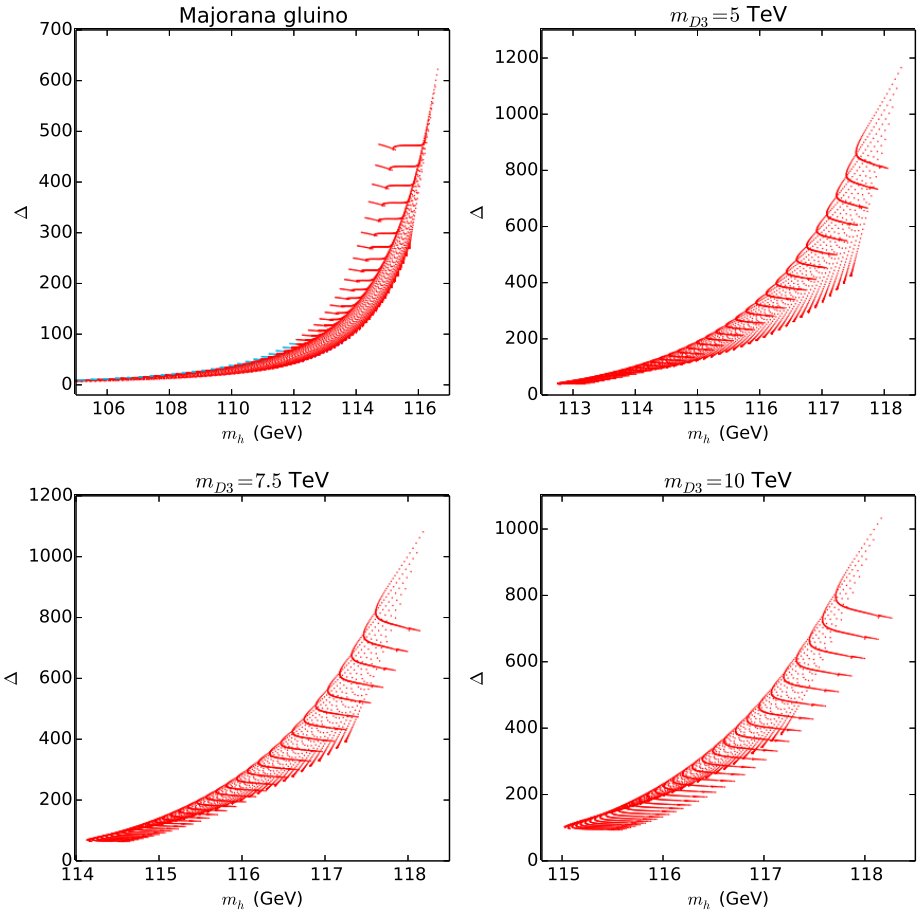

Figure 29. Fine tuning in CGGM with $t_\beta = 25$, $m_{\rm Mess} = 10^7$ GeV and m_{D3} fixed as indicated. The red and blue regions correspond to μ and Λ_S as the dominant source of tuning.

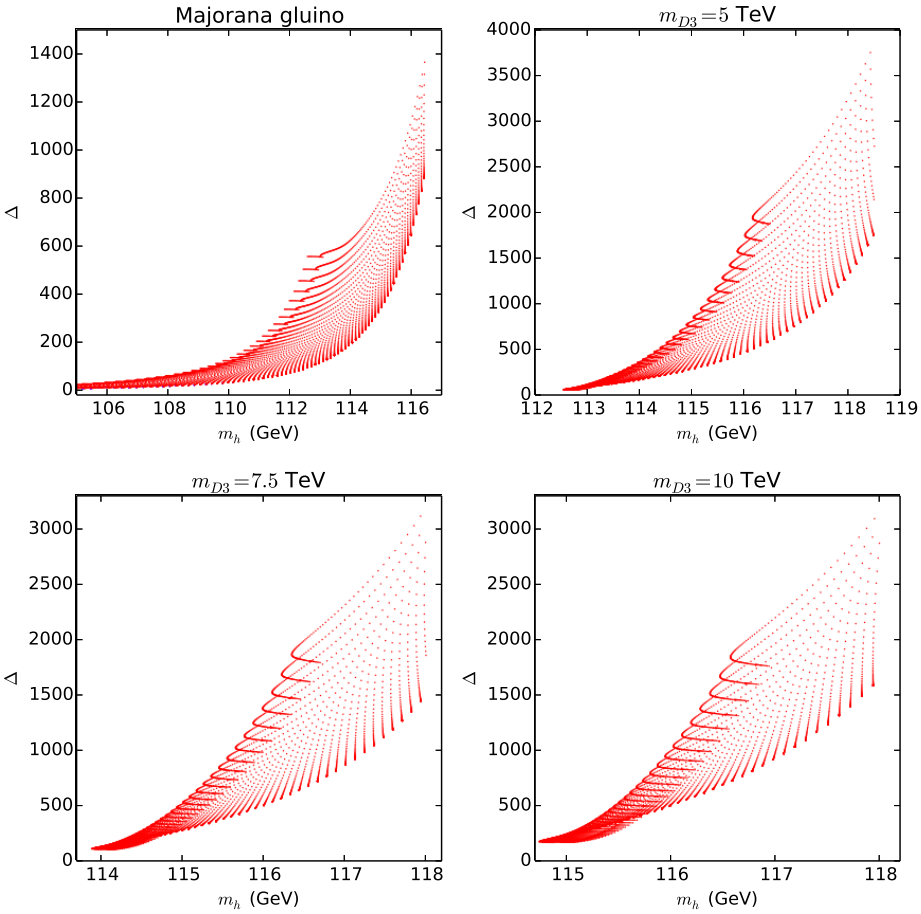

Figure 30. Fine tuning in CGGM with $t_\beta = 10$, $m_{\rm Mess} = 10^{12}$ GeV and m_{D3} fixed as indicated. The dominant source of tuning is entirely from the μ parameter.

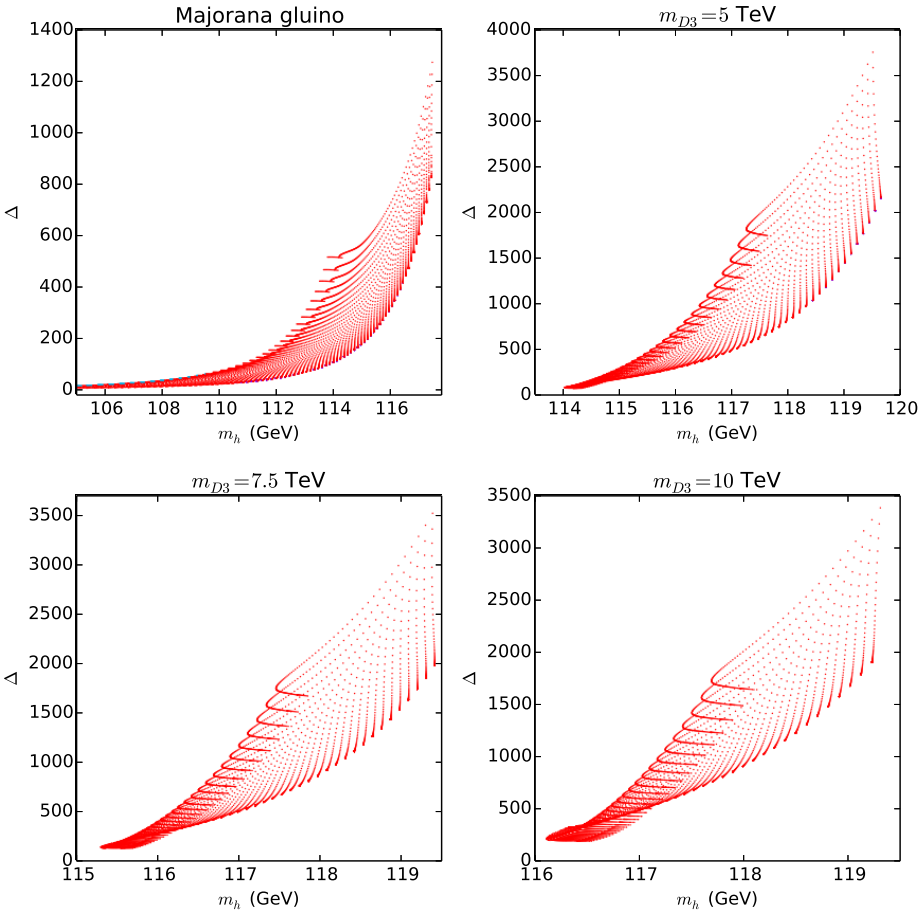

Figure 31. Fine tuning in CGGM with $t_\beta = 25$, $m_{\rm Mess} = 10^{12}$ GeV and m_{D3} fixed as indicated. The red and blue regions correspond to μ and Λ_S as the dominant source of tuning.

B Renormalisation Group equations with Dirac gluino decoupling

These RGEs were calculated using a combination of `SARAH`, `PyR@TE` [103] and results from [115, 116]. We decouple the gluino and the sgluons at renormalisation scales μ below $\mu(m_{D3}) = m_{D3} \equiv \overline{m_{D3}}$. We therefore define

$$\theta_{\tilde{g}} = 1 \quad \text{if} \quad \mu \geq \overline{m_{D3}}, \qquad\qquad \theta_{\tilde{g}} = 0 \quad \text{if} \quad \mu < \overline{m_{D3}}. \tag{B.1}$$

Decoupling is achieved at two loop accuracy for the gauge coupling for all particles, whereas the decoupling for the remaining terms is correct to one loop for all particles and correct to two loop for the sgluons and right handed gluino.

B.1 SUSY parameters

Gauge couplings

$$\beta_{g_1}^{(1)} = \frac{33}{5} g_1^3, \tag{B.2}$$

$$\beta_{g_1}^{(2)} = \frac{1}{25} g_1^3 \Big[-130 \operatorname{tr}\left(y_u y_u^\dagger\right) + 135 g_2^2 + 199 g_1^2 + 220(3 - \theta_{\tilde{g}}) g_3^2 - 70 \operatorname{tr}\left(y_d y_d^\dagger\right) - 90 \operatorname{tr}\left(y_e y_e^\dagger\right) \Big], \tag{B.3}$$

$$\beta_{g_2}^{(1)} = g_2^3, \tag{B.4}$$

$$\beta_{g_2}^{(2)} = \frac{1}{5} g_2^3 \Big[-10 \operatorname{tr}\left(y_e y_e^\dagger\right) + 60(3 - \theta_{\tilde{g}}) g_3^2 + 125 g_2^2 - 30 \operatorname{tr}\left(y_d y_d^\dagger\right) - 30 \operatorname{tr}\left(y_u y_u^\dagger\right) + 9 g_1^2 \Big], \tag{B.5}$$

$$\beta_{g_3}^{(1)} = -\frac{9}{2}(1 - \theta_{\tilde{g}}) g_3^3, \tag{B.6}$$

$$\beta_{g_3}^{(2)} = \frac{1}{5} g_3^3 \Big[11 g_1^2 - 20 \operatorname{tr}\left(y_d y_d^\dagger\right) - 20 \operatorname{tr}\left(y_u y_u^\dagger\right) + 5(39 + 29\,\theta_{\tilde{g}}) g_3^2 + 45 g_2^2 \Big]. \tag{B.7}$$

Yukawa couplings

$$\beta_{y_\mathrm{d}}^{(1)} = 3y_\mathrm{d}y_\mathrm{d}^\dagger y_\mathrm{d} + y_\mathrm{d}\Big[-3g_2^2 + 3\,\mathrm{tr}\Big(y_\mathrm{d}y_\mathrm{d}^\dagger\Big) + \frac{8}{3}\Big(\theta_{\widetilde{\mathrm{g}}} - 3\Big)g_3^2 - \frac{7}{15}g_1^2 + \mathrm{tr}\Big(y_\mathrm{e}y_\mathrm{e}^\dagger\Big)\Big] + y_\mathrm{d}y_\mathrm{u}^\dagger y_\mathrm{u}, \tag{B.8}$$

$$\begin{aligned}\beta_{y_\mathrm{d}}^{(2)} = {}& \frac{4}{5}g_1^2 y_\mathrm{d}y_\mathrm{u}^\dagger y_\mathrm{u} - 4y_\mathrm{d}y_\mathrm{d}^\dagger y_\mathrm{d}y_\mathrm{d}^\dagger y_\mathrm{d} - 2y_\mathrm{d}y_\mathrm{u}^\dagger y_\mathrm{u}y_\mathrm{d}^\dagger y_\mathrm{d} - 2y_\mathrm{d}y_\mathrm{u}^\dagger y_\mathrm{u}y_\mathrm{u}^\dagger y_\mathrm{u} \\ & + y_\mathrm{d}y_\mathrm{d}^\dagger y_\mathrm{d}\Big[6g_2^2 - 3\,\mathrm{tr}\Big(y_\mathrm{e}y_\mathrm{e}^\dagger\Big) - 9\,\mathrm{tr}\Big(y_\mathrm{d}y_\mathrm{d}^\dagger\Big) + \frac{4}{5}g_1^2\Big] - 3y_\mathrm{d}y_\mathrm{u}^\dagger y_\mathrm{u}\,\mathrm{tr}\Big(y_\mathrm{u}y_\mathrm{u}^\dagger\Big) + y_\mathrm{d}\Big[\frac{287}{90}g_1^4 \\ & + g_1^2g_2^2 + \frac{15}{2}g_2^4 + \frac{8}{9}g_1^2g_3^2 + 8g_2^2g_3^2 + \frac{128}{9}g_3^4 - \frac{2}{5}\Big(g_1^2 - 40g_3^2\Big)\,\mathrm{tr}\Big(y_\mathrm{d}y_\mathrm{d}^\dagger\Big) \\ & + \frac{6}{5}g_1^2\,\mathrm{tr}\Big(y_\mathrm{e}y_\mathrm{e}^\dagger\Big) - 9\,\mathrm{tr}\Big(y_\mathrm{d}y_\mathrm{d}^\dagger y_\mathrm{d}y_\mathrm{d}^\dagger\Big) - 3\,\mathrm{tr}\Big(y_\mathrm{d}y_\mathrm{u}^\dagger y_\mathrm{u}y_\mathrm{d}^\dagger\Big) - 3\,\mathrm{tr}\Big(y_\mathrm{e}y_\mathrm{e}^\dagger y_\mathrm{e}y_\mathrm{e}^\dagger\Big)\Big],\end{aligned} \tag{B.9}$$

$$\beta_{y_\mathrm{e}}^{(1)} = 3y_\mathrm{e}y_\mathrm{e}^\dagger y_\mathrm{e} + y_\mathrm{e}\Big[-3g_2^2 + 3\,\mathrm{tr}\Big(y_\mathrm{d}y_\mathrm{d}^\dagger\Big) - \frac{9}{5}g_1^2 + \mathrm{tr}\Big(y_\mathrm{e}y_\mathrm{e}^\dagger\Big)\Big], \tag{B.10}$$

$$\begin{aligned}\beta_{y_\mathrm{e}}^{(2)} = {}& -4y_\mathrm{e}y_\mathrm{e}^\dagger y_\mathrm{e}y_\mathrm{e}^\dagger y_\mathrm{e} + y_\mathrm{e}y_\mathrm{e}^\dagger y_\mathrm{e}\Big[-3\,\mathrm{tr}\Big(y_\mathrm{e}y_\mathrm{e}^\dagger\Big) + 6g_2^2 - 9\,\mathrm{tr}\Big(y_\mathrm{d}y_\mathrm{d}^\dagger\Big)\Big] \\ & + \frac{1}{10}y_\mathrm{e}\Big\{3\Big[45g_1^4 + 6g_1^2g_2^2 + 25g_2^4 + 4g_1^2\,\mathrm{tr}\Big(y_\mathrm{e}y_\mathrm{e}^\dagger\Big) - 30\,\mathrm{tr}\Big(y_\mathrm{d}y_\mathrm{d}^\dagger y_\mathrm{d}y_\mathrm{d}^\dagger\Big) \\ & - 10\,\mathrm{tr}\Big(y_\mathrm{d}y_\mathrm{u}^\dagger y_\mathrm{u}y_\mathrm{d}^\dagger\Big) - 10\,\mathrm{tr}\Big(y_\mathrm{e}y_\mathrm{e}^\dagger y_\mathrm{e}y_\mathrm{e}^\dagger\Big)\Big] - 4\Big(-40g_3^2 + g_1^2\Big)\,\mathrm{tr}\Big(y_\mathrm{d}y_\mathrm{d}^\dagger\Big)\Big\},\end{aligned} \tag{B.11}$$

$$\beta_{y_\mathrm{u}}^{(1)} = 3y_\mathrm{u}y_\mathrm{u}^\dagger y_\mathrm{u} - \frac{1}{15}y_\mathrm{u}\Big[13g_1^2 + 45g_2^2 - 45\,\mathrm{tr}\Big(y_\mathrm{u}y_\mathrm{u}^\dagger\Big) + 40\Big(3 - \theta_{\widetilde{\mathrm{g}}}\Big)g_3^2\Big] + y_\mathrm{u}y_\mathrm{d}^\dagger y_\mathrm{d}, \tag{B.12}$$

$$\begin{aligned}\beta_{y_\mathrm{u}}^{(2)} = {}& \frac{2}{5}g_1^2 y_\mathrm{u}y_\mathrm{u}^\dagger y_\mathrm{u} + 6g_2^2 y_\mathrm{u}y_\mathrm{u}^\dagger y_\mathrm{u} - 2y_\mathrm{u}y_\mathrm{d}^\dagger y_\mathrm{d}y_\mathrm{d}^\dagger y_\mathrm{d} - 2y_\mathrm{u}y_\mathrm{d}^\dagger y_\mathrm{d}y_\mathrm{u}^\dagger y_\mathrm{u} \\ & - 4y_\mathrm{u}y_\mathrm{u}^\dagger y_\mathrm{u}y_\mathrm{u}^\dagger y_\mathrm{u} + y_\mathrm{u}y_\mathrm{d}^\dagger y_\mathrm{d}\Big[-3\,\mathrm{tr}\Big(y_\mathrm{d}y_\mathrm{d}^\dagger\Big) + \frac{2}{5}g_1^2 - \mathrm{tr}\Big(y_\mathrm{e}y_\mathrm{e}^\dagger\Big)\Big] - 9y_\mathrm{u}y_\mathrm{u}^\dagger y_\mathrm{u}\,\mathrm{tr}\Big(y_\mathrm{u}y_\mathrm{u}^\dagger\Big) \\ & + y_\mathrm{u}\Big[\frac{2743}{450}g_1^4 + g_1^2g_2^2 + \frac{15}{2}g_2^4 + \frac{136}{45}g_1^2g_3^2 + 8g_2^2g_3^2 + \frac{128}{9}g_3^4 \\ & + \frac{4}{5}\Big(20g_3^2 + g_1^2\Big)\,\mathrm{tr}\Big(y_\mathrm{u}y_\mathrm{u}^\dagger\Big) - 3\,\mathrm{tr}\Big(y_\mathrm{d}y_\mathrm{u}^\dagger y_\mathrm{u}y_\mathrm{d}^\dagger\Big) - 9\,\mathrm{tr}\Big(y_\mathrm{u}y_\mathrm{u}^\dagger y_\mathrm{u}y_\mathrm{u}^\dagger\Big)\Big].\end{aligned} \tag{B.13}$$

SUSY masses

$$\beta_\mu^{(1)} = 3\mu\,\mathrm{tr}\Big(y_\mathrm{d}y_\mathrm{d}^\dagger\Big) - \frac{3}{5}\mu\Big(5g_2^2 - 5\,\mathrm{tr}\Big(y_\mathrm{u}y_\mathrm{u}^\dagger\Big) + g_1^2\Big) + \mu\,\mathrm{tr}\Big(y_\mathrm{e}y_\mathrm{e}^\dagger\Big), \tag{B.14}$$

$$\begin{aligned}\beta_\mu^{(2)} = {}& \frac{1}{50}\mu\Big[207g_1^4 + 90g_1^2g_2^2 + 375g_2^4 - 20\Big(-40g_3^2 + g_1^2\Big)\,\mathrm{tr}\Big(y_\mathrm{d}y_\mathrm{d}^\dagger\Big) + 60g_1^2\,\mathrm{tr}\Big(y_\mathrm{e}y_\mathrm{e}^\dagger\Big) \\ & + 800g_3^2\,\mathrm{tr}\Big(y_\mathrm{u}y_\mathrm{u}^\dagger\Big) - 450\,\mathrm{tr}\Big(y_\mathrm{d}y_\mathrm{d}^\dagger y_\mathrm{d}y_\mathrm{d}^\dagger\Big) - 300\,\mathrm{tr}\Big(y_\mathrm{d}y_\mathrm{u}^\dagger y_\mathrm{u}y_\mathrm{d}^\dagger\Big) - 150\,\mathrm{tr}\Big(y_\mathrm{e}y_\mathrm{e}^\dagger y_\mathrm{e}y_\mathrm{e}^\dagger\Big) \\ & + 40g_1^2\,\mathrm{tr}\Big(y_\mathrm{u}y_\mathrm{u}^\dagger\Big) - 450\,\mathrm{tr}\Big(y_\mathrm{u}y_\mathrm{u}^\dagger y_\mathrm{u}y_\mathrm{u}^\dagger\Big)\Big].\end{aligned} \tag{B.15}$$

B.2 SUSY breaking parameters

Majorana gaugino masses

$$\beta^{(1)}_{M_1} = \frac{66}{5} g_1^2 M_1, \tag{B.16}$$

$$\begin{aligned}\beta^{(2)}_{M_1} = \frac{2}{25} g_1^2 \Big[&398 g_1^2 M_1 + 135 g_2^2 M_1 + 440 g_3^2 M_1 + 440 g_3^2 M_3\, \theta_{\tilde{\mathrm{g}}} + 135 g_2^2 M_2 - 70 M_1 \operatorname{tr}\Big(y_{\mathrm{d}} y_{\mathrm{d}}^\dagger\Big) \\ &- 90 M_1 \operatorname{tr}\Big(y_{\mathrm{e}} y_{\mathrm{e}}^\dagger\Big) - 130 M_1 \operatorname{tr}\Big(y_{\mathrm{u}} y_{\mathrm{u}}^\dagger\Big) + 70 \operatorname{tr}\Big(y_{\mathrm{d}}^\dagger a_{\mathrm{d}}\Big) + 90 \operatorname{tr}\Big(y_{\mathrm{e}}^\dagger a_{\mathrm{e}}\Big) + 130 \operatorname{tr}\Big(y_{\mathrm{u}}^\dagger a_{\mathrm{u}}\Big)\Big],\end{aligned} \tag{B.17}$$

$$\beta^{(1)}_{M_2} = 2 g_2^2 M_2, \tag{B.18}$$

$$\begin{aligned}\beta^{(2)}_{M_2} = \frac{2}{5} g_2^2 \Big[&9 g_1^2 M_1 + 120 g_3^2 M_3\, \theta_{\tilde{\mathrm{g}}} + 9 g_1^2 M_2 + 250 g_2^2 M_2 + 120 g_3^2 M_2 - 30 M_2 \operatorname{tr}\Big(y_{\mathrm{d}} y_{\mathrm{d}}^\dagger\Big) \\ &- 10 M_2 \operatorname{tr}\Big(y_{\mathrm{e}} y_{\mathrm{e}}^\dagger\Big) - 30 M_2 \operatorname{tr}\Big(y_{\mathrm{u}} y_{\mathrm{u}}^\dagger\Big) + 30 \operatorname{tr}\Big(y_{\mathrm{d}}^\dagger a_{\mathrm{d}}\Big) + 10 \operatorname{tr}\Big(y_{\mathrm{e}}^\dagger a_{\mathrm{e}}\Big) + 30 \operatorname{tr}\Big(y_{\mathrm{u}}^\dagger a_{\mathrm{u}}\Big)\Big],\end{aligned} \tag{B.19}$$

$$\beta^{(1)}_{M_3} = 0, \tag{B.20}$$

$$\begin{aligned}\beta^{(2)}_{M_3} = \frac{2}{5} g_3^2 \Big[&11 g_1^2 M_1 + 11 g_1^2 M_3 + 45 g_2^2 M_3 + 680 g_3^2 M_3 + 45 g_2^2 M_2 - 20 M_3 \operatorname{tr}\Big(y_{\mathrm{d}} y_{\mathrm{d}}^\dagger\Big) \\ &- 20 M_3 \operatorname{tr}\Big(y_{\mathrm{u}} y_{\mathrm{u}}^\dagger\Big) + 20 \operatorname{tr}\Big(y_{\mathrm{d}}^\dagger a_{\mathrm{d}}\Big) + 20 \operatorname{tr}\Big(y_{\mathrm{u}}^\dagger a_{\mathrm{u}}\Big)\Big] \theta_{\tilde{\mathrm{g}}}.\end{aligned} \tag{B.21}$$

Dirac gluino mass

$$\beta^{(1)}_{m_{D3}} = -6\, g_3^2 m_{D3}\, \theta_{\tilde{\mathrm{g}}}, \tag{B.22}$$

$$\beta^{(2)}_{m_{D3}} = \frac{1}{5}\, g_3^2 m_{D3} \Big[11 g_1^2 + 45 g_2^2 + 520 g_3^2 - 20 \operatorname{tr}\Big(y_{\mathrm{d}} y_{\mathrm{d}}^\dagger\Big) - 20 \operatorname{tr}\Big(y_{\mathrm{u}} y_{\mathrm{u}}^\dagger\Big)\Big] \theta_{\tilde{\mathrm{g}}}. \tag{B.23}$$

Trilinear Soft-Breaking Parameters

$$\begin{aligned}\beta^{(1)}_{a_{\mathrm{d}}} = {}& 4 y_{\mathrm{d}} y_{\mathrm{d}}^\dagger a_{\mathrm{d}} + 2 y_{\mathrm{d}} y_{\mathrm{u}}^\dagger a_{\mathrm{u}} + 5 a_{\mathrm{d}} y_{\mathrm{d}}^\dagger y_{\mathrm{d}} + a_{\mathrm{d}} y_{\mathrm{u}}^\dagger y_{\mathrm{u}} - \frac{7}{15} g_1^2 a_{\mathrm{d}} - 3 g_2^2 a_{\mathrm{d}} + \frac{16}{3}\Big(\theta_{\tilde{\mathrm{g}}} - 2\Big) g_3^2 a_{\mathrm{d}} \\ &+ 3 a_{\mathrm{d}} \operatorname{tr}\Big(y_{\mathrm{d}} y_{\mathrm{d}}^\dagger\Big) + a_{\mathrm{d}} \operatorname{tr}\Big(y_{\mathrm{e}} y_{\mathrm{e}}^\dagger\Big) + y_{\mathrm{d}} \Big[2 \operatorname{tr}\Big(y_{\mathrm{e}}^\dagger a_{\mathrm{e}}\Big) + 6 g_2^2 M_2 + 6 \operatorname{tr}\Big(y_{\mathrm{d}}^\dagger a_{\mathrm{d}}\Big) \\ &+ \frac{14}{15} g_1^2 M_1 + \frac{32}{3} g_3^2 M_3\, \theta_{\tilde{\mathrm{g}}}\Big],\end{aligned} \tag{B.24}$$

$$\begin{aligned}\beta^{(2)}_{a_{\mathrm{d}}} = {}& \frac{6}{5} g_1^2 y_{\mathrm{d}} y_{\mathrm{d}}^\dagger a_{\mathrm{d}} + 6 g_2^2 y_{\mathrm{d}} y_{\mathrm{d}}^\dagger a_{\mathrm{d}} - \frac{8}{5} g_1^2 M_1 y_{\mathrm{d}} y_{\mathrm{u}}^\dagger y_{\mathrm{u}} + \frac{8}{5} g_1^2 y_{\mathrm{d}} y_{\mathrm{u}}^\dagger a_{\mathrm{u}} \\ &+ \frac{6}{5} g_1^2 a_{\mathrm{d}} y_{\mathrm{d}}^\dagger y_{\mathrm{d}} + 12 g_2^2 a_{\mathrm{d}} y_{\mathrm{d}}^\dagger y_{\mathrm{d}} + \frac{4}{5} g_1^2 a_{\mathrm{d}} y_{\mathrm{u}}^\dagger y_{\mathrm{u}} - 6 y_{\mathrm{d}} y_{\mathrm{d}}^\dagger y_{\mathrm{d}} y_{\mathrm{d}}^\dagger a_{\mathrm{d}} \\ &- 8 y_{\mathrm{d}} y_{\mathrm{d}}^\dagger a_{\mathrm{d}} y_{\mathrm{d}}^\dagger y_{\mathrm{d}} - 2 y_{\mathrm{d}} y_{\mathrm{u}}^\dagger y_{\mathrm{u}} y_{\mathrm{d}}^\dagger a_{\mathrm{d}} - 4 y_{\mathrm{d}} y_{\mathrm{u}}^\dagger y_{\mathrm{u}} y_{\mathrm{u}}^\dagger a_{\mathrm{u}} - 4 y_{\mathrm{d}} y_{\mathrm{u}}^\dagger a_{\mathrm{u}} y_{\mathrm{d}}^\dagger y_{\mathrm{d}} \\ &- 4 y_{\mathrm{d}} y_{\mathrm{u}}^\dagger a_{\mathrm{u}} y_{\mathrm{u}}^\dagger y_{\mathrm{u}} - 6 a_{\mathrm{d}} y_{\mathrm{d}}^\dagger y_{\mathrm{d}} y_{\mathrm{d}}^\dagger y_{\mathrm{d}} - 4 a_{\mathrm{d}} y_{\mathrm{u}}^\dagger y_{\mathrm{u}} y_{\mathrm{d}}^\dagger y_{\mathrm{d}} - 2 a_{\mathrm{d}} y_{\mathrm{u}}^\dagger y_{\mathrm{u}} y_{\mathrm{u}}^\dagger y_{\mathrm{u}} \\ &+ \frac{287}{90} g_1^4 a_{\mathrm{d}} + g_1^2 g_2^2 a_{\mathrm{d}} + \frac{15}{2} g_2^4 a_{\mathrm{d}} + \frac{8}{9} g_1^2 g_3^2 a_{\mathrm{d}} + 8 g_2^2 g_3^2 a_{\mathrm{d}} + \frac{128}{9} g_3^4 a_{\mathrm{d}} \\ &- 12 y_{\mathrm{d}} y_{\mathrm{d}}^\dagger a_{\mathrm{d}} \operatorname{tr}\Big(y_{\mathrm{d}} y_{\mathrm{d}}^\dagger\Big) - 15 a_{\mathrm{d}} y_{\mathrm{d}}^\dagger y_{\mathrm{d}} \operatorname{tr}\Big(y_{\mathrm{d}} y_{\mathrm{d}}^\dagger\Big) - \frac{2}{5} g_1^2 a_{\mathrm{d}} \operatorname{tr}\Big(y_{\mathrm{d}} y_{\mathrm{d}}^\dagger\Big) \\ &+ 16 g_3^2 a_{\mathrm{d}} \operatorname{tr}\Big(y_{\mathrm{d}} y_{\mathrm{d}}^\dagger\Big) - 4 y_{\mathrm{d}} y_{\mathrm{d}}^\dagger a_{\mathrm{d}} \operatorname{tr}\Big(y_{\mathrm{e}} y_{\mathrm{e}}^\dagger\Big) - 5 a_{\mathrm{d}} y_{\mathrm{d}}^\dagger y_{\mathrm{d}} \operatorname{tr}\Big(y_{\mathrm{e}} y_{\mathrm{e}}^\dagger\Big) \\ &+ \frac{6}{5} g_1^2 a_{\mathrm{d}} \operatorname{tr}\Big(y_{\mathrm{e}} y_{\mathrm{e}}^\dagger\Big) - 6 y_{\mathrm{d}} y_{\mathrm{u}}^\dagger a_{\mathrm{u}} \operatorname{tr}\Big(y_{\mathrm{u}} y_{\mathrm{u}}^\dagger\Big) - 3 a_{\mathrm{d}} y_{\mathrm{u}}^\dagger y_{\mathrm{u}} \operatorname{tr}\Big(y_{\mathrm{u}} y_{\mathrm{u}}^\dagger\Big)\end{aligned}$$

$$
\begin{aligned}
&- \frac{2}{5} y_{\mathrm{d}} y_{\mathrm{d}}^{\dagger} y_{\mathrm{d}} \Big[15 \operatorname{tr}\Big(y_{\mathrm{e}}^{\dagger} a_{\mathrm{e}} \Big) + 30 g_2^2 M_2 + 45 \operatorname{tr}\Big(y_{\mathrm{d}}^{\dagger} a_{\mathrm{d}} \Big) + 4 g_1^2 M_1 \Big] - 6 y_{\mathrm{d}} y_{\mathrm{u}}^{\dagger} y_{\mathrm{u}} \operatorname{tr}\Big(y_{\mathrm{u}}^{\dagger} a_{\mathrm{u}} \Big) \\
&- 9 a_{\mathrm{d}} \operatorname{tr}\Big(y_{\mathrm{d}} y_{\mathrm{d}}^{\dagger} y_{\mathrm{d}} y_{\mathrm{d}}^{\dagger} \Big) - 3 a_{\mathrm{d}} \operatorname{tr}\Big(y_{\mathrm{d}} y_{\mathrm{u}}^{\dagger} y_{\mathrm{u}} y_{\mathrm{d}}^{\dagger} \Big) - 3 a_{\mathrm{d}} \operatorname{tr}\Big(y_{\mathrm{e}} y_{\mathrm{e}}^{\dagger} y_{\mathrm{e}} y_{\mathrm{e}}^{\dagger} \Big) \\
&- \frac{2}{45} y_{\mathrm{d}} \Big[287 g_1^4 M_1 + 45 g_1^2 g_2^2 M_1 + 40 g_1^2 g_3^2 M_1 + 40 g_1^2 g_3^2 M_3 \, \theta_{\widetilde{\mathrm{g}}} + 360 g_2^2 g_3^2 M_3 \, \theta_{\widetilde{\mathrm{g}}} \\
&+ 1280 g_3^4 M_3 \, \theta_{\widetilde{\mathrm{g}}} + 45 g_1^2 g_2^2 M_2 + 675 g_2^4 M_2 + 360 g_2^2 g_3^2 M_2 + 18 \Big(40 g_3^2 M_3 \, \theta_{\widetilde{\mathrm{g}}} - g_1^2 M_1 \Big) \operatorname{tr}\Big(y_{\mathrm{d}} y_{\mathrm{d}}^{\dagger} \Big) \\
&+ 54 g_1^2 M_1 \operatorname{tr}\Big(y_{\mathrm{e}} y_{\mathrm{e}}^{\dagger} \Big) + 18 g_1^2 \operatorname{tr}\Big(y_{\mathrm{d}}^{\dagger} a_{\mathrm{d}} \Big) - 720 g_3^2 \operatorname{tr}\Big(y_{\mathrm{d}}^{\dagger} a_{\mathrm{d}} \Big) - 54 g_1^2 \operatorname{tr}\Big(y_{\mathrm{e}}^{\dagger} a_{\mathrm{e}} \Big) + 810 \operatorname{tr}\Big(y_{\mathrm{d}} y_{\mathrm{d}}^{\dagger} a_{\mathrm{d}} y_{\mathrm{d}}^{\dagger} \Big) \\
&+ 135 \operatorname{tr}\Big(y_{\mathrm{d}} y_{\mathrm{u}}^{\dagger} a_{\mathrm{u}} y_{\mathrm{d}}^{\dagger} \Big) + 270 \operatorname{tr}\Big(y_{\mathrm{e}} y_{\mathrm{e}}^{\dagger} a_{\mathrm{e}} y_{\mathrm{e}}^{\dagger} \Big) + 135 \operatorname{tr}\Big(y_{\mathrm{u}} y_{\mathrm{d}}^{\dagger} a_{\mathrm{d}} y_{\mathrm{u}}^{\dagger} \Big) \Big],
\end{aligned} \tag{B.25}
$$

$$
\begin{aligned}
\beta_{a_{\mathrm{e}}}^{(1)} &= 4 y_{\mathrm{e}} y_{\mathrm{e}}^{\dagger} a_{\mathrm{e}} + 5 a_{\mathrm{e}} y_{\mathrm{e}}^{\dagger} y_{\mathrm{e}} - \frac{9}{5} g_1^2 a_{\mathrm{e}} - 3 g_2^2 a_{\mathrm{e}} + 3 a_{\mathrm{e}} \operatorname{tr}\Big(y_{\mathrm{d}} y_{\mathrm{d}}^{\dagger} \Big) + a_{\mathrm{e}} \operatorname{tr}\Big(y_{\mathrm{e}} y_{\mathrm{e}}^{\dagger} \Big) \\
&+ y_{\mathrm{e}} \Big[2 \operatorname{tr}\Big(y_{\mathrm{e}}^{\dagger} a_{\mathrm{e}} \Big) + 6 g_2^2 M_2 + 6 \operatorname{tr}\Big(y_{\mathrm{d}}^{\dagger} a_{\mathrm{d}} \Big) + \frac{18}{5} g_1^2 M_1 \Big],
\end{aligned} \tag{B.26}
$$

$$
\begin{aligned}
\beta_{a_{\mathrm{e}}}^{(2)} &= + \frac{6}{5} g_1^2 y_{\mathrm{e}} y_{\mathrm{e}}^{\dagger} a_{\mathrm{e}} + 6 g_2^2 y_{\mathrm{e}} y_{\mathrm{e}}^{\dagger} a_{\mathrm{e}} - \frac{6}{5} g_1^2 a_{\mathrm{e}} y_{\mathrm{e}}^{\dagger} y_{\mathrm{e}} + 12 g_2^2 a_{\mathrm{e}} y_{\mathrm{e}}^{\dagger} y_{\mathrm{e}} \\
&- 6 y_{\mathrm{e}} y_{\mathrm{e}}^{\dagger} y_{\mathrm{e}} y_{\mathrm{e}}^{\dagger} a_{\mathrm{e}} - 8 y_{\mathrm{e}} y_{\mathrm{e}}^{\dagger} a_{\mathrm{e}} y_{\mathrm{e}}^{\dagger} y_{\mathrm{e}} - 6 a_{\mathrm{e}} y_{\mathrm{e}}^{\dagger} y_{\mathrm{e}} y_{\mathrm{e}}^{\dagger} y_{\mathrm{e}} + \frac{27}{2} g_1^4 a_{\mathrm{e}} + \frac{9}{5} g_1^2 g_2^2 a_{\mathrm{e}} + \frac{15}{2} g_2^4 a_{\mathrm{e}} \\
&- 12 y_{\mathrm{e}} y_{\mathrm{e}}^{\dagger} a_{\mathrm{e}} \operatorname{tr}\Big(y_{\mathrm{d}} y_{\mathrm{d}}^{\dagger} \Big) - 15 a_{\mathrm{e}} y_{\mathrm{e}}^{\dagger} y_{\mathrm{e}} \operatorname{tr}\Big(y_{\mathrm{d}} y_{\mathrm{d}}^{\dagger} \Big) - \frac{2}{5} g_1^2 a_{\mathrm{e}} \operatorname{tr}\Big(y_{\mathrm{d}} y_{\mathrm{d}}^{\dagger} \Big) \\
&+ 16 g_3^2 a_{\mathrm{e}} \operatorname{tr}\Big(y_{\mathrm{d}} y_{\mathrm{d}}^{\dagger} \Big) - 4 y_{\mathrm{e}} y_{\mathrm{e}}^{\dagger} a_{\mathrm{e}} \operatorname{tr}\Big(y_{\mathrm{e}} y_{\mathrm{e}}^{\dagger} \Big) - 5 a_{\mathrm{e}} y_{\mathrm{e}}^{\dagger} y_{\mathrm{e}} \operatorname{tr}\Big(y_{\mathrm{e}} y_{\mathrm{e}}^{\dagger} \Big) \\
&+ \frac{6}{5} g_1^2 a_{\mathrm{e}} \operatorname{tr}\Big(y_{\mathrm{e}} y_{\mathrm{e}}^{\dagger} \Big) - 6 y_{\mathrm{e}} y_{\mathrm{e}}^{\dagger} y_{\mathrm{e}} \Big[2 g_2^2 M_2 + 3 \operatorname{tr}\Big(y_{\mathrm{d}}^{\dagger} a_{\mathrm{d}} \Big) + \operatorname{tr}\Big(y_{\mathrm{e}}^{\dagger} a_{\mathrm{e}} \Big) \Big] - 9 a_{\mathrm{e}} \operatorname{tr}\Big(y_{\mathrm{d}} y_{\mathrm{d}}^{\dagger} y_{\mathrm{d}} y_{\mathrm{d}}^{\dagger} \Big) \\
&- 3 a_{\mathrm{e}} \operatorname{tr}\Big(y_{\mathrm{d}} y_{\mathrm{u}}^{\dagger} y_{\mathrm{u}} y_{\mathrm{d}}^{\dagger} \Big) - 3 a_{\mathrm{e}} \operatorname{tr}\Big(y_{\mathrm{e}} y_{\mathrm{e}}^{\dagger} y_{\mathrm{e}} y_{\mathrm{e}}^{\dagger} \Big) \\
&- \frac{2}{5} y_{\mathrm{e}} \Big[135 g_1^4 M_1 + 9 g_1^2 g_2^2 M_1 + 9 g_1^2 g_2^2 M_2 + 75 g_2^4 M_2 + \Big(- 2 g_1^2 M_1 + 80 g_3^2 M_3 \, \theta_{\widetilde{\mathrm{g}}} \Big) \operatorname{tr}\Big(y_{\mathrm{d}} y_{\mathrm{d}}^{\dagger} \Big) \\
&+ 6 g_1^2 M_1 \operatorname{tr}\Big(y_{\mathrm{e}} y_{\mathrm{e}}^{\dagger} \Big) + 2 g_1^2 \operatorname{tr}\Big(y_{\mathrm{d}}^{\dagger} a_{\mathrm{d}} \Big) - 80 g_3^2 \operatorname{tr}\Big(y_{\mathrm{d}}^{\dagger} a_{\mathrm{d}} \Big) - 6 g_1^2 \operatorname{tr}\Big(y_{\mathrm{e}}^{\dagger} a_{\mathrm{e}} \Big) \\
&+ 90 \operatorname{tr}\Big(y_{\mathrm{d}} y_{\mathrm{d}}^{\dagger} a_{\mathrm{d}} y_{\mathrm{d}}^{\dagger} \Big) + 15 \operatorname{tr}\Big(y_{\mathrm{d}} y_{\mathrm{u}}^{\dagger} a_{\mathrm{u}} y_{\mathrm{d}}^{\dagger} \Big) + 30 \operatorname{tr}\Big(y_{\mathrm{e}} y_{\mathrm{e}}^{\dagger} a_{\mathrm{e}} y_{\mathrm{e}}^{\dagger} \Big) + 15 \operatorname{tr}\Big(y_{\mathrm{u}} y_{\mathrm{d}}^{\dagger} a_{\mathrm{d}} y_{\mathrm{u}}^{\dagger} \Big) \Big],
\end{aligned} \tag{B.27}
$$

$$
\begin{aligned}
\beta_{a_{\mathrm{u}}}^{(1)} &= 2 y_{\mathrm{u}} y_{\mathrm{d}}^{\dagger} a_{\mathrm{d}} + 4 y_{\mathrm{u}} y_{\mathrm{u}}^{\dagger} a_{\mathrm{u}} + a_{\mathrm{u}} y_{\mathrm{d}}^{\dagger} y_{\mathrm{d}} + 5 a_{\mathrm{u}} y_{\mathrm{u}}^{\dagger} y_{\mathrm{u}} - \frac{13}{15} g_1^2 a_{\mathrm{u}} - 3 g_2^2 a_{\mathrm{u}} + \frac{16}{3} \Big(\theta_{\widetilde{\mathrm{g}}} - 2 \Big) g_3^2 a_{\mathrm{u}} \\
&+ 3 a_{\mathrm{u}} \operatorname{tr}\Big(y_{\mathrm{u}} y_{\mathrm{u}}^{\dagger} \Big) + y_{\mathrm{u}} \Big[6 g_2^2 M_2 + 6 \operatorname{tr}\Big(y_{\mathrm{u}}^{\dagger} a_{\mathrm{u}} \Big) + \frac{26}{15} g_1^2 M_1 + \frac{32}{3} g_3^2 M_3 \, \theta_{\widetilde{\mathrm{g}}} \Big],
\end{aligned} \tag{B.28}
$$

$$
\begin{aligned}
\beta_{a_{\mathrm{u}}}^{(2)} &= \frac{4}{5} g_1^2 y_{\mathrm{u}} y_{\mathrm{d}}^{\dagger} a_{\mathrm{d}} - \frac{4}{5} g_1^2 M_1 y_{\mathrm{u}} y_{\mathrm{u}}^{\dagger} y_{\mathrm{u}} - 12 g_2^2 M_2 y_{\mathrm{u}} y_{\mathrm{u}}^{\dagger} y_{\mathrm{u}} + \frac{6}{5} g_1^2 y_{\mathrm{u}} y_{\mathrm{u}}^{\dagger} a_{\mathrm{u}} \\
&+ 6 g_2^2 y_{\mathrm{u}} y_{\mathrm{u}}^{\dagger} a_{\mathrm{u}} + \frac{2}{5} g_1^2 a_{\mathrm{u}} y_{\mathrm{d}}^{\dagger} y_{\mathrm{d}} + 12 g_2^2 a_{\mathrm{u}} y_{\mathrm{u}}^{\dagger} y_{\mathrm{u}} - 4 y_{\mathrm{u}} y_{\mathrm{d}}^{\dagger} y_{\mathrm{d}} y_{\mathrm{d}}^{\dagger} a_{\mathrm{d}} \\
&- 2 y_{\mathrm{u}} y_{\mathrm{d}}^{\dagger} y_{\mathrm{d}} y_{\mathrm{u}}^{\dagger} a_{\mathrm{u}} - 4 y_{\mathrm{u}} y_{\mathrm{d}}^{\dagger} a_{\mathrm{d}} y_{\mathrm{d}}^{\dagger} y_{\mathrm{d}} - 4 y_{\mathrm{u}} y_{\mathrm{d}}^{\dagger} a_{\mathrm{d}} y_{\mathrm{u}}^{\dagger} y_{\mathrm{u}} - 6 y_{\mathrm{u}} y_{\mathrm{u}}^{\dagger} y_{\mathrm{u}} y_{\mathrm{u}}^{\dagger} a_{\mathrm{u}} \\
&- 8 y_{\mathrm{u}} y_{\mathrm{u}}^{\dagger} a_{\mathrm{u}} y_{\mathrm{u}}^{\dagger} y_{\mathrm{u}} - 2 a_{\mathrm{u}} y_{\mathrm{d}}^{\dagger} y_{\mathrm{d}} y_{\mathrm{d}}^{\dagger} y_{\mathrm{d}} - 4 a_{\mathrm{u}} y_{\mathrm{d}}^{\dagger} y_{\mathrm{d}} y_{\mathrm{u}}^{\dagger} y_{\mathrm{u}} - 6 a_{\mathrm{u}} y_{\mathrm{u}}^{\dagger} y_{\mathrm{u}} y_{\mathrm{u}}^{\dagger} y_{\mathrm{u}} + \frac{2743}{450} g_1^4 a_{\mathrm{u}} \\
&+ g_1^2 g_2^2 a_{\mathrm{u}} + \frac{15}{2} g_2^4 a_{\mathrm{u}} + \frac{136}{45} g_1^2 g_3^2 a_{\mathrm{u}} + 8 g_2^2 g_3^2 a_{\mathrm{u}} + \frac{128}{9} g_3^4 a_{\mathrm{u}} - 6 y_{\mathrm{u}} y_{\mathrm{d}}^{\dagger} a_{\mathrm{d}} \operatorname{tr}\Big(y_{\mathrm{d}} y_{\mathrm{d}}^{\dagger} \Big) \\
&- 3 a_{\mathrm{u}} y_{\mathrm{d}}^{\dagger} y_{\mathrm{d}} \operatorname{tr}\Big(y_{\mathrm{d}} y_{\mathrm{d}}^{\dagger} \Big) - 2 y_{\mathrm{u}} y_{\mathrm{d}}^{\dagger} a_{\mathrm{d}} \operatorname{tr}\Big(y_{\mathrm{e}} y_{\mathrm{e}}^{\dagger} \Big) - a_{\mathrm{u}} y_{\mathrm{d}}^{\dagger} y_{\mathrm{d}} \operatorname{tr}\Big(y_{\mathrm{e}} y_{\mathrm{e}}^{\dagger} \Big) \\
&- 12 y_{\mathrm{u}} y_{\mathrm{u}}^{\dagger} a_{\mathrm{u}} \operatorname{tr}\Big(y_{\mathrm{u}} y_{\mathrm{u}}^{\dagger} \Big) - 15 a_{\mathrm{u}} y_{\mathrm{u}}^{\dagger} y_{\mathrm{u}} \operatorname{tr}\Big(y_{\mathrm{u}} y_{\mathrm{u}}^{\dagger} \Big) + \frac{4}{5} g_1^2 a_{\mathrm{u}} \operatorname{tr}\Big(y_{\mathrm{u}} y_{\mathrm{u}}^{\dagger} \Big) \\
&+ 16 g_3^2 a_{\mathrm{u}} \operatorname{tr}\Big(y_{\mathrm{u}} y_{\mathrm{u}}^{\dagger} \Big) - \frac{2}{5} y_{\mathrm{u}} y_{\mathrm{d}}^{\dagger} y_{\mathrm{d}} \Big[15 \operatorname{tr}\Big(y_{\mathrm{d}}^{\dagger} a_{\mathrm{d}} \Big) + 2 g_1^2 M_1 + 5 \operatorname{tr}\Big(y_{\mathrm{e}}^{\dagger} a_{\mathrm{e}} \Big) \Big]
\end{aligned}
$$

$$
\begin{aligned}
&- 18 y_{\mathrm{u}} y_{\mathrm{u}}^{\dagger} y_{\mathrm{u}} \operatorname{tr}\Big(y_{\mathrm{u}}^{\dagger} a_{\mathrm{u}}\Big) - 3 a_{\mathrm{u}} \operatorname{tr}\Big(y_{\mathrm{d}} y_{\mathrm{u}}^{\dagger} y_{\mathrm{u}} y_{\mathrm{d}}^{\dagger}\Big) - 9 a_{\mathrm{u}} \operatorname{tr}\Big(y_{\mathrm{u}} y_{\mathrm{u}}^{\dagger} y_{\mathrm{u}} y_{\mathrm{u}}^{\dagger}\Big) \\
&- \frac{2}{225} y_{\mathrm{u}} \Big\{ 2743 g_1^4 M_1 + 225 g_1^2 g_2^2 M_1 + 680 g_1^2 g_3^2 M_1 + 680 g_1^2 g_3^2 M_3 \, \theta_{\widetilde{\mathrm{g}}} + 1800 g_2^2 g_3^2 M_3 \, \theta_{\widetilde{\mathrm{g}}} \\
&+ 6400 g_3^4 M_3 \, \theta_{\widetilde{\mathrm{g}}} + 225 g_1^2 g_2^2 M_2 + 3375 g_2^4 M_2 + 1800 g_2^2 g_3^2 M_2 \\
&- 180 \Big(20 g_3^2 + g_1^2\Big) \operatorname{tr}\Big(y_{\mathrm{u}}^{\dagger} a_{\mathrm{u}}\Big) + 675 \operatorname{tr}\Big(y_{\mathrm{d}} y_{\mathrm{u}}^{\dagger} a_{\mathrm{u}} y_{\mathrm{d}}^{\dagger}\Big) + 675 \operatorname{tr}\Big(y_{\mathrm{u}} y_{\mathrm{d}}^{\dagger} a_{\mathrm{d}} y_{\mathrm{u}}^{\dagger}\Big) \\
&+ 4050 \operatorname{tr}\Big[y_{\mathrm{u}} y_{\mathrm{u}}^{\dagger} a_{\mathrm{u}} y_{\mathrm{u}}^{\dagger} + 180 \Big(20 g_3^2 M_3 \, \theta_{\widetilde{\mathrm{g}}} + g_1^2 M_1\Big) \operatorname{tr}\Big(y_{\mathrm{u}} y_{\mathrm{u}}^{\dagger}\Big)\Big] \Big\}. \qquad \text{(B.29)}
\end{aligned}
$$

Bilinear Soft-Breaking Parameters

$$
\begin{aligned}
\beta_{B_\mu}^{(1)} &= \frac{6}{5} g_1^2 M_1 \mu + 6 g_2^2 M_2 \mu + B_\mu \Big[3 \operatorname{tr}\Big(y_{\mathrm{d}} y_{\mathrm{d}}^{\dagger}\Big) - 3 g_2^2 + 3 \operatorname{tr}\Big(y_{\mathrm{u}} y_{\mathrm{u}}^{\dagger}\Big) - \frac{3}{5} g_1^2 + \operatorname{tr}\Big(y_{\mathrm{e}} y_{\mathrm{e}}^{\dagger}\Big)\Big] \\
&\quad + 6 \mu \operatorname{tr}\Big(y_{\mathrm{d}}^{\dagger} a_{\mathrm{d}}\Big) + 2 \mu \operatorname{tr}\Big(y_{\mathrm{e}}^{\dagger} a_{\mathrm{e}}\Big) + 6 \mu \operatorname{tr}\Big(y_{\mathrm{u}}^{\dagger} a_{\mathrm{u}}\Big), \qquad \text{(B.30)} \\
\beta_{B_\mu}^{(2)} &= B_\mu \Big[\frac{207}{50} g_1^4 + \frac{9}{5} g_1^2 g_2^2 + \frac{15}{2} g_2^4 + \frac{2}{5} \Big(g_1^2 - 40 g_3^2\Big) \operatorname{tr}\Big(y_{\mathrm{d}} y_{\mathrm{d}}^{\dagger}\Big) + \frac{6}{5} g_1^2 \operatorname{tr}\Big(y_{\mathrm{e}} y_{\mathrm{e}}^{\dagger}\Big) + \frac{4}{5} g_1^2 \operatorname{tr}\Big(y_{\mathrm{u}} y_{\mathrm{u}}^{\dagger}\Big) \\
&\quad + 16 g_3^2 \operatorname{tr}\Big(y_{\mathrm{u}} y_{\mathrm{u}}^{\dagger}\Big) - 9 \operatorname{tr}\Big(y_{\mathrm{d}} y_{\mathrm{d}}^{\dagger} y_{\mathrm{d}} y_{\mathrm{d}}^{\dagger}\Big) - 6 \operatorname{tr}\Big(y_{\mathrm{d}} y_{\mathrm{u}}^{\dagger} y_{\mathrm{u}} y_{\mathrm{d}}^{\dagger}\Big) - 3 \operatorname{tr}\Big(y_{\mathrm{e}} y_{\mathrm{e}}^{\dagger} y_{\mathrm{e}} y_{\mathrm{e}}^{\dagger}\Big) \\
&\quad - 9 \operatorname{tr}\Big(y_{\mathrm{u}} y_{\mathrm{u}}^{\dagger} y_{\mathrm{u}} y_{\mathrm{u}}^{\dagger}\Big)\Big] - \frac{2}{25} \mu \Big[207 g_1^4 M_1 + 45 g_1^2 g_2^2 M_1 + 45 g_1^2 g_2^2 M_2 + 375 g_2^4 M_2 \\
&\quad + 30 g_1^2 M_1 \operatorname{tr}\Big(y_{\mathrm{e}} y_{\mathrm{e}}^{\dagger}\Big) + 10 \Big(g_1^2 M_1 - 40 g_3^2 M_3 \, \theta_{\widetilde{\mathrm{g}}}\Big) \operatorname{tr}\Big(y_{\mathrm{d}} y_{\mathrm{d}}^{\dagger}\Big) + 20 g_1^2 M_1 \operatorname{tr}\Big(y_{\mathrm{u}} y_{\mathrm{u}}^{\dagger}\Big) \\
&\quad + 400 g_3^2 M_3 \, \theta_{\widetilde{\mathrm{g}}} \operatorname{tr}\Big(y_{\mathrm{u}} y_{\mathrm{u}}^{\dagger}\Big) + 10 g_1^2 \operatorname{tr}\Big(y_{\mathrm{d}}^{\dagger} a_{\mathrm{d}}\Big) - 400 g_3^2 \operatorname{tr}\Big(y_{\mathrm{d}}^{\dagger} a_{\mathrm{d}}\Big) - 30 g_1^2 \operatorname{tr}\Big(y_{\mathrm{e}}^{\dagger} a_{\mathrm{e}}\Big) - 20 g_1^2 \operatorname{tr}\Big(y_{\mathrm{u}}^{\dagger} a_{\mathrm{u}}\Big) \\
&\quad + 450 \operatorname{tr}\Big(y_{\mathrm{d}} y_{\mathrm{d}}^{\dagger} a_{\mathrm{d}} y_{\mathrm{d}}^{\dagger}\Big) + 150 \operatorname{tr}\Big(y_{\mathrm{d}} y_{\mathrm{u}}^{\dagger} a_{\mathrm{u}} y_{\mathrm{d}}^{\dagger}\Big) + 150 \operatorname{tr}\Big(y_{\mathrm{e}} y_{\mathrm{e}}^{\dagger} a_{\mathrm{e}} y_{\mathrm{e}}^{\dagger}\Big) + 150 \operatorname{tr}\Big(y_{\mathrm{u}} y_{\mathrm{d}}^{\dagger} a_{\mathrm{d}} y_{\mathrm{u}}^{\dagger}\Big) \\
&\quad + 450 \operatorname{tr}\Big(y_{\mathrm{u}} y_{\mathrm{u}}^{\dagger} a_{\mathrm{u}} y_{\mathrm{u}}^{\dagger}\Big) - 400 g_3^2 \operatorname{tr}\Big(y_{\mathrm{u}}^{\dagger} a_{\mathrm{u}}\Big)\Big], \qquad \text{(B.31)} \\
\beta_{B_3}^{(1)} &= -12 g_3^2 B_3, \qquad \text{(B.32)} \\
\beta_{B_3}^{(2)} &= 72 g_3^4 B_3. \qquad \text{(B.33)}
\end{aligned}
$$

Soft-Breaking Scalar Masses

$$\sigma_{1,1} = \sqrt{\frac{3}{5}} g_1 \Big[m^2_{\mathrm{H}_u} - 2\,\mathrm{tr}\Big(m^2_{\mathrm{u}}\Big) - \mathrm{tr}\Big(m^2_{\ell}\Big) - m^2_{\mathrm{H}_d} + \mathrm{tr}\Big(m^2_{\mathrm{d}}\Big) + \mathrm{tr}\Big(m^2_{\mathrm{e}}\Big) + \mathrm{tr}\Big(m^2_{q}\Big)\Big], \tag{B.34}$$

$$\sigma_{2,11} = \frac{1}{10} g_1^2 \Big[2\,\mathrm{tr}\Big(m^2_{\mathrm{d}}\Big) + 3\,\mathrm{tr}\Big(m^2_{\ell}\Big) + 3m^2_{\mathrm{H}_d} + 3m^2_{\mathrm{H}_u} + 6\,\mathrm{tr}\Big(m^2_{\mathrm{e}}\Big) + 8\,\mathrm{tr}\Big(m^2_{\mathrm{u}}\Big) + \mathrm{tr}\Big(m^2_{q}\Big)\Big], \tag{B.35}$$

$$\begin{aligned}
\sigma_{3,1} = \frac{1}{20\sqrt{15}} g_1 \Big[& 9g_1^2 m^2_{\mathrm{H}_u} - 9g_1^2 m^2_{\mathrm{H}_d} - 45g_2^2 m^2_{\mathrm{H}_d} + 45g_2^2 m^2_{\mathrm{H}_u} + 4\Big(20g_3^2 + g_1^2\Big)\,\mathrm{tr}\Big(m^2_{\mathrm{d}}\Big) \\
& - 9g_1^2\,\mathrm{tr}\Big(m^2_{\ell}\Big) - 45g_2^2\,\mathrm{tr}\Big(m^2_{\ell}\Big) + g_1^2\,\mathrm{tr}\Big(m^2_{q}\Big) + 45g_2^2\,\mathrm{tr}\Big(m^2_{q}\Big) + 80g_3^2\,\mathrm{tr}\Big(m^2_{q}\Big) - 32g_1^2\,\mathrm{tr}\Big(m^2_{\mathrm{u}}\Big) \\
& - 160g_3^2\,\mathrm{tr}\Big(m^2_{q}\Big) + 90m^2_{\mathrm{H}_d}\,\mathrm{tr}\Big(y_{\mathrm{d}} y^{\dagger}_{\mathrm{d}}\Big) + 30m^2_{\mathrm{H}_d}\,\mathrm{tr}\Big(y_{\mathrm{e}} y^{\dagger}_{\mathrm{e}}\Big) - 90m^2_{\mathrm{H}_u}\,\mathrm{tr}\Big(y_{\mathrm{u}} y^{\dagger}_{\mathrm{u}}\Big) \\
& - 30\,\mathrm{tr}\Big(y_{\mathrm{d}} m^{2*}_{q} y^{\dagger}_{\mathrm{d}}\Big) - 60\,\mathrm{tr}\Big(y_{\mathrm{e}} y^{\dagger}_{\mathrm{e}} m^{2*}_{\mathrm{e}}\Big) + 30\,\mathrm{tr}\Big(y_{\mathrm{e}} m^{2*}_{\ell} y^{\dagger}_{\mathrm{e}}\Big) + 120\,\mathrm{tr}\Big(y_{\mathrm{u}} y^{\dagger}_{\mathrm{u}} m^{2*}_{\mathrm{u}}\Big) \\
& - 30\,\mathrm{tr}\Big(y_{\mathrm{u}} m^{2*}_{q} y^{\dagger}_{\mathrm{u}}\Big) + 36g_1^2\,\mathrm{tr}\Big(m^2_{\mathrm{e}}\Big) - 60\,\mathrm{tr}\Big(y_{\mathrm{d}} y^{\dagger}_{\mathrm{d}} m^{2*}_{\mathrm{d}}\Big)\Big],
\end{aligned} \tag{B.36}$$

$$\sigma_{2,2} = \frac{1}{2}\Big[3\,\mathrm{tr}\Big(m^2_{q}\Big) + m^2_{\mathrm{H}_d} + m^2_{\mathrm{H}_u} + \mathrm{tr}\Big(m^2_{\ell}\Big)\Big], \tag{B.37}$$

$$\sigma_{2,3} = \frac{1}{2}\Big[2\,\mathrm{tr}\Big(m^2_{q}\Big) + 3(1+\theta_{\widetilde{\mathrm{g}}}) m_3^2 + \mathrm{tr}\Big(m^2_{\mathrm{d}}\Big) + \mathrm{tr}\Big(m^2_{\mathrm{u}}\Big)\Big]. \tag{B.38}$$

$$\begin{aligned}
\beta^{(1)}_{m^2_q} = & -\frac{2}{15} g_1^2 |M_1|^2 - \frac{32}{3} g_3^2 |M_3|^2\,\theta_{\widetilde{\mathrm{g}}} - 6g_2^2 |M_2|^2 + 2m^2_{\mathrm{H}_d} y^{\dagger}_{\mathrm{d}} y_{\mathrm{d}} + 2m^2_{\mathrm{H}_u} y^{\dagger}_{\mathrm{u}} y_{\mathrm{u}} + 2a^{\dagger}_{\mathrm{d}} a_{\mathrm{d}} \\
& + 2a^{\dagger}_{\mathrm{u}} a_{\mathrm{u}} + m^2_q y^{\dagger}_{\mathrm{d}} y_{\mathrm{d}} + m^2_q y^{\dagger}_{\mathrm{u}} y_{\mathrm{u}} + 2y^{\dagger}_{\mathrm{d}} m^2_{\mathrm{d}} y_{\mathrm{d}} + y^{\dagger}_{\mathrm{d}} y_{\mathrm{d}} m^2_q + 2y^{\dagger}_{\mathrm{u}} m^2_{\mathrm{u}} y_{\mathrm{u}} \\
& + y^{\dagger}_{\mathrm{u}} y_{\mathrm{u}} m^2_q + \frac{1}{\sqrt{15}} g_1 \sigma_{1,1},
\end{aligned} \tag{B.39}$$

$$\begin{aligned}
\beta^{(2)}_{m^2_q} = & \frac{2}{5} g_1^2 g_2^2 |M_2|^2 + 33 g_2^4 |M_2|^2 + 32 g_2^2 g_3^2 |M_2|^2 \\
& + \frac{16}{45} g_3^2 \Big\{ 15\Big[10 g_3^2 M_3\,\theta_{\widetilde{\mathrm{g}}} + 3g_2^2\Big(2M_3\,\theta_{\widetilde{\mathrm{g}}} + M_2\Big)\Big] + g_1^2\Big[2M_3\,\theta_{\widetilde{\mathrm{g}}} + M_1\Big]\Big\} M_3^*\,\theta_{\widetilde{\mathrm{g}}} + \frac{1}{5} g_1^2 g_2^2 M_1 M_2^* \\
& + 16 g_2^2 g_3^2 M_3 M_2^*\,\theta_{\widetilde{\mathrm{g}}} + \frac{4}{5} g_1^2 m^2_{\mathrm{H}_d} y^{\dagger}_{\mathrm{d}} y_{\mathrm{d}} + \frac{8}{5} g_1^2 m^2_{\mathrm{H}_u} y^{\dagger}_{\mathrm{u}} y_{\mathrm{u}} \\
& + \frac{1}{225} g_1^2 M_1^* \Big[\Big\{ 5\Big[16 g_3^2\Big(2M_1 + M_3\,\theta_{\widetilde{\mathrm{g}}}\Big) + 9g_2^2\Big(2M_1 + M_2\Big)\Big] + 597 g_1^2 M_1 \Big\} \\
& + 180\Big\{ 2M_1 y^{\dagger}_{\mathrm{d}} y_{\mathrm{d}} - 2y^{\dagger}_{\mathrm{u}} a_{\mathrm{u}} + 4M_1 y^{\dagger}_{\mathrm{u}} y_{\mathrm{u}} - y^{\dagger}_{\mathrm{d}} a_{\mathrm{d}} \Big\} \Big] \\
& - \frac{4}{5} g_1^2 M_1 a^{\dagger}_{\mathrm{d}} y_{\mathrm{d}} + \frac{4}{5} g_1^2 a^{\dagger}_{\mathrm{d}} a_{\mathrm{d}} - \frac{8}{5} g_1^2 M_1 a^{\dagger}_{\mathrm{u}} y_{\mathrm{u}} + \frac{8}{5} g_1^2 a^{\dagger}_{\mathrm{u}} a_{\mathrm{u}} \\
& + \frac{2}{5} g_1^2 m^2_q y^{\dagger}_{\mathrm{d}} y_{\mathrm{d}} + \frac{4}{5} g_1^2 m^2_q y^{\dagger}_{\mathrm{u}} y_{\mathrm{u}} + \frac{4}{5} g_1^2 y^{\dagger}_{\mathrm{d}} m^2_{\mathrm{d}} y_{\mathrm{d}} + \frac{2}{5} g_1^2 y^{\dagger}_{\mathrm{d}} y_{\mathrm{d}} m^2_q \\
& + \frac{8}{5} g_1^2 y^{\dagger}_{\mathrm{u}} m^2_{\mathrm{u}} y_{\mathrm{u}} + \frac{4}{5} g_1^2 y^{\dagger}_{\mathrm{u}} y_{\mathrm{u}} m^2_q - 8 m^2_{\mathrm{H}_d} y^{\dagger}_{\mathrm{d}} y_{\mathrm{d}} y^{\dagger}_{\mathrm{d}} y_{\mathrm{d}} - 4 y^{\dagger}_{\mathrm{d}} y_{\mathrm{d}} a^{\dagger}_{\mathrm{d}} a_{\mathrm{d}} \\
& - 4 y^{\dagger}_{\mathrm{d}} a_{\mathrm{d}} a^{\dagger}_{\mathrm{d}} y_{\mathrm{d}} - 8 m^2_{\mathrm{H}_u} y^{\dagger}_{\mathrm{u}} y_{\mathrm{u}} y^{\dagger}_{\mathrm{u}} y_{\mathrm{u}} - 4 y^{\dagger}_{\mathrm{u}} y_{\mathrm{u}} a^{\dagger}_{\mathrm{u}} a_{\mathrm{u}} - 4 y^{\dagger}_{\mathrm{u}} a_{\mathrm{u}} a^{\dagger}_{\mathrm{u}} y_{\mathrm{u}} \\
& - 4 a^{\dagger}_{\mathrm{d}} y_{\mathrm{d}} y^{\dagger}_{\mathrm{d}} a_{\mathrm{d}} - 4 a^{\dagger}_{\mathrm{d}} a_{\mathrm{d}} y^{\dagger}_{\mathrm{d}} y_{\mathrm{d}} - 4 a^{\dagger}_{\mathrm{u}} y_{\mathrm{u}} y^{\dagger}_{\mathrm{u}} a_{\mathrm{u}} - 4 a^{\dagger}_{\mathrm{u}} a_{\mathrm{u}} y^{\dagger}_{\mathrm{u}} y_{\mathrm{u}} \\
& - 2 m^2_q y^{\dagger}_{\mathrm{d}} y_{\mathrm{d}} y^{\dagger}_{\mathrm{d}} y_{\mathrm{d}} - 2 m^2_q y^{\dagger}_{\mathrm{u}} y_{\mathrm{u}} y^{\dagger}_{\mathrm{u}} y_{\mathrm{u}} - 4 y^{\dagger}_{\mathrm{d}} m^2_{\mathrm{d}} y_{\mathrm{d}} y^{\dagger}_{\mathrm{d}} y_{\mathrm{d}} - 4 y^{\dagger}_{\mathrm{d}} y_{\mathrm{d}} m^2_q y^{\dagger}_{\mathrm{d}} y_{\mathrm{d}} \\
& - 4 y^{\dagger}_{\mathrm{d}} y_{\mathrm{d}} y^{\dagger}_{\mathrm{d}} m^2_{\mathrm{d}} y_{\mathrm{d}} - 2 y^{\dagger}_{\mathrm{d}} y_{\mathrm{d}} y^{\dagger}_{\mathrm{d}} y_{\mathrm{d}} m^2_q - 4 y^{\dagger}_{\mathrm{u}} m^2_{\mathrm{u}} y_{\mathrm{u}} y^{\dagger}_{\mathrm{u}} y_{\mathrm{u}} - 4 y^{\dagger}_{\mathrm{u}} y_{\mathrm{u}} m^2_q y^{\dagger}_{\mathrm{u}} y_{\mathrm{u}} \\
& - 4 y^{\dagger}_{\mathrm{u}} y_{\mathrm{u}} y^{\dagger}_{\mathrm{u}} m^2_{\mathrm{u}} y_{\mathrm{u}} - 2 y^{\dagger}_{\mathrm{u}} y_{\mathrm{u}} y^{\dagger}_{\mathrm{u}} y_{\mathrm{u}} m^2_q + 6 g_2^4 \sigma_{2,2} + \frac{32}{3} g_3^4 \sigma_{2,3} + \frac{2}{15} g_1^2 \sigma_{2,11} + 4 \frac{1}{\sqrt{15}} g_1 \sigma_{3,1}
\end{aligned}$$

$$
\begin{aligned}
&- 12m^2_{\mathrm{H}_d} y_{\mathrm{d}}^\dagger y_{\mathrm{d}} \operatorname{tr}\Big(y_{\mathrm{d}} y_{\mathrm{d}}^\dagger\Big) - 6a_{\mathrm{d}}^\dagger a_{\mathrm{d}} \operatorname{tr}\Big(y_{\mathrm{d}} y_{\mathrm{d}}^\dagger\Big) - 3m_q^2 y_{\mathrm{d}}^\dagger y_{\mathrm{d}} \operatorname{tr}\Big(y_{\mathrm{d}} y_{\mathrm{d}}^\dagger\Big) \\
&- 6y_{\mathrm{d}}^\dagger m_{\mathrm{d}}^2 y_{\mathrm{d}} \operatorname{tr}\Big(y_{\mathrm{d}} y_{\mathrm{d}}^\dagger\Big) - 3y_{\mathrm{d}}^\dagger y_{\mathrm{d}} m_q^2 \operatorname{tr}\Big(y_{\mathrm{d}} y_{\mathrm{d}}^\dagger\Big) - 4m^2_{\mathrm{H}_d} y_{\mathrm{d}}^\dagger y_{\mathrm{d}} \operatorname{tr}\Big(y_{\mathrm{e}} y_{\mathrm{e}}^\dagger\Big) \\
&- 2a_{\mathrm{d}}^\dagger a_{\mathrm{d}} \operatorname{tr}\Big(y_{\mathrm{e}} y_{\mathrm{e}}^\dagger\Big) - m_q^2 y_{\mathrm{d}}^\dagger y_{\mathrm{d}} \operatorname{tr}\Big(y_{\mathrm{e}} y_{\mathrm{e}}^\dagger\Big) - 2y_{\mathrm{d}}^\dagger m_{\mathrm{d}}^2 y_{\mathrm{d}} \operatorname{tr}\Big(y_{\mathrm{e}} y_{\mathrm{e}}^\dagger\Big) \\
&- y_{\mathrm{d}}^\dagger y_{\mathrm{d}} m_q^2 \operatorname{tr}\Big(y_{\mathrm{e}} y_{\mathrm{e}}^\dagger\Big) - 12m^2_{\mathrm{H}_u} y_{\mathrm{u}}^\dagger y_{\mathrm{u}} \operatorname{tr}\Big(y_{\mathrm{u}} y_{\mathrm{u}}^\dagger\Big) - 6a_{\mathrm{u}}^\dagger a_{\mathrm{u}} \operatorname{tr}\Big(y_{\mathrm{u}} y_{\mathrm{u}}^\dagger\Big) \\
&- 3m_q^2 y_{\mathrm{u}}^\dagger y_{\mathrm{u}} \operatorname{tr}\Big(y_{\mathrm{u}} y_{\mathrm{u}}^\dagger\Big) - 6y_{\mathrm{u}}^\dagger m_{\mathrm{u}}^2 y_{\mathrm{u}} \operatorname{tr}\Big(y_{\mathrm{u}} y_{\mathrm{u}}^\dagger\Big) - 3y_{\mathrm{u}}^\dagger y_{\mathrm{u}} m_q^2 \operatorname{tr}\Big(y_{\mathrm{u}} y_{\mathrm{u}}^\dagger\Big) \\
&- 6a_{\mathrm{d}}^\dagger y_{\mathrm{d}} \operatorname{tr}\Big(y_{\mathrm{d}}^\dagger a_{\mathrm{d}}\Big) - 2a_{\mathrm{d}}^\dagger y_{\mathrm{d}} \operatorname{tr}\Big(y_{\mathrm{e}}^\dagger a_{\mathrm{e}}\Big) - 6a_{\mathrm{u}}^\dagger y_{\mathrm{u}} \operatorname{tr}\Big(y_{\mathrm{u}}^\dagger a_{\mathrm{u}}\Big) \\
&- 6y_{\mathrm{d}}^\dagger a_{\mathrm{d}} \operatorname{tr}\Big(a_{\mathrm{d}}^* y_{\mathrm{d}}^T\Big) - 6y_{\mathrm{d}}^\dagger y_{\mathrm{d}} \operatorname{tr}\Big(a_{\mathrm{d}}^* a_{\mathrm{d}}^T\Big) - 2y_{\mathrm{d}}^\dagger a_{\mathrm{d}} \operatorname{tr}\Big(a_{\mathrm{e}}^* y_{\mathrm{e}}^T\Big) \\
&- 2y_{\mathrm{d}}^\dagger y_{\mathrm{d}} \operatorname{tr}\Big(a_{\mathrm{e}}^* a_{\mathrm{e}}^T\Big) - 6y_{\mathrm{u}}^\dagger a_{\mathrm{u}} \operatorname{tr}\Big(a_{\mathrm{u}}^* y_{\mathrm{u}}^T\Big) - 6y_{\mathrm{u}}^\dagger y_{\mathrm{u}} \operatorname{tr}\Big(a_{\mathrm{u}}^* a_{\mathrm{u}}^T\Big) \\
&- 6y_{\mathrm{d}}^\dagger y_{\mathrm{d}} \operatorname{tr}\Big(m_{\mathrm{d}}^2 y_{\mathrm{d}} y_{\mathrm{d}}^\dagger\Big) - 2y_{\mathrm{d}}^\dagger y_{\mathrm{d}} \operatorname{tr}\Big(m_{\mathrm{e}}^2 y_{\mathrm{e}} y_{\mathrm{e}}^\dagger\Big) - 2y_{\mathrm{d}}^\dagger y_{\mathrm{d}} \operatorname{tr}\Big(m_\ell^2 y_{\mathrm{e}}^\dagger y_{\mathrm{e}}\Big) \\
&- 6y_{\mathrm{d}}^\dagger y_{\mathrm{d}} \operatorname{tr}\Big(m_q^2 y_{\mathrm{d}}^\dagger y_{\mathrm{d}}\Big) - 6y_{\mathrm{u}}^\dagger y_{\mathrm{u}} \operatorname{tr}\Big(m_q^2 y_{\mathrm{u}}^\dagger y_{\mathrm{u}}\Big) - 6y_{\mathrm{u}}^\dagger y_{\mathrm{u}} \operatorname{tr}\Big(m_{\mathrm{u}}^2 y_{\mathrm{u}} y_{\mathrm{u}}^\dagger\Big),
\end{aligned}
\tag{B.40}
$$

$$
\begin{aligned}
\beta^{(1)}_{m_\ell^2} = &-\frac{6}{5} g_1^2 |M_1|^2 - 6g_2^2 |M_2|^2 + 2m^2_{\mathrm{H}_d} y_{\mathrm{e}}^\dagger y_{\mathrm{e}} + 2a_{\mathrm{e}}^\dagger a_{\mathrm{e}} + m_\ell^2 y_{\mathrm{e}}^\dagger y_{\mathrm{e}} + 2y_{\mathrm{e}}^\dagger m_{\mathrm{e}}^2 y_{\mathrm{e}} \\
&+ y_{\mathrm{e}}^\dagger y_{\mathrm{e}} m_\ell^2 - \sqrt{\frac{3}{5}} g_1 \sigma_{1,1},
\end{aligned}
\tag{B.41}
$$

$$
\begin{aligned}
\beta^{(2)}_{m_\ell^2} = &\frac{3}{5} g_2^2 \Big[3g_1^2 \Big(2M_2 + M_1\Big) + 55 g_2^2 M_2\Big] M_2^* + \frac{12}{5} g_1^2 m^2_{\mathrm{H}_d} y_{\mathrm{e}}^\dagger y_{\mathrm{e}} \\
&+ \frac{3}{25} g_1^2 M_1^* \Big\{ - 20 y_{\mathrm{e}}^\dagger a_{\mathrm{e}} + 3\Big[5g_2^2 \Big(2M_1 + M_2\Big) + 69 g_1^2 M_1\Big] + 40 M_1 y_{\mathrm{e}}^\dagger y_{\mathrm{e}}\Big\} - \frac{12}{5} g_1^2 M_1 a_{\mathrm{e}}^\dagger y_{\mathrm{e}} \\
&+ \frac{12}{5} g_1^2 a_{\mathrm{e}}^\dagger a_{\mathrm{e}} + \frac{6}{5} g_1^2 m_\ell^2 y_{\mathrm{e}}^\dagger y_{\mathrm{e}} + \frac{12}{5} g_1^2 y_{\mathrm{e}}^\dagger m_{\mathrm{e}}^2 y_{\mathrm{e}} + \frac{6}{5} g_1^2 y_{\mathrm{e}}^\dagger y_{\mathrm{e}} m_\ell^2 \\
&- 8m^2_{\mathrm{H}_d} y_{\mathrm{e}}^\dagger y_{\mathrm{e}} y_{\mathrm{e}}^\dagger y_{\mathrm{e}} - 4y_{\mathrm{e}}^\dagger y_{\mathrm{e}} a_{\mathrm{e}}^\dagger a_{\mathrm{e}} - 4y_{\mathrm{e}}^\dagger a_{\mathrm{e}} a_{\mathrm{e}}^\dagger y_{\mathrm{e}} - 4a_{\mathrm{e}}^\dagger y_{\mathrm{e}} y_{\mathrm{e}}^\dagger a_{\mathrm{e}} \\
&- 4a_{\mathrm{e}}^\dagger a_{\mathrm{e}} y_{\mathrm{e}}^\dagger y_{\mathrm{e}} - 2m_\ell^2 y_{\mathrm{e}}^\dagger y_{\mathrm{e}} y_{\mathrm{e}}^\dagger y_{\mathrm{e}} - 4y_{\mathrm{e}}^\dagger m_{\mathrm{e}}^2 y_{\mathrm{e}} y_{\mathrm{e}}^\dagger y_{\mathrm{e}} - 4y_{\mathrm{e}}^\dagger y_{\mathrm{e}} m_\ell^2 y_{\mathrm{e}}^\dagger y_{\mathrm{e}} \\
&- 4y_{\mathrm{e}}^\dagger y_{\mathrm{e}} y_{\mathrm{e}}^\dagger m_{\mathrm{e}}^2 y_{\mathrm{e}} - 2y_{\mathrm{e}}^\dagger y_{\mathrm{e}} y_{\mathrm{e}}^\dagger y_{\mathrm{e}} m_\ell^2 + 6g_2^4 \sigma_{2,2} + \frac{6}{5} g_1^2 \sigma_{2,11} - 4\sqrt{\frac{3}{5}} g_1 \sigma_{3,1} \\
&- 12m^2_{\mathrm{H}_d} y_{\mathrm{e}}^\dagger y_{\mathrm{e}} \operatorname{tr}\Big(y_{\mathrm{d}} y_{\mathrm{d}}^\dagger\Big) - 6a_{\mathrm{e}}^\dagger a_{\mathrm{e}} \operatorname{tr}\Big(y_{\mathrm{d}} y_{\mathrm{d}}^\dagger\Big) - 3m_\ell^2 y_{\mathrm{e}}^\dagger y_{\mathrm{e}} \operatorname{tr}\Big(y_{\mathrm{d}} y_{\mathrm{d}}^\dagger\Big) \\
&- 6y_{\mathrm{e}}^\dagger m_{\mathrm{e}}^2 y_{\mathrm{e}} \operatorname{tr}\Big(y_{\mathrm{d}} y_{\mathrm{d}}^\dagger\Big) - 3y_{\mathrm{e}}^\dagger y_{\mathrm{e}} m_\ell^2 \operatorname{tr}\Big(y_{\mathrm{d}} y_{\mathrm{d}}^\dagger\Big) - 4m^2_{\mathrm{H}_d} y_{\mathrm{e}}^\dagger y_{\mathrm{e}} \operatorname{tr}\Big(y_{\mathrm{e}} y_{\mathrm{e}}^\dagger\Big) \\
&- 2a_{\mathrm{e}}^\dagger a_{\mathrm{e}} \operatorname{tr}\Big(y_{\mathrm{e}} y_{\mathrm{e}}^\dagger\Big) - m_\ell^2 y_{\mathrm{e}}^\dagger y_{\mathrm{e}} \operatorname{tr}\Big(y_{\mathrm{e}} y_{\mathrm{e}}^\dagger\Big) - 2y_{\mathrm{e}}^\dagger m_{\mathrm{e}}^2 y_{\mathrm{e}} \operatorname{tr}\Big(y_{\mathrm{e}} y_{\mathrm{e}}^\dagger\Big) \\
&- y_{\mathrm{e}}^\dagger y_{\mathrm{e}} m_\ell^2 \operatorname{tr}\Big(y_{\mathrm{e}} y_{\mathrm{e}}^\dagger\Big) - 6a_{\mathrm{e}}^\dagger y_{\mathrm{e}} \operatorname{tr}\Big(y_{\mathrm{d}}^\dagger a_{\mathrm{d}}\Big) - 2a_{\mathrm{e}}^\dagger y_{\mathrm{e}} \operatorname{tr}\Big(y_{\mathrm{e}}^\dagger a_{\mathrm{e}}\Big) \\
&- 6y_{\mathrm{e}}^\dagger a_{\mathrm{e}} \operatorname{tr}\Big(a_{\mathrm{d}}^* y_{\mathrm{d}}^T\Big) - 6y_{\mathrm{e}}^\dagger y_{\mathrm{e}} \operatorname{tr}\Big(a_{\mathrm{d}}^* a_{\mathrm{d}}^T\Big) - 2y_{\mathrm{e}}^\dagger a_{\mathrm{e}} \operatorname{tr}\Big(a_{\mathrm{e}}^* y_{\mathrm{e}}^T\Big) \\
&- 2y_{\mathrm{e}}^\dagger y_{\mathrm{e}} \operatorname{tr}\Big(a_{\mathrm{e}}^* a_{\mathrm{e}}^T\Big) - 6y_{\mathrm{e}}^\dagger y_{\mathrm{e}} \operatorname{tr}\Big(m_{\mathrm{d}}^2 y_{\mathrm{d}} y_{\mathrm{d}}^\dagger\Big) - 2y_{\mathrm{e}}^\dagger y_{\mathrm{e}} \operatorname{tr}\Big(m_{\mathrm{e}}^2 y_{\mathrm{e}} y_{\mathrm{e}}^\dagger\Big) \\
&- 2y_{\mathrm{e}}^\dagger y_{\mathrm{e}} \operatorname{tr}\Big(m_\ell^2 y_{\mathrm{e}}^\dagger y_{\mathrm{e}}\Big) - 6y_{\mathrm{e}}^\dagger y_{\mathrm{e}} \operatorname{tr}\Big(m_q^2 y_{\mathrm{d}}^\dagger y_{\mathrm{d}}\Big),
\end{aligned}
\tag{B.42}
$$

$$
\begin{aligned}
\beta^{(1)}_{m^2_{\mathrm{H}_d}} = &-\frac{6}{5} g_1^2 |M_1|^2 - 6g_2^2 |M_2|^2 - \sqrt{\frac{3}{5}} g_1 \sigma_{1,1} + 6m^2_{\mathrm{H}_d} \operatorname{tr}\Big(y_{\mathrm{d}} y_{\mathrm{d}}^\dagger\Big) + 2m^2_{\mathrm{H}_d} \operatorname{tr}\Big(y_{\mathrm{e}} y_{\mathrm{e}}^\dagger\Big) + 6 \operatorname{tr}\Big(a_{\mathrm{d}}^* a_{\mathrm{d}}^T\Big) \\
&+ 2 \operatorname{tr}\Big(a_{\mathrm{e}}^* a_{\mathrm{e}}^T\Big) + 6 \operatorname{tr}\Big(m_{\mathrm{d}}^2 y_{\mathrm{d}} y_{\mathrm{d}}^\dagger\Big) + 2 \operatorname{tr}\Big(m_{\mathrm{e}}^2 y_{\mathrm{e}} y_{\mathrm{e}}^\dagger\Big) + 2 \operatorname{tr}\Big(m_\ell^2 y_{\mathrm{e}}^\dagger y_{\mathrm{e}}\Big) + 6 \operatorname{tr}\Big(m_q^2 y_{\mathrm{d}}^\dagger y_{\mathrm{d}}\Big),
\end{aligned}
\tag{B.43}
$$

$$
\begin{aligned}
\beta^{(2)}_{m^2_{\mathrm{H}_d}} &= \frac{1}{25}\Big\{15g_2^2\Big[3g_1^2\Big(2M_2+M_1\Big)+55g_2^2M_2\Big]M_2^*+g_1^2M_1^*\Big[621g_1^2M_1+90g_2^2M_1+45g_2^2M_2\\
&\quad-40M_1\,\mathrm{tr}\Big(y_{\mathrm{d}}y_{\mathrm{d}}^\dagger\Big)+120M_1\,\mathrm{tr}\Big(y_{\mathrm{e}}y_{\mathrm{e}}^\dagger\Big)+20\,\mathrm{tr}\Big(y_{\mathrm{d}}^\dagger a_{\mathrm{d}}\Big)-60\,\mathrm{tr}\Big(y_{\mathrm{e}}^\dagger a_{\mathrm{e}}\Big)\Big]\\
&\quad+10\Big[15g_2^4\sigma_{2,2}+3g_1^2\sigma_{2,11}-2\sqrt{15}g_1\sigma_{3,1}+\Big(160g_3^2|M_3|^2\,\theta_{\tilde{\mathrm{g}}}-2g_1^2m^2_{\mathrm{H}_d}+80g_3^2m^2_{\mathrm{H}_d}\Big)\,\mathrm{tr}\Big(y_{\mathrm{d}}y_{\mathrm{d}}^\dagger\Big)\\
&\quad+6g_1^2m^2_{\mathrm{H}_d}\,\mathrm{tr}\Big(y_{\mathrm{e}}y_{\mathrm{e}}^\dagger\Big)-80g_3^2M_3^*\,\mathrm{tr}\Big(y_{\mathrm{d}}^\dagger a_{\mathrm{d}}\Big)\,\theta_{\tilde{\mathrm{g}}}+2g_1^2M_1\,\mathrm{tr}\Big(a_{\mathrm{d}}^*y_{\mathrm{d}}^T\Big)-80g_3^2M_3\,\mathrm{tr}\Big(a_{\mathrm{d}}^*y_{\mathrm{d}}^T\Big)\,\theta_{\tilde{\mathrm{g}}}\\
&\quad-2g_1^2\,\mathrm{tr}\Big(a_{\mathrm{d}}^*a_{\mathrm{d}}^T\Big)+80g_3^2\,\mathrm{tr}\Big(a_{\mathrm{d}}^*a_{\mathrm{d}}^T\Big)-6g_1^2M_1\,\mathrm{tr}\Big(a_{\mathrm{e}}^*y_{\mathrm{e}}^T\Big)+6g_1^2\,\mathrm{tr}\Big(a_{\mathrm{e}}^*a_{\mathrm{e}}^T\Big)\\
&\quad-2g_1^2\,\mathrm{tr}\Big(m_{\mathrm{d}}^2y_{\mathrm{d}}y_{\mathrm{d}}^\dagger\Big)+80g_3^2\,\mathrm{tr}\Big(m_{\mathrm{d}}^2y_{\mathrm{d}}y_{\mathrm{d}}^\dagger\Big)+6g_1^2\,\mathrm{tr}\Big(m_{\mathrm{e}}^2y_{\mathrm{e}}y_{\mathrm{e}}^\dagger\Big)+6g_1^2\,\mathrm{tr}\Big(m_\ell^2y_{\mathrm{e}}^\dagger y_{\mathrm{e}}\Big)\\
&\quad-2g_1^2\,\mathrm{tr}\Big(m_q^2y_{\mathrm{d}}^\dagger y_{\mathrm{d}}\Big)+80g_3^2\,\mathrm{tr}\Big(m_q^2y_{\mathrm{d}}^\dagger y_{\mathrm{d}}\Big)-90m^2_{\mathrm{H}_d}\,\mathrm{tr}\Big(y_{\mathrm{d}}y_{\mathrm{d}}^\dagger y_{\mathrm{d}}y_{\mathrm{d}}^\dagger\Big)-90\,\mathrm{tr}\Big(y_{\mathrm{d}}y_{\mathrm{d}}^\dagger a_{\mathrm{d}}a_{\mathrm{d}}^\dagger\Big)\\
&\quad-15m^2_{\mathrm{H}_d}\,\mathrm{tr}\Big(y_{\mathrm{d}}y_{\mathrm{u}}^\dagger y_{\mathrm{u}}y_{\mathrm{d}}^\dagger\Big)-15m^2_{\mathrm{H}_u}\,\mathrm{tr}\Big(y_{\mathrm{d}}y_{\mathrm{u}}^\dagger y_{\mathrm{u}}y_{\mathrm{d}}^\dagger\Big)-15\,\mathrm{tr}\Big(y_{\mathrm{d}}y_{\mathrm{u}}^\dagger a_{\mathrm{u}}a_{\mathrm{d}}^\dagger\Big)\\
&\quad-90\,\mathrm{tr}\Big(y_{\mathrm{d}}a_{\mathrm{d}}^\dagger a_{\mathrm{d}}y_{\mathrm{d}}^\dagger\Big)-15\,\mathrm{tr}\Big(y_{\mathrm{d}}a_{\mathrm{u}}^\dagger a_{\mathrm{u}}y_{\mathrm{d}}^\dagger\Big)-30m^2_{\mathrm{H}_d}\,\mathrm{tr}\Big(y_{\mathrm{e}}y_{\mathrm{e}}^\dagger y_{\mathrm{e}}y_{\mathrm{e}}^\dagger\Big)-30\,\mathrm{tr}\Big(y_{\mathrm{e}}y_{\mathrm{e}}^\dagger a_{\mathrm{e}}a_{\mathrm{e}}^\dagger\Big)\\
&\quad-30\,\mathrm{tr}\Big(y_{\mathrm{e}}a_{\mathrm{e}}^\dagger a_{\mathrm{e}}y_{\mathrm{e}}^\dagger\Big)-15\,\mathrm{tr}\Big(y_{\mathrm{u}}y_{\mathrm{d}}^\dagger a_{\mathrm{d}}a_{\mathrm{u}}^\dagger\Big)-15\,\mathrm{tr}\Big(y_{\mathrm{u}}a_{\mathrm{d}}^\dagger a_{\mathrm{d}}y_{\mathrm{u}}^\dagger\Big)-90\,\mathrm{tr}\Big(m_{\mathrm{d}}^2y_{\mathrm{d}}y_{\mathrm{d}}^\dagger y_{\mathrm{d}}y_{\mathrm{d}}^\dagger\Big)\\
&\quad-15\,\mathrm{tr}\Big(m_{\mathrm{d}}^2y_{\mathrm{d}}y_{\mathrm{u}}^\dagger y_{\mathrm{u}}y_{\mathrm{d}}^\dagger\Big)-30\,\mathrm{tr}\Big(m_{\mathrm{e}}^2y_{\mathrm{e}}y_{\mathrm{e}}^\dagger y_{\mathrm{e}}y_{\mathrm{e}}^\dagger\Big)-30\,\mathrm{tr}\Big(m_\ell^2y_{\mathrm{e}}^\dagger y_{\mathrm{e}}y_{\mathrm{e}}^\dagger y_{\mathrm{e}}\Big)\\
&\quad-90\,\mathrm{tr}\Big(m_q^2y_{\mathrm{d}}^\dagger y_{\mathrm{d}}y_{\mathrm{d}}^\dagger y_{\mathrm{d}}\Big)-15\,\mathrm{tr}\Big(m_q^2y_{\mathrm{d}}^\dagger y_{\mathrm{d}}y_{\mathrm{u}}^\dagger y_{\mathrm{u}}\Big)-15\,\mathrm{tr}\Big(m_q^2y_{\mathrm{u}}^\dagger y_{\mathrm{u}}y_{\mathrm{d}}^\dagger y_{\mathrm{d}}\Big)\\
&\quad-15\,\mathrm{tr}\Big(m_{\mathrm{u}}^2y_{\mathrm{u}}y_{\mathrm{d}}^\dagger y_{\mathrm{d}}y_{\mathrm{u}}^\dagger\Big)\Big]\Big\},
\end{aligned}
\tag{B.44}
$$

$$
\begin{aligned}
\beta^{(1)}_{m^2_{\mathrm{H}_u}} &= -\frac{6}{5}g_1^2|M_1|^2-6g_2^2|M_2|^2+\sqrt{\frac{3}{5}}g_1\sigma_{1,1}+6m^2_{\mathrm{H}_u}\,\mathrm{tr}\Big(y_{\mathrm{u}}y_{\mathrm{u}}^\dagger\Big)+6\,\mathrm{tr}\Big(a_{\mathrm{u}}^*a_{\mathrm{u}}^T\Big)+6\,\mathrm{tr}\Big(m_q^2y_{\mathrm{u}}^\dagger y_{\mathrm{u}}\Big)\\
&\quad+6\,\mathrm{tr}\Big(m_{\mathrm{u}}^2y_{\mathrm{u}}y_{\mathrm{u}}^\dagger\Big),
\end{aligned}
\tag{B.45}
$$

$$
\begin{aligned}
\beta^{(2)}_{m^2_{\mathrm{H}_u}} &= \frac{3}{5}g_2^2\Big[3g_1^2\Big(2M_2+M_1\Big)+55g_2^2M_2\Big]M_2^*+6g_2^4\sigma_{2,2}+\frac{6}{5}g_1^2\sigma_{2,11}+4\sqrt{\frac{3}{5}}g_1\sigma_{3,1}\\
&\quad+\frac{8}{5}g_1^2m^2_{\mathrm{H}_u}\,\mathrm{tr}\Big(y_{\mathrm{u}}y_{\mathrm{u}}^\dagger\Big)+32g_3^2m^2_{\mathrm{H}_u}\,\mathrm{tr}\Big(y_{\mathrm{u}}y_{\mathrm{u}}^\dagger\Big)+64g_3^2|M_3|^2\,\mathrm{tr}\Big(y_{\mathrm{u}}y_{\mathrm{u}}^\dagger\Big)\,\theta_{\tilde{\mathrm{g}}}\\
&\quad+\frac{1}{25}g_1^2M_1^*\Big[-40\,\mathrm{tr}\Big(y_{\mathrm{u}}^\dagger a_{\mathrm{u}}\Big)+45g_2^2M_2+621g_1^2M_1+80M_1\,\mathrm{tr}\Big(y_{\mathrm{u}}y_{\mathrm{u}}^\dagger\Big)+90g_2^2M_1\Big]\\
&\quad-32g_3^2M_3^*\,\mathrm{tr}\Big(y_{\mathrm{u}}^\dagger a_{\mathrm{u}}\Big)\,\theta_{\tilde{\mathrm{g}}}-\frac{8}{5}g_1^2M_1\,\mathrm{tr}\Big(a_{\mathrm{u}}^*y_{\mathrm{u}}^T\Big)-32g_3^2M_3\,\mathrm{tr}\Big(a_{\mathrm{u}}^*y_{\mathrm{u}}^T\Big)\,\theta_{\tilde{\mathrm{g}}}+\frac{8}{5}g_1^2\,\mathrm{tr}\Big(a_{\mathrm{u}}^*a_{\mathrm{u}}^T\Big)\\
&\quad+32g_3^2\,\mathrm{tr}\Big(a_{\mathrm{u}}^*a_{\mathrm{u}}^T\Big)+\frac{8}{5}g_1^2\,\mathrm{tr}\Big(m_q^2y_{\mathrm{u}}^\dagger y_{\mathrm{u}}\Big)+32g_3^2\,\mathrm{tr}\Big(m_q^2y_{\mathrm{u}}^\dagger y_{\mathrm{u}}\Big)+\frac{8}{5}g_1^2\,\mathrm{tr}\Big(m_{\mathrm{u}}^2y_{\mathrm{u}}y_{\mathrm{u}}^\dagger\Big)\\
&\quad+32g_3^2\,\mathrm{tr}\Big(m_{\mathrm{u}}^2y_{\mathrm{u}}y_{\mathrm{u}}^\dagger\Big)-6m^2_{\mathrm{H}_d}\,\mathrm{tr}\Big(y_{\mathrm{d}}y_{\mathrm{u}}^\dagger y_{\mathrm{u}}y_{\mathrm{d}}^\dagger\Big)-6m^2_{\mathrm{H}_u}\,\mathrm{tr}\Big(y_{\mathrm{d}}y_{\mathrm{u}}^\dagger y_{\mathrm{u}}y_{\mathrm{d}}^\dagger\Big)\\
&\quad-6\,\mathrm{tr}\Big(y_{\mathrm{d}}y_{\mathrm{u}}^\dagger a_{\mathrm{u}}a_{\mathrm{d}}^\dagger\Big)-6\,\mathrm{tr}\Big(y_{\mathrm{d}}a_{\mathrm{u}}^\dagger a_{\mathrm{u}}y_{\mathrm{d}}^\dagger\Big)-6\,\mathrm{tr}\Big(y_{\mathrm{u}}y_{\mathrm{d}}^\dagger a_{\mathrm{d}}a_{\mathrm{u}}^\dagger\Big)-36m^2_{\mathrm{H}_u}\,\mathrm{tr}\Big(y_{\mathrm{u}}y_{\mathrm{u}}^\dagger y_{\mathrm{u}}y_{\mathrm{u}}^\dagger\Big)\\
&\quad-36\,\mathrm{tr}\Big(y_{\mathrm{u}}y_{\mathrm{u}}^\dagger a_{\mathrm{u}}a_{\mathrm{u}}^\dagger\Big)-6\,\mathrm{tr}\Big(y_{\mathrm{u}}a_{\mathrm{d}}^\dagger a_{\mathrm{d}}y_{\mathrm{u}}^\dagger\Big)-36\,\mathrm{tr}\Big(y_{\mathrm{u}}a_{\mathrm{u}}^\dagger a_{\mathrm{u}}y_{\mathrm{u}}^\dagger\Big)\\
&\quad-6\,\mathrm{tr}\Big(m_{\mathrm{d}}^2y_{\mathrm{d}}y_{\mathrm{u}}^\dagger y_{\mathrm{u}}y_{\mathrm{d}}^\dagger\Big)-6\,\mathrm{tr}\Big(m_q^2y_{\mathrm{d}}^\dagger y_{\mathrm{d}}y_{\mathrm{u}}^\dagger y_{\mathrm{u}}\Big)-6\,\mathrm{tr}\Big(m_q^2y_{\mathrm{u}}^\dagger y_{\mathrm{u}}y_{\mathrm{d}}^\dagger y_{\mathrm{d}}\Big)\\
&\quad-36\,\mathrm{tr}\Big(m_q^2y_{\mathrm{u}}^\dagger y_{\mathrm{u}}y_{\mathrm{u}}^\dagger y_{\mathrm{u}}\Big)-6\,\mathrm{tr}\Big(m_{\mathrm{u}}^2y_{\mathrm{u}}y_{\mathrm{d}}^\dagger y_{\mathrm{d}}y_{\mathrm{u}}^\dagger\Big)-36\,\mathrm{tr}\Big(m_{\mathrm{u}}^2y_{\mathrm{u}}y_{\mathrm{u}}^\dagger y_{\mathrm{u}}y_{\mathrm{u}}^\dagger\Big),
\end{aligned}
\tag{B.46}
$$

$$
\begin{aligned}
\beta^{(1)}_{m^2_{\mathrm{d}}} &= -\frac{8}{15}g_1^2|M_1|^2-\frac{32}{3}g_3^2|M_3|^2\,\theta_{\tilde{\mathrm{g}}}+4m^2_{\mathrm{H}_d}y_{\mathrm{d}}y_{\mathrm{d}}^\dagger+4a_{\mathrm{d}}a_{\mathrm{d}}^\dagger+2m_{\mathrm{d}}^2y_{\mathrm{d}}y_{\mathrm{d}}^\dagger+4y_{\mathrm{d}}m_q^2y_{\mathrm{d}}^\dagger\\
&\quad+2y_{\mathrm{d}}y_{\mathrm{d}}^\dagger m_{\mathrm{d}}^2+2\frac{1}{\sqrt{15}}g_1\sigma_{1,1},
\end{aligned}
\tag{B.47}
$$

$$
\begin{aligned}
\beta^{(2)}_{m^2_{\rm d}} &= \frac{32}{45}g_3^2\Big[2g_1^2\Big(2M_3+M_1\Big)+75g_3^2M_3\Big]M_3^*\,\theta_{\widetilde{\rm g}}+\frac{4}{5}g_1^2m^2_{{\rm H}_d}y_{\rm d}y_{\rm d}^\dagger+12g_2^2m^2_{{\rm H}_d}y_{\rm d}y_{\rm d}^\dagger\\
&+24g_2^2|M_2|^2y_{\rm d}y_{\rm d}^\dagger-\frac{4}{5}g_1^2M_1y_{\rm d}a_{\rm d}^\dagger-12g_2^2M_2y_{\rm d}a_{\rm d}^\dagger\\
&+\frac{4}{225}g_1^2M_1^*\Big\{2\Big[303g_1^2M_1+40g_3^2\Big(2M_1+M_3\,\theta_{\widetilde{\rm g}}\Big)\Big]-45a_{\rm d}y_{\rm d}^\dagger+90M_1y_{\rm d}y_{\rm d}^\dagger\Big\}-12g_2^2M_2^*a_{\rm d}y_{\rm d}^\dagger\\
&+\frac{4}{5}g_1^2a_{\rm d}a_{\rm d}^\dagger+12g_2^2a_{\rm d}a_{\rm d}^\dagger+\frac{2}{5}g_1^2m_{\rm d}^2y_{\rm d}y_{\rm d}^\dagger+6g_2^2m_{\rm d}^2y_{\rm d}y_{\rm d}^\dagger\\
&+\frac{4}{5}g_1^2y_{\rm d}m_q^2y_{\rm d}^\dagger+12g_2^2y_{\rm d}m_q^2y_{\rm d}^\dagger+\frac{2}{5}g_1^2y_{\rm d}y_{\rm d}^\dagger m_{\rm d}^2+6g_2^2y_{\rm d}y_{\rm d}^\dagger m_{\rm d}^2\\
&-8m^2_{{\rm H}_d}y_{\rm d}y_{\rm d}^\dagger y_{\rm d}y_{\rm d}^\dagger-4y_{\rm d}y_{\rm d}^\dagger a_{\rm d}a_{\rm d}^\dagger-4m^2_{{\rm H}_d}y_{\rm d}y_{\rm u}^\dagger y_{\rm u}y_{\rm d}^\dagger\\
&-4m^2_{{\rm H}_u}y_{\rm d}y_{\rm u}^\dagger y_{\rm u}y_{\rm d}^\dagger-4y_{\rm d}y_{\rm u}^\dagger a_{\rm u}a_{\rm d}^\dagger-4y_{\rm d}a_{\rm d}^\dagger a_{\rm d}y_{\rm d}^\dagger-4y_{\rm d}a_{\rm u}^\dagger a_{\rm u}y_{\rm d}^\dagger\\
&-4a_{\rm d}y_{\rm d}^\dagger y_{\rm d}a_{\rm d}^\dagger-4a_{\rm d}y_{\rm u}^\dagger y_{\rm u}a_{\rm d}^\dagger-4a_{\rm d}a_{\rm d}^\dagger y_{\rm d}y_{\rm d}^\dagger-4a_{\rm d}a_{\rm u}^\dagger y_{\rm u}y_{\rm d}^\dagger\\
&-2m_{\rm d}^2y_{\rm d}y_{\rm d}^\dagger y_{\rm d}y_{\rm d}^\dagger-2m_{\rm d}^2y_{\rm d}y_{\rm u}^\dagger y_{\rm u}y_{\rm d}^\dagger-4y_{\rm d}m_q^2y_{\rm d}^\dagger y_{\rm d}y_{\rm d}^\dagger-4y_{\rm d}m_q^2y_{\rm u}^\dagger y_{\rm u}y_{\rm d}^\dagger\\
&-4y_{\rm d}y_{\rm d}^\dagger m_{\rm d}^2y_{\rm d}y_{\rm d}^\dagger-4y_{\rm d}y_{\rm d}^\dagger y_{\rm d}m_q^2y_{\rm d}^\dagger-2y_{\rm d}y_{\rm d}^\dagger y_{\rm d}y_{\rm d}^\dagger m_{\rm d}^2-4y_{\rm d}y_{\rm u}^\dagger m_{\rm u}^2y_{\rm u}y_{\rm d}^\dagger\\
&-4y_{\rm d}y_{\rm u}^\dagger y_{\rm u}m_q^2y_{\rm d}^\dagger-2y_{\rm d}y_{\rm u}^\dagger y_{\rm u}y_{\rm d}^\dagger m_{\rm d}^2+\frac{32}{3}g_3^4\sigma_{2,3}+\frac{8}{15}g_1^2\sigma_{2,11}+8\frac{1}{\sqrt{15}}g_1\sigma_{3,1}\\
&-24m^2_{{\rm H}_d}y_{\rm d}y_{\rm d}^\dagger\,{\rm tr}\Big(y_{\rm d}y_{\rm d}^\dagger\Big)-12a_{\rm d}a_{\rm d}^\dagger\,{\rm tr}\Big(y_{\rm d}y_{\rm d}^\dagger\Big)-6m_{\rm d}^2y_{\rm d}y_{\rm d}^\dagger\,{\rm tr}\Big(y_{\rm d}y_{\rm d}^\dagger\Big)\\
&-12y_{\rm d}m_q^2y_{\rm d}^\dagger\,{\rm tr}\Big(y_{\rm d}y_{\rm d}^\dagger\Big)-6y_{\rm d}y_{\rm d}^\dagger m_{\rm d}^2\,{\rm tr}\Big(y_{\rm d}y_{\rm d}^\dagger\Big)-8m^2_{{\rm H}_d}y_{\rm d}y_{\rm d}^\dagger\,{\rm tr}\Big(y_{\rm e}y_{\rm e}^\dagger\Big)\\
&-4a_{\rm d}a_{\rm d}^\dagger\,{\rm tr}\Big(y_{\rm e}y_{\rm e}^\dagger\Big)-2m_{\rm d}^2y_{\rm d}y_{\rm d}^\dagger\,{\rm tr}\Big(y_{\rm e}y_{\rm e}^\dagger\Big)-4y_{\rm d}m_q^2y_{\rm d}^\dagger\,{\rm tr}\Big(y_{\rm e}y_{\rm e}^\dagger\Big)\\
&-2y_{\rm d}y_{\rm d}^\dagger m_{\rm d}^2\,{\rm tr}\Big(y_{\rm e}y_{\rm e}^\dagger\Big)-12y_{\rm d}a_{\rm d}^\dagger\,{\rm tr}\Big(y_{\rm d}^\dagger a_{\rm d}\Big)-4y_{\rm d}a_{\rm d}^\dagger\,{\rm tr}\Big(y_{\rm e}^\dagger a_{\rm e}\Big)\\
&-12a_{\rm d}y_{\rm d}^\dagger\,{\rm tr}\Big(a_{\rm d}^*y_{\rm d}^T\Big)-12y_{\rm d}y_{\rm d}^\dagger\,{\rm tr}\Big(a_{\rm d}^*a_{\rm d}^T\Big)-4a_{\rm d}y_{\rm d}^\dagger\,{\rm tr}\Big(a_{\rm e}^*y_{\rm e}^T\Big)\\
&-4y_{\rm d}y_{\rm d}^\dagger\,{\rm tr}\Big(a_{\rm e}^*a_{\rm e}^T\Big)-12y_{\rm d}y_{\rm d}^\dagger\,{\rm tr}\Big(m_{\rm d}^2y_{\rm d}y_{\rm d}^\dagger\Big)-4y_{\rm d}y_{\rm d}^\dagger\,{\rm tr}\Big(m_{\rm e}^2y_{\rm e}y_{\rm e}^\dagger\Big)\\
&-4y_{\rm d}y_{\rm d}^\dagger\,{\rm tr}\Big(m_\ell^2y_{\rm e}^\dagger y_{\rm e}\Big)-12y_{\rm d}y_{\rm d}^\dagger\,{\rm tr}\Big(m_q^2y_{\rm d}^\dagger y_{\rm d}\Big),
\end{aligned}
\tag{B.48}
$$

$$
\begin{aligned}
\beta^{(1)}_{m^2_{\rm u}} &= -\frac{32}{15}g_1^2|M_1|^2-\frac{32}{3}g_3^2|M_3|^2\,\theta_{\widetilde{\rm g}}+4m^2_{{\rm H}_u}y_{\rm u}y_{\rm u}^\dagger+4a_{\rm u}a_{\rm u}^\dagger+2m_q^2y_{\rm u}y_{\rm u}^\dagger+4y_{\rm u}m_q^2y_{\rm u}^\dagger\\
&+2y_{\rm u}y_{\rm u}^\dagger m_{\rm u}^2-4\frac{1}{\sqrt{15}}g_1\sigma_{1,1},
\end{aligned}
\tag{B.49}
$$

$$
\begin{aligned}
\beta^{(2)}_{m^2_{\rm u}} &= \frac{32}{45}g_3^2\Big[75g_3^2M_3\,\theta_{\widetilde{\rm g}}+8g_1^2\Big(2M_3+M_1\Big)\Big]M_3^*\,\theta_{\widetilde{\rm g}}-\frac{4}{5}g_1^2m^2_{{\rm H}_u}y_{\rm u}y_{\rm u}^\dagger+12g_2^2m^2_{{\rm H}_u}y_{\rm u}y_{\rm u}^\dagger\\
&+24g_2^2|M_2|^2y_{\rm u}y_{\rm u}^\dagger+\frac{4}{5}g_1^2M_1y_{\rm u}a_{\rm u}^\dagger-12g_2^2M_2y_{\rm u}a_{\rm u}^\dagger-12g_2^2M_2^*a_{\rm u}y_{\rm u}^\dagger\\
&+\frac{4}{225}g_1^2M_1^*\Big\{45\Big[-2M_1y_{\rm u}y_{\rm u}^\dagger+a_{\rm u}y_{\rm u}^\dagger\Big]+8\Big[321g_1^2M_1+40g_3^2\Big(2M_1+M_3\,\theta_{\widetilde{\rm g}}\Big)\Big]\Big\}-\frac{4}{5}g_1^2a_{\rm u}a_{\rm u}^\dagger\\
&+12g_2^2a_{\rm u}a_{\rm u}^\dagger-\frac{2}{5}g_1^2m_{\rm u}^2y_{\rm u}y_{\rm u}^\dagger+6g_2^2m_{\rm u}^2y_{\rm u}y_{\rm u}^\dagger-\frac{4}{5}g_1^2y_{\rm u}m_q^2y_{\rm u}^\dagger\\
&+12g_2^2y_{\rm u}m_q^2y_{\rm u}^\dagger-\frac{2}{5}g_1^2y_{\rm u}y_{\rm u}^\dagger m_{\rm u}^2+6g_2^2y_{\rm u}y_{\rm u}^\dagger m_{\rm u}^2-4m^2_{{\rm H}_d}y_{\rm u}y_{\rm d}^\dagger y_{\rm d}y_{\rm u}^\dagger\\
&-4m^2_{{\rm H}_u}y_{\rm u}y_{\rm d}^\dagger y_{\rm d}y_{\rm u}^\dagger-4y_{\rm u}y_{\rm d}^\dagger a_{\rm d}a_{\rm u}^\dagger-8m^2_{{\rm H}_u}y_{\rm u}y_{\rm u}^\dagger y_{\rm u}y_{\rm u}^\dagger-4y_{\rm u}y_{\rm u}^\dagger a_{\rm u}a_{\rm u}^\dagger\\
&-4y_{\rm u}a_{\rm d}^\dagger a_{\rm d}y_{\rm u}^\dagger-4y_{\rm u}a_{\rm u}^\dagger a_{\rm u}y_{\rm u}^\dagger-4a_{\rm u}y_{\rm d}^\dagger y_{\rm d}a_{\rm u}^\dagger-4a_{\rm u}y_{\rm u}^\dagger y_{\rm u}a_{\rm u}^\dagger\\
&-4a_{\rm u}a_{\rm d}^\dagger y_{\rm d}y_{\rm u}^\dagger-4a_{\rm u}a_{\rm u}^\dagger y_{\rm u}y_{\rm u}^\dagger-2m_{\rm u}^2y_{\rm u}y_{\rm d}^\dagger y_{\rm d}y_{\rm u}^\dagger-2m_{\rm u}^2y_{\rm u}y_{\rm u}^\dagger y_{\rm u}y_{\rm u}^\dagger
\end{aligned}
$$

$$
\begin{aligned}
&- 4y_{\rm u}m_q^2y_{\rm d}^\dagger y_{\rm d}y_{\rm u}^\dagger - 4y_{\rm u}m_q^2y_{\rm u}^\dagger y_{\rm u}y_{\rm u}^\dagger - 4y_{\rm u}y_{\rm d}^\dagger m_{\rm d}^2y_{\rm d}y_{\rm u}^\dagger \\
&- 4y_{\rm u}y_{\rm d}^\dagger y_{\rm d}m_q^2y_{\rm u}^\dagger - 2y_{\rm u}y_{\rm d}^\dagger y_{\rm d}y_{\rm u}^\dagger m_{\rm u}^2 - 4y_{\rm u}y_{\rm u}^\dagger m_{\rm u}^2y_{\rm u}y_{\rm u}^\dagger - 4y_{\rm u}y_{\rm u}^\dagger y_{\rm u}m_q^2y_{\rm u}^\dagger \\
&- 2y_{\rm u}y_{\rm u}^\dagger y_{\rm u}y_{\rm u}^\dagger m_{\rm u}^2 + \frac{32}{3}g_3^4\sigma_{2,3} + \frac{32}{15}g_1^2\sigma_{2,11} - 16\frac{1}{\sqrt{15}}g_1\sigma_{3,1} - 24m_{{\rm H}_u}^2y_{\rm u}y_{\rm u}^\dagger\,{\rm tr}\Big(y_{\rm u}y_{\rm u}^\dagger\Big) \\
&- 12a_{\rm u}a_{\rm u}^\dagger\,{\rm tr}\Big(y_{\rm u}y_{\rm u}^\dagger\Big) - 6m_{\rm u}^2y_{\rm u}y_{\rm u}^\dagger\,{\rm tr}\Big(y_{\rm u}y_{\rm u}^\dagger\Big) - 12y_{\rm u}m_q^2y_{\rm u}^\dagger\,{\rm tr}\Big(y_{\rm u}y_{\rm u}^\dagger\Big) \\
&- 6y_{\rm u}y_{\rm u}^\dagger m_{\rm u}^2\,{\rm tr}\Big(y_{\rm u}y_{\rm u}^\dagger\Big) - 12y_{\rm u}a_{\rm u}^\dagger\,{\rm tr}\Big(y_{\rm u}^\dagger a_{\rm u}\Big) - 12a_{\rm u}y_{\rm u}^\dagger\,{\rm tr}\Big(a_{\rm u}^*y_{\rm u}^T\Big) \\
&- 12y_{\rm u}y_{\rm u}^\dagger\,{\rm tr}\Big(a_{\rm u}^*a_{\rm u}^T\Big) - 12y_{\rm u}y_{\rm u}^\dagger\,{\rm tr}\Big(m_q^2y_{\rm u}^\dagger y_{\rm u}\Big) - 12y_{\rm u}y_{\rm u}^\dagger\,{\rm tr}\Big(m_{\rm u}^2y_{\rm u}y_{\rm u}^\dagger\Big),
\end{aligned}
\tag{B.50}
$$

$$
\begin{aligned}
\beta_{m_{\rm e}^2}^{(1)} &= -\frac{24}{5}g_1^2|M_1|^2 + 2\Big(2m_{{\rm H}_d}^2y_{\rm e}y_{\rm e}^\dagger + 2a_{\rm e}a_{\rm e}^\dagger + 2y_{\rm e}m_\ell^2y_{\rm e}^\dagger + m_{\rm e}^2y_{\rm e}y_{\rm e}^\dagger + y_{\rm e}y_{\rm e}^\dagger m_{\rm e}^2\Big) \\
&+ 2\sqrt{\frac{3}{5}}g_1\sigma_{1,1},
\end{aligned}
\tag{B.51}
$$

$$
\begin{aligned}
\beta_{m_{\rm e}^2}^{(2)} &= \frac{2}{25}\Big[6g_1^2M_1^*\Big\{234g_1^2M_1 + 5\Big[-2M_1y_{\rm e}y_{\rm e}^\dagger + a_{\rm e}y_{\rm e}^\dagger\Big]\Big\} + 20g_1\Big(3g_1\sigma_{2,11} + \sqrt{15}\sigma_{3,1}\Big) \\
&- 5\Big\{30g_2^2M_2^*a_{\rm e}y_{\rm e}^\dagger + 6g_1^2a_{\rm e}a_{\rm e}^\dagger - 30g_2^2a_{\rm e}a_{\rm e}^\dagger + 3g_1^2m_{\rm e}^2y_{\rm e}y_{\rm e}^\dagger \\
&- 15g_2^2m_{\rm e}^2y_{\rm e}y_{\rm e}^\dagger + 6g_1^2y_{\rm e}m_\ell^2y_{\rm e}^\dagger - 30g_2^2y_{\rm e}m_\ell^2y_{\rm e}^\dagger + 3g_1^2y_{\rm e}y_{\rm e}^\dagger m_{\rm e}^2 \\
&- 15g_2^2y_{\rm e}y_{\rm e}^\dagger m_{\rm e}^2 + 20m_{{\rm H}_d}^2y_{\rm e}y_{\rm e}^\dagger y_{\rm e}y_{\rm e}^\dagger + 10y_{\rm e}y_{\rm e}^\dagger a_{\rm e}a_{\rm e}^\dagger + 10y_{\rm e}a_{\rm e}^\dagger a_{\rm e}y_{\rm e}^\dagger \\
&+ 10a_{\rm e}y_{\rm e}^\dagger y_{\rm e}a_{\rm e}^\dagger + 10a_{\rm e}a_{\rm e}^\dagger y_{\rm e}y_{\rm e}^\dagger + 5m_{\rm e}^2y_{\rm e}y_{\rm e}^\dagger y_{\rm e}y_{\rm e}^\dagger + 10y_{\rm e}m_\ell^2y_{\rm e}^\dagger y_{\rm e}y_{\rm e}^\dagger \\
&+ 10y_{\rm e}y_{\rm e}^\dagger m_{\rm e}^2y_{\rm e}y_{\rm e}^\dagger + 10y_{\rm e}y_{\rm e}^\dagger y_{\rm e}m_\ell^2y_{\rm e}^\dagger + 5y_{\rm e}y_{\rm e}^\dagger y_{\rm e}y_{\rm e}^\dagger m_{\rm e}^2 + 30a_{\rm e}a_{\rm e}^\dagger\,{\rm tr}\Big(y_{\rm d}y_{\rm d}^\dagger\Big) \\
&+ 15m_{\rm e}^2y_{\rm e}y_{\rm e}^\dagger\,{\rm tr}\Big(y_{\rm d}y_{\rm d}^\dagger\Big) + 30y_{\rm e}m_\ell^2y_{\rm e}^\dagger\,{\rm tr}\Big(y_{\rm d}y_{\rm d}^\dagger\Big) + 15y_{\rm e}y_{\rm e}^\dagger m_{\rm e}^2\,{\rm tr}\Big(y_{\rm d}y_{\rm d}^\dagger\Big) \\
&+ 10a_{\rm e}a_{\rm e}^\dagger\,{\rm tr}\Big(y_{\rm e}y_{\rm e}^\dagger\Big) + 5m_{\rm e}^2y_{\rm e}y_{\rm e}^\dagger\,{\rm tr}\Big(y_{\rm e}y_{\rm e}^\dagger\Big) + 10y_{\rm e}m_\ell^2y_{\rm e}^\dagger\,{\rm tr}\Big(y_{\rm e}y_{\rm e}^\dagger\Big) \\
&+ 5y_{\rm e}y_{\rm e}^\dagger m_{\rm e}^2\,{\rm tr}\Big(y_{\rm e}y_{\rm e}^\dagger\Big) + y_{\rm e}a_{\rm e}^\dagger\Big[10\,{\rm tr}\Big(y_{\rm e}^\dagger a_{\rm e}\Big) + 30g_2^2M_2 + 30\,{\rm tr}\Big(y_{\rm d}^\dagger a_{\rm d}\Big) - 6g_1^2M_1\Big] \\
&+ 30a_{\rm e}y_{\rm e}^\dagger\,{\rm tr}\Big(a_{\rm d}^*y_{\rm d}^T\Big) + 10a_{\rm e}y_{\rm e}^\dagger\,{\rm tr}\Big(a_{\rm e}^*y_{\rm e}^T\Big) + 2y_{\rm e}y_{\rm e}^\dagger\Big[3g_1^2m_{{\rm H}_d}^2 - 15g_2^2m_{{\rm H}_d}^2 - 30g_2^2|M_2|^2 \\
&+ 30m_{{\rm H}_d}^2\,{\rm tr}\Big(y_{\rm d}y_{\rm d}^\dagger\Big) + 10m_{{\rm H}_d}^2\,{\rm tr}\Big(y_{\rm e}y_{\rm e}^\dagger\Big) + 15\,{\rm tr}\Big(a_{\rm d}^*a_{\rm d}^T\Big) + 5\,{\rm tr}\Big(a_{\rm e}^*a_{\rm e}^T\Big) \\
&+ 15\,{\rm tr}\Big(m_{\rm d}^2y_{\rm d}y_{\rm d}^\dagger\Big) + 5\,{\rm tr}\Big(m_{\rm e}^2y_{\rm e}y_{\rm e}^\dagger\Big) + 5\,{\rm tr}\Big(m_\ell^2y_{\rm e}^\dagger y_{\rm e}\Big) + 15\,{\rm tr}\Big(m_q^2y_{\rm d}^\dagger y_{\rm d}\Big)\Big]\Big\}\Big],
\end{aligned}
\tag{B.52}
$$

$$
\beta_{m_{\tilde{\rm g}}^2}^{(1)} = -24g_3^2|M_3|^2\,\theta_{\tilde{\rm g}},
\tag{B.53}
$$

$$
\beta_{m_{\tilde{\rm g}}^2}^{(2)} = 24g_3^4\Big(15|M_3|^2\,\theta_{\tilde{\rm g}} + \sigma_{2,3}\Big).
\tag{B.54}
$$

References

[1] The ATLAS Collaboration, *Observation of a new particle in the search for the Standard Model Higgs boson with the ATLAS detector at the LHC*, arXiv:1207.7214.

[2] The CMS Collaboration, *Observation of a new boson at a mass of 125 GeV with the CMS experiment at the LHC*, arXiv:1207.7235.

[3] J. Beringer et al. (Particle Data Group), *Review of Particle Physics*, *Physical Review D* **86** (July, 2012) 010001.

[4] The ATLAS Collaboration, *Search for squarks and gluinos with the ATLAS detector in final states with jets and missing transverse momentum and 20.3 fb-1 of sqrt(s) = 8 TeV proton-proton collision data*, .

[5] The CMS Collaboration, *Search for new physics in the multijet and missing transverse momentum final state in proton-proton collisions at sqrt(s) = 8 TeV*, arXiv:1402.4770.

[6] U. Ellwanger and C. Hugonie, *The upper bound on the lightest Higgs Mass in the NMSSM revisited*, *Modern Physics Letters A* **22** (July, 2007) 1581–1590, [0612133].

[7] U. Ellwanger, C. Hugonie, and A. M. Teixeira, *The Next-to-Minimal Supersymmetric Standard Model*, *Physics Reports* **496** (Nov., 2010) 1–77, [arXiv:0910.1785].

[8] T. Basak and S. Mohanty, *Triplet-singlet extension of the MSSM with a 125 GeV Higgs boson and dark matter*, *Physical Review D* **86** (Oct., 2012) 075031, [arXiv:1204.6592].

[9] T. Basak and S. Mohanty, *130 GeV gamma ray line and enhanced Higgs di-photon rate from Triplet-Singlet extended MSSM*, arXiv:1304.6856.

[10] T. J. LeCompte and S. P. Martin, *Large Hadron Collider reach for supersymmetric models with compressed mass spectra*, *Physical Review D* **84** (July, 2011) 015004, [arXiv:1105.4304].

[11] H. K. Dreiner, M. Krämer, and J. Tattersall, *How low can SUSY go? Matching, monojets and compressed spectra*, arXiv:1207.1613.

[12] B. Bhattacherjee, A. Choudhury, K. Ghosh, and S. Poddar, *Compressed supersymmetry at 14 TeV LHC*, *Physical Review D* **89** (Feb., 2014) 037702, [arXiv:1308.1526].

[13] R. Barbier, C. Bérat, M. Besançon, M. Chemtob, A. Deandrea, E. Dudas, P. Fayet, S. Lavignac, G. Moreau, E. Perez, and Y. Sirois, *R-Parity-violating supersymmetry*, *Physics Reports* **420** (Nov., 2005) 1–195, [0406039].

[14] M. Abdullah, I. Galon, Y. Shadmi, and Y. Shirman, *Flavored Gauge Mediation, A Heavy Higgs, and Supersymmetric Alignment*, arXiv:1209.4904.

[15] I. Galon, G. Perez, and Y. Shadmi, *Non-Degenerate Squarks from Flavored Gauge Mediation*, arXiv:1306.6631.

[16] P. J. Fox, A. E. Nelson, and N. Weiner, *Dirac Gaugino Masses and Supersoft Supersymmetry Breaking*, *Journal of High Energy Physics* **2002** (Aug., 2002) 035–035, [0206096].

[17] P. Fayet, *Massive gluinos*, *Physics Letters B* **78** (1978), no. 4 417–420.

[18] J. Polchinski and L. Susskind, *Breaking of supersymmetry at intermediate energy*, *Physical Review D* **26** (1982), no. 12 3661–3673.

[19] L. J. Hall and L. Randall, *$U(1)_R$ symmetric supersymmetry*, *Nuclear Physics B* **352** (1991) 289–308.

[20] A. E. Nelson, N. Rius, V. Sanz, and M. Unsal, *The MSSM without mu term*, 0211102.

[21] I. Antoniadis, A. Delgado, K. Benakli, M. Quirós, and M. Tuckmantel, *Splitting extended supersymmetry*, *Physics Letters B* **634** (Mar., 2006) 302–306, [0507192].

[22] I. Antoniadis, K. Benakli, A. Delgado, and M. Quiros, *A New Gauge Mediation Theory*, 0610265.

[23] I. Antoniadis, K. Benakli, A. Delgado, M. Quirós, and M. Tuckmantel, *Split extended supersymmetry from intersecting branes*, *Nuclear Physics B* **744** (June, 2006) 156–179, [0601003].

[24] K. Hsieh, *Pseudo-Dirac bino dark matter*, *Physical Review D* **77** (Jan., 2008) 015004, [arXiv:0708.3970].

[25] S. D. L. Amigo, A. E. Blechman, P. J. Fox, and E. Poppitz, *R -symmetric gauge mediation*, *Journal of High Energy Physics* **2009** (Jan., 2009) 018–018, [arXiv:0809.1112].

[26] S. Choi, M. Drees, A. Freitas, and P. Zerwas, *Testing the Majorana nature of gluinos and neutralinos*, *Physical Review D* **78** (Nov., 2008) 095007, [arXiv:0808.2410].

[27] S. Choi, M. Drees, J. Kalinowski, J. Kim, E. Popenda, and P. Zerwas, *Color-octet scalars of supersymmetry at the LHC*, *Physics Letters B* **672** (Feb., 2009) 246–252, [arXiv:0812.3586].

[28] A. E. Blechman, *R-symmetric Gauge Mediation and the MRSSM*, *Modern Physics Letters A* **24** (Mar., 2009) 14, [arXiv:0903.2822].

[29] K. Benakli and M. D. Goodsell, *Dirac gauginos in general gauge mediation*, *Nuclear Physics B* **816** (July, 2009) 185–203, [arXiv:0811.4409].

[30] G. Belanger, K. Benakli, M. D. Goodsell, C. Moura, and A. Pukhov, *Dark matter with Dirac and Majorana gaugino masses*, *Journal of Cosmology and Astroparticle Physics* **2009** (Aug., 2009) 027–027, [arXiv:0905.1043].

[31] S. Choi, J. Kalinowski, J. Kim, and E. Popenda, *Scalar gluons and Dirac gluinos at the LHC*, arXiv:0911.1951.

[32] K. Benakli and M. D. Goodsell, *Dirac gauginos and kinetic mixing*, *Nuclear Physics B* **830** (Mar., 2010) 315–329, [arXiv:1003.4957].

[33] E. J. Chun, J.-C. Park, and S. Scopel, *Dirac gaugino as leptophilic dark matter*, *Journal of Cosmology and Astroparticle Physics* **2010** (Feb., 2010) 015–015, [arXiv:0911.5273].

[34] K. Benakli and M. D. Goodsell, *Dirac Gauginos, Gauge Mediation and Unification*, arXiv:1003.4957.

[35] L. M. Carpenter, *Dirac Gauginos, Negative Supertraces and Gauge Mediation*, arXiv:1007.0017.

[36] G. D. Kribs, T. Okui, and T. Roy, *Viable gravity-mediated supersymmetry breaking*, *Physical Review D* (2010).

[37] S. Choi, D. Choudhury, A. Freitas, J. Kalinowski, J. Kim, and P. M. Zerwas, *Dirac neutralinos and electroweak scalar bosons of $N = 1/N = 2$ hybrid supersymmetry at colliders*, *Journal of High Energy Physics* **2010** (Aug., 2010) 25, [arXiv:1005.0818].

[38] S. Abel and M. D. Goodsell, *Easy Dirac gauginos*, *Journal of High Energy Physics* **2011** (June, 2011) 64, [arXiv:1102.0014].

[39] R. Davies, J. March-Russell, and M. McCullough, *A supersymmetric one Higgs doublet model*, *Journal of High Energy Physics* **2011** (Apr., 2011) 108, [arXiv:1103.1647].

[40] K. Benakli, M. D. Goodsell, and A.-K. Maier, *Generating μ and $B\mu$ in models with Dirac gauginos*, *Nuclear Physics B* **851** (Oct., 2011) 445–461.

[41] K. Benakli, *Dirac Gauginos: A User Manual*, *ArXiv* (June, 2011) 4, [arXiv:1106.1649].

[42] M. Heikinheimo, M. Kellerstein, and V. Sanz, *How Many Supersymmetries?*, *Simulation* (Nov., 2011) 7, [arXiv:1111.4322].

[43] H. Itoyama and N. Maru, *D-term Dynamical Supersymmetry Breaking Generating Split N=2 Gaugino Masses of Mixed Majorana-Dirac Type*, arXiv:1109.2276.

[44] G. D. Kribs and A. Martin, *Supersoft supersymmetry is super-safe*, *Physical Review D* **85** (June, 2012) 115014, [arXiv:1203.4821].

[45] R. Davies, *Dirac gauginos and unification in F-theory*, *Journal of High Energy Physics* **2012** (Oct., 2012) 10, [arXiv:1205.1942].

[46] M. D. Goodsell, *Two-loop RGEs with Dirac gaugino masses*, arXiv:1206.6697.

[47] K. Benakli, M. D. Goodsell, and F. Staub, *Dirac Gauginos and the 125 GeV Higgs*, arXiv:1211.0552.

[48] C. Frugiuele and T. Grégoire, *Making the sneutrino a Higgs particle with a $U(1)_R$ lepton number*, *Physical Review D* **85** (Jan., 2012) 015016, [arXiv:1107.4634].

[49] C. Frugiuele, T. Gregoire, P. Kumar, and E. Ponton, *"L=R" - $U(1)_R$ as the Origin of Leptonic 'RPV'*, arXiv:1210.0541.

[50] E. Bertuzzo and C. Frugiuele, *Fitting neutrino physics with a U(1) R lepton number*, *Journal of High Energy Physics* **2012** (May, 2012) 100, [arXiv:1203.5340].

[51] F. Riva, C. Biggio, and A. Pomarol, *Is the 125 GeV Higgs the superpartner of a neutrino?*, arXiv:1211.4526.

[52] C. Frugiuele, T. Gregoire, P. Kumar, and E. Ponton, *"L=R" – $U(1)_R$ Lepton Number at the LHC*, arXiv:1210.5257.

[53] H. Itoyama and N. Maru, *D-term Triggered Dynamical Supersymmetry Breaking*, arXiv:1301.7548.

[54] S. Abel and D. Busbridge, *Mapping Dirac gaugino masses*, *Journal of High Energy Physics* (June, 2013) 37, [arXiv:1306.6323].

[55] G. D. Kribs and A. Martin, *Dirac Gauginos in Supersymmetry – Suppressed Jets + MET Signals: A Snowmass Whitepaper*, arXiv:1308.3468.

[56] G. D. Kribs and N. Raj, *Mixed Gauginos Sending Mixed Messages to the LHC*, arXiv:1307.7197.

[57] T. Banks, *Dirac Gluinos in the Pyramid Scheme*, *arXiv preprint arXiv:1311.4410* **30** (2013) 1–11, [arXiv:1311.4410].

[58] C. Csáki, J. Goodman, R. Pavesi, and Y. Shirman, *The m_D-b_M Problem of Dirac Gauginos and its solutions*, arXiv:1310.4504.

[59] E. Dudas, M. D. Goodsell, L. Heurtier, and P. Tziveloglou, *Flavour models with Dirac and fake gluinos*, arXiv:1312.2011.

[60] E. Bertuzzo, C. Frugiuele, T. Gregoire, and E. Ponton, *Dirac gauginos, R symmetry and the 125 GeV Higgs*, arXiv:1402.5432.

[61] K. Benakli, M. D. Goodsell, F. Staub, and W. Porod, *The Constrained Minimal Dirac Gaugino Supersymmetric Standard Model*, arXiv:1403.5122.

[62] P. J. Fox, G. D. Kribs, and A. Martin, *Split Dirac Supersymmetry: An Ultraviolet Completion of Higgsino Dark Matter*, arXiv:1405.3692.

[63] M. D. Goodsell and P. Tziveloglou, *Dirac Gauginos in Low Scale Supersymmetry Breaking*, arXiv:1407.5076.

[64] S. Ipek, D. McKeen, and A. E. Nelson, *CP Violation in Pseudo-Dirac Fermion Oscillations*, arXiv:1407.8193.

[65] G. Gamberini, G. Ridolfi, and F. Zwirner, *On radiative gauge symmetry breaking in the minimal supersymmetric model*, *Nuclear Physics B* **331** (1990) 331–349.

[66] P. Nath and R. Arnowitt, *Loop corrections to radiative breaking of electroweak symmetry in supersymmetry*, *Physical Review D* **46** (1992), no. 9 3981.

[67] B. de Carlos and J. A. Casas, *One-loop analysis of the electroweak breaking in supersymmetric models and the fine-tuning problem*, *Physics Letters B* **309** (1993), no. 3 320–328.

[68] J. Jaeckel, V. V. Khoze, T. Plehn, and P. Richardson, *Travels on the squark-gluino mass plane*, *Physical Review D* **85** (Jan., 2012) 015015, [arXiv:1109.2072].

[69] A. Arvanitaki, M. Baryakhtar, X. Huang, K. Van Tilburg, and G. Villadoro, *The Last Vestiges of Naturalness*, *arXiv preprint arXiv: ...* (Sept., 2013) 22, [arXiv:1309.3568].

[70] S. P. Martin, *A Supersymmetry Primer*, *Nature* (Sept., 1997) 152, [9709356].

[71] S. P. Martin, *Generalized messengers of supersymmetry breaking and the sparticle mass spectrum*, *Physical Review D* **55** (Mar., 1997) 3177–3187, [9608224].

[72] M. Dine and A. E. Nelson, *Dynamical supersymmetry breaking at low energies*, *Physical Review D* (1993).

[73] M. Dine, A. Nelson, and Y. Shirman, *Low energy dynamical supersymmetry breaking simplified*, *Physical Review D* **51** (1995), no. 3 1362–1370.

[74] M. Dine, A. E. Nelson, Y. Nir, and Y. Shirman, *New tools for low energy dynamical supersymmetry breaking.*, *Physical review D: Particles and fields* **53** (Mar., 1996) 2658–2669.

[75] S. Dimopoulos and S. Raby, *Supercolor*, *Nuclear Physics B* **192** (1981), no. 1981 353–368.

[76] M. Dine, W. Fischler, and M. Srednicki, *Supersymmetric technicolor*, *Nuclear Physics B* **189** (1981) 575–593.

[77] M. Dine and W. Fischler, *A phenomenological model of particle physics based on supersymmetry*, *Physics Letters B* **110** (1982), no. 3 227–231.

[78] M. Dine and W. Fischler, *A supersymmetric gut*, *Nuclear Physics B* **204** (1982) 346–364.

[79] C. R. Nappi and B. A. Ovrut, *Supersymmetric extension of the SU(3)SU(2)U(1) model*, *Physics Letters B* **113** (June, 1982) 175–179.

[80] L. Alvarez-Gaume, M. Claudson, and M. Wise, *Low-energy supersymmetry*, *Nuclear Physics B* **207** (1982) 96–110.

[81] S. Abel, M. J. Dolan, J. Jaeckel, and V. V. Khoze, *Phenomenology of Pure General Gauge Mediation*, *Physics* (Oct., 2009) 30, [arXiv:0910.2674].

[82] S. Abel, M. J. Dolan, J. Jaeckel, and V. V. Khoze, *Pure General Gauge Mediation for Early LHC Searches*, *Physics* (Sept., 2010) 22, [arXiv:1009.1164].

[83] M. J. Dolan, D. Grellscheid, J. Jaeckel, V. V. Khoze, and P. Richardson, *New Constraints on Gauge Mediation and Beyond from LHC SUSY Searches at 7 TeV*, *Constraints* (Apr., 2011) 20, [arXiv:1104.0585].

[84] D. Grellscheid, J. Jaeckel, V. V. Khoze, P. Richardson, and C. Wymant, *Direct SUSY Searches at the LHC in the light of LEP Higgs Bounds*, *Physics* (Nov., 2011) 13, [arXiv:1111.3365].

[85] I. Jack and D. R. T. Jones, *Non-standard soft supersymmetry breaking*, *Physics Letters B* **61** (Mar., 1999) 12, [9903365].

[86] D. M. Pierce, J. A. Bagger, K. T. Matchev, and R.-J. Zhang, *Precision Corrections in the Minimal Supersymmetric Standard Model*, *Energy* (June, 1996) 57, [9606211].

[87] R. Ellis and G. Zanderighi, *Scalar one-loop integrals for QCD*, *Journal of High Energy Physics* (2008) 0–27, [arXiv:0712.1851].

[88] L. J. Hall, *Grand unification of effective gauge theories*, *Nuclear Physics B* **178** (1981).

[89] F. Staub, *Sarah*, arXiv:0806.0538.

[90] F. Staub, *From superpotential to model files for FeynArts and CalcHep/CompHEP*, *Computer Physics Communications* (2010) [0909.2863].

[91] F. Staub, *Automatic calculation of supersymmetric renormalization group equations and loop corrections*, *Computer Physics Communications* (2011) 1–32, [1002.0840].

[92] F. Staub, *SARAH 3.2: Dirac gauginos, UFO output, and more*, *Computer Physics Communications* (July, 2013) 1–24, [arXiv:1207.0906].

[93] F. Staub, *SARAH 4: A tool for (not only SUSY) model builders*, *arXiv preprint arXiv:1309.7223* (Sept., 2013) 24, [arXiv:1309.7223].

[94] W. Porod, F. Staub, and A. Vicente, *A Flavor Kit for BSM models*, arXiv:1405.1434.

[95] W. Porod, *SPheno, a program for calculating supersymmetric spectra, SUSY particle decays and SUSY particle production at e+e colliders*, *Computer Physics Communications* **153** (June, 2003) 275–315.

[96] W. Porod and F. Staub, *SPheno 3.1: extensions including flavour, CP-phases and models beyond the MSSM*, *Computer Physics Communications* **183** (Nov., 2012) 2458–2469.

[97] The DELPHI Collaboration and J. Abdallah, *Photon events with missing energy in e + e- collisions at* $\sqrt{s} =$ *130 to 209 GeV*, *The European Physical Journal C* **38** (Jan., 2005) 395–411, [0406019].

[98] The OPAL Collaboration and G. Abbiendi, *Searches for Gauge-Mediated Supersymmetry Breaking topologies in* e^+e^- *collisions at centre-of-mass energies up to* $\sqrt{s} = 209$GeV, *The European Physical Journal C* **46** (Mar., 2006) 307–341, [0507048].

[99] LEPSUSYWG, ALEPH, DELPHI, L3, and OPAL Experiments, *Combined LEP Chargino Results, up to 208 GeV for large m0, note LEPSUSYWG/01-03*, 2001.

[100] LEPSUSYWG, ALEPH, DELPHI, L3, and OPAL Experiments, *Combined LEP Chargino Results, up to 208 GeV for low DM, note LEPSUSYWG/02-04*, 2002.

[101] LEPSUSYWG, ALEPH, DELPHI, L3, and OPAL Experiments, *Combined LEP Selectron/Smuon/Stau Results, 183-208 GeV, note LEPSUSYWG/04-01*, 2004.

[102] M. D. Goodsell and P. Slavich, *No title, in preparatation* (2014).

[103] F. Lyonnet, I. Schienbein, F. Staub, and A. Wingerter, *PyR@TE: Renormalization Group Equations for General Gauge Theories*, arXiv:1309.7030.

[104] G. Bhattacharyya and T. Ray, *Pushing the SUSY Higgs mass towards 125 GeV with a color adjoint*, *Physical Review D* **87** (Jan., 2013) 015017.

[105] P. Grajek, A. Mariotti, and D. Redigolo, *Phenomenology of General Gauge Mediation in light of a 125 GeV Higgs*, arXiv:1303.0870.

[106] N. Arkani-Hamed, A. Delgado, and G. F. Giudice, *The well-tempered neutralino*, *Nuclear Physics B* **741** (May, 2006) 108–130, [0601041].

[107] R. Brock, M. E. Peskin, K. Agashe, M. Artuso, J. Campbell, S. Dawson, R. Erbacher, C. Gerber, Y. Gershtein, A. Gritsan, K. Hatakeyama, J. Huston, A. Kotwal, H. Logan, M. Luty, K. Melnikov, M. Narain, M. Papucci, F. Petriello, S. Prell, J. Qian, R. Schwienhorst, C. Tully, R. Van Kooten, D. Wackeroth, L. Wang, and D. Whiteson, *Planning the Future of U.S. Particle Physics (Snowmass 2013): Chapter 3: Energy Frontier*, arXiv:1401.6081.

[108] M. Berggren, T. Han, J. List, S. Padhi, S. Su, and T. Tanabe, *Electroweakino Searches: A Comparative Study for LHC and ILC (A Snowmass White Paper)*, arXiv:1309.7342.

[109] S. Raby, *Gauge-mediated SUSY Breaking with a Gluino LSP*, 9712254.

[110] S. Raby and K. Tobe, *The phenomenology of SUSY models with a gluino LSP*, *Nuclear Physics B* **539** (Jan., 1999) 3–22, [9807281].

[111] H. Baer, K. Cheung, and J. Gunion, *Heavy gluino as the lightest supersymmetric particle*, *Physical Review D* **59** (1999) 1–30.

[112] The ATLAS Collaboration, *Search for strongly produced supersymmetric particles in final states with two same-sign leptons and jets with the ATLAS detector using 21 fb1 of proton-proton collisions at* $\sqrt{s} = 8$ *TeV*, in *ATLAS NOTE, ATLAS-CONF-2013-007*, pp. 0–26, 2013.

[113] R. Barbieri and G. F. Giudice, *Upper bounds on supersymmetric particle masses*, *Nuclear Physics B* **306** (1988) 63–76.

[114] S. P. Martin and M. T. Vaughn, *Regularization Dependence of Running Couplings in Softly Broken Supersymmetry*, 9308222.

[115] A. D. Box and X. Tata, *Threshold and flavor effects in the renormalization group equations of the MSSM. II*, *Physical Review D* **82** (Dec., 2010) 119905, [arXiv:0810.5765].

[116] A. D. Box and X. Tata, *Threshold and flavor effects in the renormalization group equations of the MSSM: Dimensionless couplings*, *Physical Review D* **82** (Dec., 2010) 119904, [arXiv:0712.2858].